THE REACTIVITY AND CATALYTIC ACTIVITY OF BIDENTATE INDENYL-PHOSPHINE TETHERED COMPLEXES OF RHODIUM AND RUTHENIUM

DAVID CHARLES PUGH, B.Sc.

A thesis submitted to the University of Southampton in accordance with the requirements of the degree of M.Phil. in the Faculty of Science.

Department of Chemistry, January 2005

UNIVERSITY OF SOUTHAMPTON

ABSTRACT

FACULTY OF PHYSICAL SCIENCES
SCHOOL OF CHEMISTRY

MASTER OF PHILOSOPHY

THE REACTIVITY AND CATALYTIC ACTIVITY OF BIDENTATE INDENYL-PHOSPHINE TETHERED COMPLEXES OF RHODIUM AND RUTHENIUM

by David Charles Pugh

A higher-yielding route to racemic ligand 2-cyclohexyl-2-(3'*H*-1'-indenyl)ethyl diphenylphosphine has been adapted from the known route to the chiral phosphine. Protection *via* formation of the borane adduct allows easy handling of the air-sensitive phosphine and has improved overall yields of known complexes (η^5:η^1-indenyl-CH(Cy)-CH_2PPh_2)Rh(CO) and (η^5:η^1-indenyl-CH(Cy)-CH_2PPh_2)RuCl(PPh_3). Tetrahydroindenyl and cationic derivatives have been synthesised from the ruthenium complex and all the complexes have been tested for catalytic activity, along with (η^5:η^1-indenyl-CH(Cy)-$CH_2CH_2PPh_2$)RuCl(PPh_3) and [(η^5:η^1-indenyl-CH(Cy)-$CH_2CH_2PPh_2$)Ru(PPh_3)]$^+$[PF_6]$^-$ (from P. Wright).

Catalytic activity was seen for the transfer hydrogenation of acetophenone, but the resulting alcohol was racemic. It was also seen for the hydrogenation of iminium tetrafluroroborate salts, though the amount of reduction seen was too small to observe a reproducible e.e. The complexes were catalytically inactive for the nucleophilic displacement of allylic acetates, the cyclopropanation of styrene and the Diels-Alder reaction between cyclopentadiene and methacrolein.

It has also been shown that displacement of PPh_3 from ruthenium complex (η^5:η^1-indenyl-CH(Cy)-CH_2PPh_2)RuCl(PPh_3) with more electron-rich phosphines occurs with retention of stereochemistry at the metal centre. X-ray structures of the tetrahydroindenyl and cationic ruthenium complexes, as well as the complexes formed by phosphine displacement, have been obtained.

ACKNOWLEDGEMENTS

Firstly, I would like to thank Professor Richard Whitby for allowing me the opportunity to undertake this degree. His advice, encouragement and support have been invaluable in allowing me to complete the work.

The past year would have been much duller without the Whitby group members past and present: Emma Thomas, Peter Wright and Drs Sally Dixon, Rupert Hunter and David Norton (many thanks to Emma and Pete for proofing this thesis). Thanks also to Thomas, Pam, Sofia and Lionel, who shared a lab with me, and the other members of the Brown group for the laughs and many trips to The Crown.

I would also like to thank the superb analytical services at Southampton: Joan Street and Neil Wells for NMR and John Langley and Julie Herniman for Mass Spec. Special thanks to Susanne Huth from the EPSRC crystallography service, who ran my X-ray structures and had to put up with a lot of my pestering.

Thanks to Johnny, Ben, Sarah, Andrea and Sky, my housemates over the past year, for the laughs, card games, pool and drunken antics (especially in The Gate!) and last, but by no means least, my family for their support, encouragement and financial assistance over the years.

LIST OF ABBREVIATIONS

Ac	Acetyl
BINAP	2,2'-*bis*(diphenylphosphino)-1,1'-binapthyl
biphop-F	1,2-*bis*[*bis*(pentafluorophenyl)phosphanyloxy]-1,2-diphenylethane
Bn	Benzyl
Cp	Cyclopentadienyl
Cp*	Pentamethylcyclopentadienyl
DCM	Dichloromethane
DKR	Dynamic Kinetic Resolution
DMAP	N,N-Dimethylaminopyridine
DME	1,2-dimethoxyethane
DMPM	*bis*(dimethylphosphino)methane
DMS	Dimethylsulfide
DPPE	*bis*(diphenylphosphino)ethane
EDA	Ethyl diazoacetate
EI	Electron Impact (MS)
ES	Electrospray (MS)
GC	Gas Chromatography
HMPA	Hexamethylphosphoramide
HRMS	High Resolution Mass Spectrometry
Ind	Indenyl
IPA	Isopropanol
^{i}Pr	*iso*-propyl
IR	Infra-Red (spectroscopy)
LRMS	Low Resolution Mass Spectrometry
MA	Methacrolein
MP	Melting Point
MPV	Meerwein-Ponndorf-Verley
Ms	Mesyl (methanesulfonyl)
m/z	Mass to Charge Ratio

^{n}Bu	*n*-butyl
NMR	Nuclear Magnetic Resonance (spectroscopy)
RCM	Ring Closing Metathesis
ROMP	Ring Opening Metathesis Polymerisation
RT	Room Temperature
TBDMS	*tert*-butyl dimethylsilyl
^{t}Bu	*tert*-butyl
TEA	Triethylamine
TEAF	Triethylamine/Formic Acid
Tf	Triflyl (trifluoromethanesulfonyl)
THF	Tetrahydrofuran
TLC	Thin Layer Chromatography
Ts	Tosyl (*p*-toluenesulfonyl)
w/v	Weight per Volume

CONTENTS

ABSTRACT i

ACKNOWLEDGEMENTS ii

ABBREVIATIONS iii

CONTENTS v

1.0 INTRODUCTION 1

1.1 GENERAL INTRODUCTION 1

1.2 BIDENTATE CYCLOPENTADIENYL-PHOSPHINE COMPLEXES I – PLANAR CHIRALITY AND THE EFFECT OF CHANGING THE CP-PHOSPHINE LIGAND 3

1.21 Rhodium Complexes 3

1.22 Ruthenium Complexes 5

1.3 BIDENTATE CYCLOPENTADIENYL-PHOSPHINE COMPLEXES II – VARYING THE LIGAND ENVIRONMENT AROUND THE METAL CENTRE 8

1.31 Varying the Metal Source 8

1.32 PPh_3 Substitution 9

1.33 Chloride Displacement 11

1.34 Reactions at the Rhodium Centre 13

1.4 REACTIONS CATALYSED BY RHODIUM AND RUTHENIUM CP-PHOSPHINE COMPLEXES 15

1.41 Hydrogenation 16

1.42 Transfer Hydrogenation 17

1.43 Allylic Displacement 19

1.44 Diels-Alder Reaction 20

1.45 Cyclopropanation of Olefins 21

2.0 SYNTHESIS OF RHODIUM AND RUTHENIUM COMPLEXES 23

2.1 BACKGROUND AND AIMS 23

2.2 BIDENTATE INDENYL-PHOSPHINE SYNTHESIS 25

2.3 SYNTHESIS OF RHODIUM COMPLEX **22** 28

2.4 SYNTHESIS OF RUTHENIUM COMPLEXES 30

2.5 CONCLUSIONS 34

3.0 CATALYTIC STUDIES OF RHODIUM AND RUTHENIUM COMPLEXES **35**

3.1 HYDROGENATION 35

3.2 TRANSFER HYDROGENATION 37

3.3 ALLYLIC DISPLACEMENT 39

3.4 DIELS-ALDER REACTION 40

3.5 CYCLOPROPANATION 41

3.6 STOICHIOMETRIC REACTIONS 42

3.7 CONCLUSIONS 43

3.8 FUTURE WORK 44

4.0 EXPERIMENTAL **45**

5.0 REFERENCES **67**

APPENDICES

Appendix I **Specific details of the catalytic studies**

Appendix II **X-Ray structure of ruthenium complex 80**

Appendix III **X-Ray structure of ruthenium complex 81**

Appendix IV **X-Ray structure of ruthenium complex 82**

Appendix V **X-Ray structure of ruthenium complex 112**

Appendix VI **X-Ray structure of ruthenium complex 113**

1.0: INTRODUCTION

1.1 – General Introduction

Over the past couple of decades, there has been much research into the use of transition metal complexes as catalysts for organic transformations. In particular, metal-cyclopentadienyl complexes have proved successful, due to their synthetic diversity and stability imparted by the strength of the metal-cyclopentadienyl bond. More recent research has looked into the use of chiral transition metal complexes to effect enantioselective transformations, thus enabling savings of time and cost to be made in the syntheses of complex chiral molecules.

In order for a chiral complex to be a successful catalyst for asymmetric reactions, the stereochemistry of the catalytic site must be controlled. In transition metal catalysis, the active site is the metal centre, and the surrounding environment is controlled by the ligands attached to the metal. Chirality in transition metal complexes can arise in several different ways: from a chiral ligand (ligand-derived chirality, **1**),[1] at the metal centre itself (metal-centred chirality, **2**)[2] or by planar chirality of a bound achiral ligand (**3**)[3] (Figure 1).

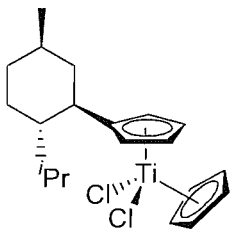

1
Ligand-derived chirality

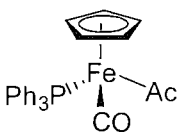

2
Metal-centred chirality

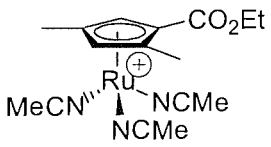

3
Planar chirality

Figure 1

Planar-chiral transition metal complexes enable chirality to be placed very close to the metal centre with no danger of racemisation, due to the strength of the metal-Cp bond. However, accessing single enantiomers often involves a costly resolution step. Despite this, planar-chiral complexes of titanium and zirconium (in particular, their *ansa*-metallocenes (Figure 2)) are active catalysts for a range of organic transformations, including hydrogenation,[4] Diels-Alder reactions[5] and carbomagnesiation reactions.[6]

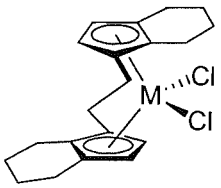

4 - M = Ti
5 - M = Zr
6 - M = Hf

Figure 2

Previous research within the Whitby group led to the development of a C_1-symmetric catalyst model for early transition metals, which achieved good results in asymmetric catalysis (Figure 3).[7]

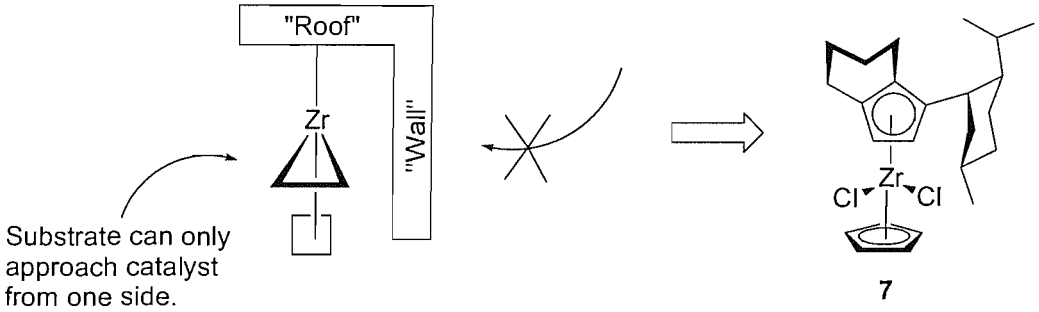

Figure 3

Subsequent work to apply this model to late transition metal complexes focused initially on the 1-neomenthylindene ligand **8**, with the neomenthyl group acting as the 'wall' and the indenyl ligand the 'roof' (Scheme 1).[8]

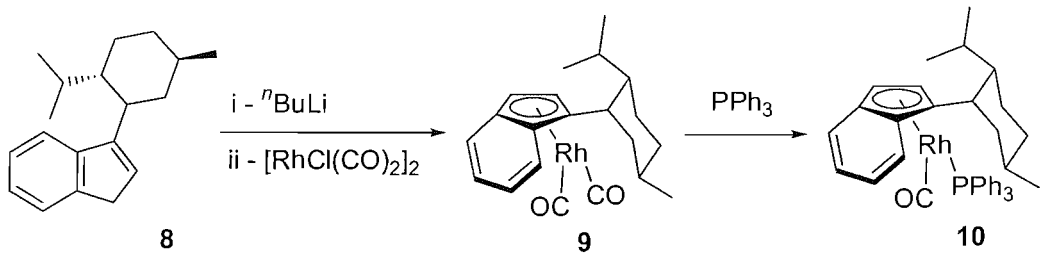

Scheme 1

Although complex **9** and its derivative **10** were synthesised, they were not isolated. Instead, the successful complexation of a substituted indenyl ligand to rhodium encouraged the development of indenyl-phosphine bidentate complexes which fitted the 'roof-wall' model.

1.2 – Bidentate Cyclopentadienyl-Phosphine Complexes I – Planar Chirality and the Effect of Changing the Cyclopentadienyl-Phosphine Ligand

Cp-heteroatom bidentate ligands are an important class of ligand, especially because these complexes are expected to have properties different to monodentate Cp or heteroatom complexes. Cp-phosphine complexes in particular have been studied in some detail.[9]

11 **12**

Figure 4

Complexes **11** and **12** are the first reported example of Cp-phosphine complexes of rhodium and ruthenium respectively. Prepared by the reaction of the lithium anion of the Cp-phosphine ligand with $[RhCl(CO)_2]_2$[10] and $RuCl_2(PPh_3)_3$[11], these, and their derivatives, have found applications in catalysis.

These complexes also have enormous potential for variability, allowing them to be 'tuned' for specific reactions. For example, a variant of **12** where the Cp-phosphine tether has 4, rather than 2, carbon atoms is the most effective chiral catalyst for Trost's 'reconstitutive condensation' reaction (Scheme 2).[12]

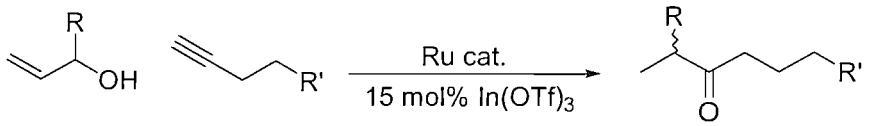

Scheme 2

1.21 – Rhodium Complexes

Although **11** is not a chiral complex, there are many ways of making it so. Perhaps the most obvious is to introduce a source of chirality onto the alkyl tether (Figure 5):

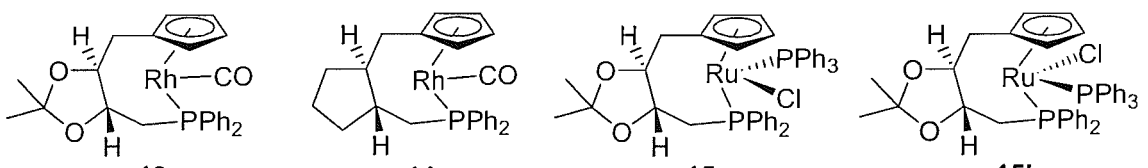

13 **14** **15a** **15b**

Figure 5

Complexes **13** and **15** have a chiral tether derived from *L*-threitol and **14** from *trans*-dimethylenecyclopentane. They were prepared by the reaction of the lithium salts of the Cp-phosphine ligand with $[RhCl(CO)_2]_2$[13] and $RuCl_2(PPh_3)_3$[12]. However, the reported complexation yields for the rhodium complexes were modest: 22% (**13**) and <20% (**14**) whilst the ruthenium complex was synthesised in 49% yield and a 41:59 ratio of diastereomers.

16 **17**

Figure 6

Salzer *et al* reported the chiral Cp-phosphine complex **16** (Figure 6).[14] Its indenyl-phosphine analogue, **17**, was synthesised by Brookings within the Whitby group.[8] Both complexes were prepared via similar synthetic routes and the complexation step for **17** occurs with some degree of planar-chirality induction, despite the chiral information being remote from the metal centre. This induction may be explained by using Poilblanc's suggested mechanism for complexation.[10] If phosphine co-ordination is the first step, chloride displacement then takes place *via* a cyclic transition state (Figure 7) and the remote chiral phenyl group is responsible for the induction of planar chirality.

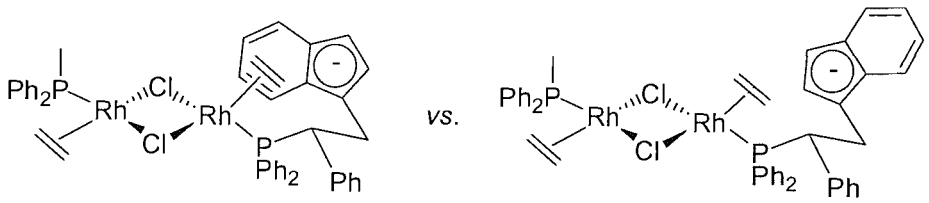

Figure 7

For indenyl-phosphine bidentate ligands where the tether is attached to the 1- or 3- position, these can be classed as unsymmetrically substituted Cp ligands. As such, they will form planar-chiral complexes irrespective of the arrangement of ligands around the metal atom. Indenyl ligands can also form η^3-indenyl complexes, freeing up a co-ordination site on the metal (ring slippage) and reducing the electron count by 2, often leading to a dramatic increase in the rate of associative reactions.[15] This peculiarity has been termed the "indenyl ligand effect" (also see section 1.4).

Tani's indenyl-phosphine analogue of complex **13** was synthesised in 38% d.e., showing that the remote chiral information is capable of inducing planar-chirality.[13] Further work into

indenyl-phosphines with chiral groups attached directly to the indene moiety showed that the neoisomenthyl group gave the highest d.e. upon complexation to $[RhCl(CO)_2]_2$ (Figure 8).

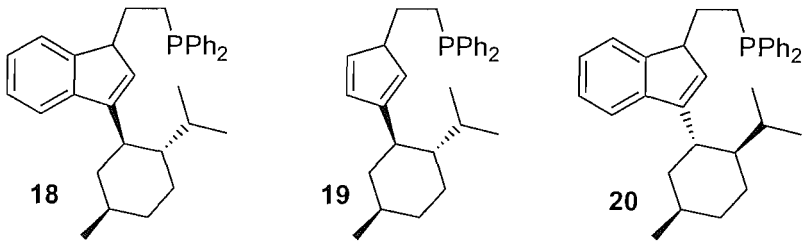

24% d.e. 8% d.e. 74% d.e.

Figure 8

The increased d.e. shown with the indenyl ligands shows the importance of the extra aromatic group in discriminating between the diastereotopic faces. The low d.e. seen with ligand **18** was repeated when complexation of the lithium salt of **18** to $[RhCl(COD)_2]_2$ showed only a 20% d.e.[16]

Previous work within the Whitby group on placing the chiral information on the tether has resulted in a reasonably high d.e. upon complexation to rhodium. Complex **17** was synthesised in 50% d.e. and **21** in 40%.[8] Changing the length of the phosphine tether resulted in a slight drop in the d.e.: **22** was synthesised in 56% d.e. and **23**, with one extra carbon, in 48% d.e. (Figure 9).[17] It should be noted that in each case, it is possible to separate the major isomer by crystallisation.

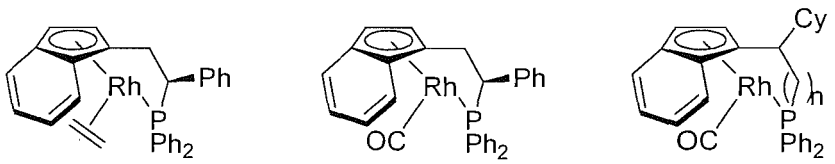

Figure 9

1.22 – Ruthenium Complexes

Ruthenium complex **12** (Figure 4) is chiral due to the asymmetric arrangement of ligands around the ruthenium atom. Although **12** was synthesised as a racemate, complex **15** (Figure 5) was synthesised in 18% d.e. Further investigation into the effect of the protecting group on the d.e. showed that the diol (**24a**) and the dibenzyl ether (**24b**) complexes retained the 18% d.e., whereas the *bis*-TBDMS complex (**24c**) was synthesised in 43% d.e. (Figure 10).[12]

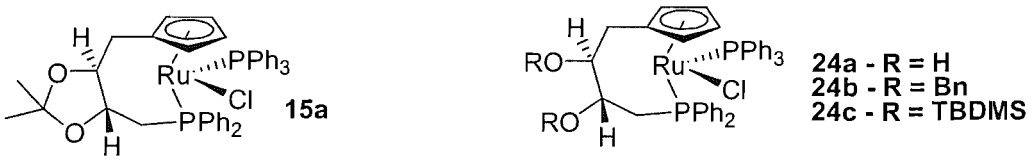

Figure 10

Increasing the d.e. of the complexation step to almost 100% is possible with more exotic ligands. The lithium salts of tethered Cp-ferrocenyl phosphole ligands were reacted with $RuCl_2(PPh_3)_3$ to form the ruthenium complexes **25** and **26** in 63% and 68% yield, but 90% and >98% d.e. respectively (Figure 11).[18]

Figure 11

Harrison synthesised a variety of chiral indenyl-phosphine ruthenium complexes, showing a varying degree of enantioselectivity (Figure 12). Interestingly, the extra carbon in the tether between complexes **27** and **28** results in an increase in the observed d.e. upon complexation: 60% d.e. (rising to 84% after purification) for **27** and 66% d.e. (diastereomers separable by flash chromatography) for **28**. This is at odds with the rhodium indenyl-phosphine complexes **22** and **23**, where increasing the tether length saw a decrease in the d.e. Complex **29** was formed in 82% d.e. and **30** in 66% d.e., but crystallisation of the diastereomeric mixture resulted in purely the major isomer in all cases.[17] It should also be noted that complexes **27-29** showed complete control of the arrangement of the ligands at the metal centre and the d.e. is a reflection of the facial selectivity of the indenyl ligand, whereas for complex **30**, 66% d.e. represents the metal-centred asymmetry only.

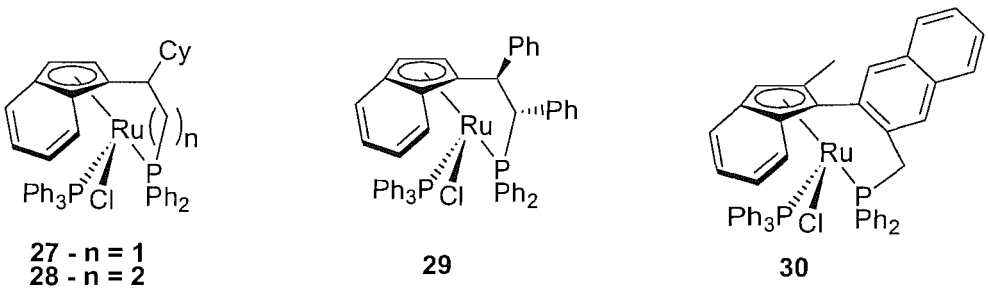

Figure 12

Although there are many more examples of Cp- and indenyl-phosphine bidentate complexes of mid-late transition metals in the literature, this project is more concerned with the catalytic applications of these complexes; hence the remainder of this introduction will concentrate on the reactions and catalytic applications of such complexes.

1.3 – Bidentate Cyclopentadienyl-Phosphine Complexes II – Varying the Ligand Environment Around the Metal Centre

Varying the Cp-phosphine ligand itself is probably the most obvious way of changing a complex to suit a particular reaction. However, it is also possible to vary the ligand environment around the metal centre without affecting the Cp-phosphine ligand, often whilst retaining/improving upon any diastereomeric selectivity induced upon complexation of the Cp-phosphine ligand to the metal.

1.31 – Varying the Metal Source

Perhaps the simplest way of changing the ligand environment is to vary the metal source used for complexation of the ligand. By far the most widely used metal source for ruthenium-based Cp complexes is $RuCl_2(PPh_3)_3$. It reacts with Cp-phosphine ligands to form neutral, 18-electron ruthenium (II) complexes (Scheme 3) and has been the metal source of choice within the Whitby group.[17] Other ruthenium sources include $[RuCl_2(C_6H_6)_2]_2$[3] and $RuCl_2(CO)_3$.[19]

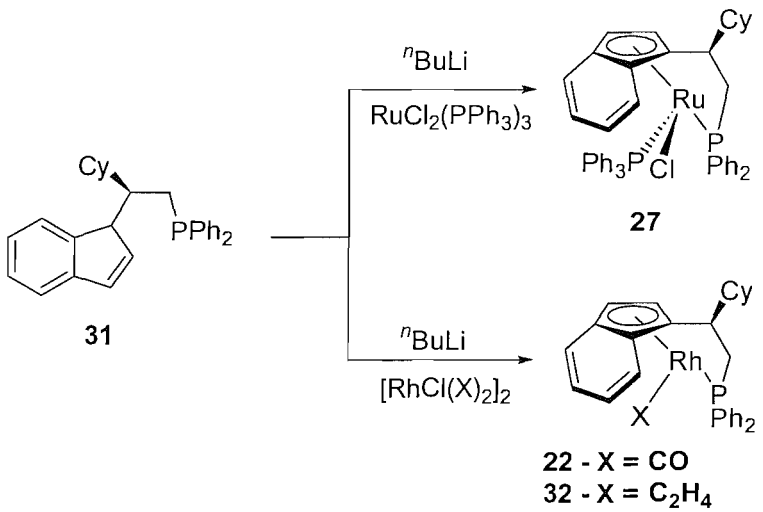

Scheme 3

In contrast with ruthenium, there are many common metal sources for rhodium-based complexes. Within the Whitby group, $[RhCl(C_2H_4)_2]_2$[8] (Figure 5) and $[RhCl(CO)_2]_2$[17] (Figure 8) have been used and both form 18-electron rhodium (I) complexes, but experience within the Whitby group has shown that the carbonyl complex of Cp-phosphine ligands is the easiest to handle (Scheme 3); being air- and moisture-stable in the solid form, though considerably less stable when in solution.[17]

Substitution of the other ligands at the metal centre is another way of varying the ligand environment. For ruthenium (II) complexes based on $RuCl_2(PPh_3)_3$, substitution of both the chloride and PPh_3 is possible. For rhodium (I) complexes, there is only one possible ligand to substitute, the nature of which depends on the starting material.

1.32 – PPh_3 Substitution

The PPh_3 ligand can be substituted by more electron-rich neutral donor ligands, such as alkyl phosphines and amines. Whilst refining his olefin metathesis catalysts, Grubbs tried a variety of different phosphine ligands to see which proved the most effective.[20] Using phenyldiazomethane to oxidise the ruthenium (II) centre to ruthenium (IV), reaction of the diazo compound and the phosphine in one pot furnished the metathesis catalyst (Scheme 4).

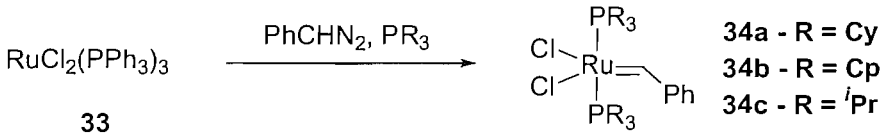

33

Scheme 4

Although phosphine displacement occurred at the same time as oxidation, further work established that the free alkyl phosphine would displace PPh_3 simply by stirring a solution of the vinylidene complex and the free alkyl phosphine in DCM (Scheme 5).[21]

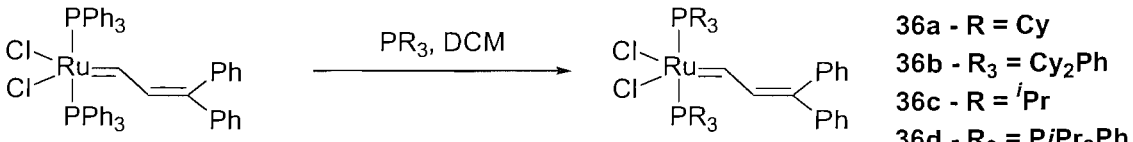

35

Scheme 5

Catalyst	Activity (turnovers/h)
32a	19.0
32b	8.0
32c	17.5
32d	5.5

Table 1

Table 1 shows the relative activities of catalysts **36a-d** in the RCM of diethyldiallylmalonate, using a 20:1 ratio of substrate:catalyst in DCM.[21] The tricyclohexylphosphine catalyst **36a** proved the most active: indeed, similar catalyst **34a** is widely known as Grubbs' 1st-generation olefin metathesis catalyst.

Displacement of PPh_3 has also been used to synthesise the complex $RuCl_2(dmpm)_2$, where dmpm = *bis*(dimethylphosphino)methane.[22] Similarly to Grubbs' method above, $RuCl_2(PPh_3)_3$ was suspended in petroleum ether and stirred for 2 hours with an excess of dmpm (it was noted that if ethanol was used as solvent, $RuCl_2(dmpm)_3$ was obtained).[23]

As well as electronic effects, steric effects play a huge part in phosphine displacement. For the equilibrium in Scheme 6, phosphines show a bonding order R' = $P(OMe)_2Ph$ > PMe_2Ph ~ $P(OEt)_3$ > PEt_3 > PEt_2Ph ~ PPr_2Ph ~ PBu_2Ph.[24] With the exception of $P(OEt)_3$, the order of the phosphine ligands correlate with the increasing cone angle, θ, of the phosphine.

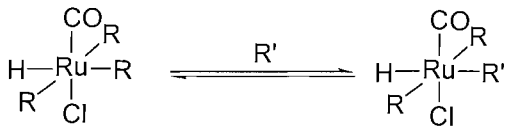

R = PEt_2Ph, PPr_2Ph or PBu_2Ph

Scheme 6

Displacement of phosphines with other group XV ligands is less-well-known. For example, arsines R' = $AsMe_2Ph$ and $AsEt_2Ph$ will not displace R = PEt_2Ph, PPr_2Ph or PBu_2Ph (Scheme 5).[24] However, neutral amine ligands will displace PPh_3 from $CpRu(PPh_3)_2Cl$; in particular, pyridine (Scheme 7) and picolines.[25]

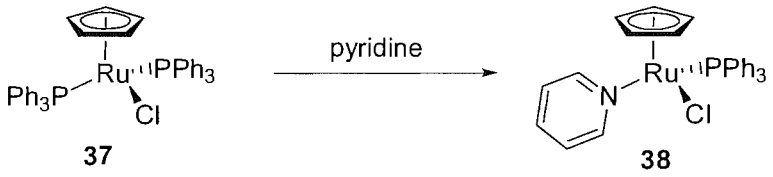

37 **38**

Scheme 7

In addition to aromatic amines, aliphatic amines will also displace PPh_3. The terdentate amine ligand 2,6-[*bis*(dimethylamino)methyl]pyridine will react with $RuCl_2(PPh_3)_3$, displacing 2 phosphines (Scheme 8).[26]

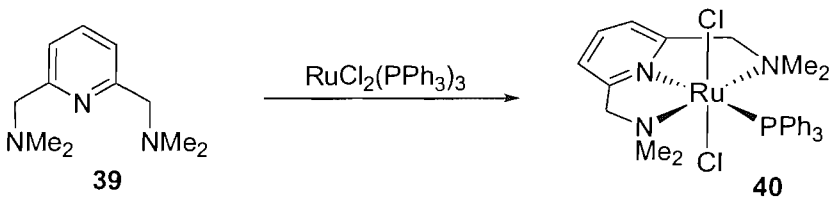

39 **40**

Scheme 8

1.33 – Chloride Displacement

The chloride ligand can be replaced with a wide range of anionic ligands. Direct substitution results in the formation of thiocyanate, cyanate, cyanide, hydride and deuteride complexes, with the other halide complexes being formed by reaction of HX with the hydride complex (Scheme 9).[27]

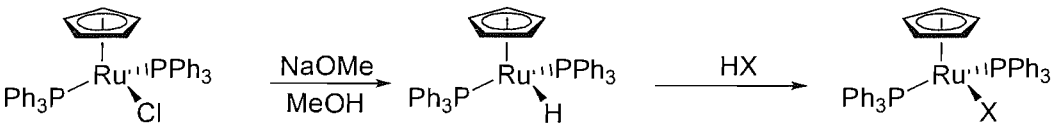

37 41 42

Scheme 9

Of the substituted complexes, hydride **41** has proved to be the most useful, being an active catalyst for the hydrogenation of iminium salts (see section 1.41).[28] The deuteride complex is synthesised using CD_3ONa in CD_3OD. The hydride has also been synthesised from the chloride using KOMe in MeOH[29] and K_2CO_3 in refluxing MeOH.[30]

With use of an appropriate chloride scavenger, it is possible to form a stable cationic ruthenium complex. Refluxing complex **37** in MeCN with NH_4PF_6 results in the formation of an air- and moisture-stable ruthenium cationic complex (Scheme 10).[31]

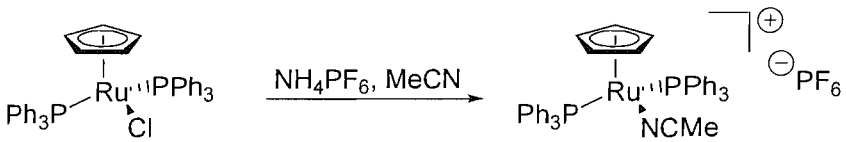

37 43

Scheme 10

Other neutral 2-electron donor ligands have been used to stabilise the cationic complex, notably acetone[32] and THF.[33] The MeCN complexes are by far the most stable, but the THF complex is generally used when a reactive cationic ruthenium intermediate is needed. Other counterions can be used, in particular BF_4^- and BPh_4^-.[31] Ag^+ is another widely used, but more expensive and less stable, chloride scavenger.

Bidentate amine ligands will also displace Cl^- from complex **37**, forming a mono-co-ordinated cationic amine complex **44** (Scheme 11).[34]

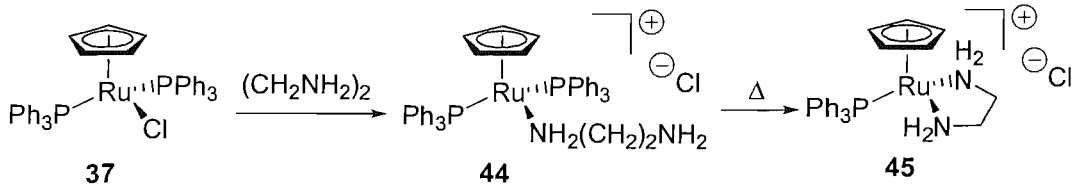

Scheme 11

After heating, the un-co-ordinated end of the *bis*-amine will displace one of the PPh_3 ligands, forming bidentate amine complex **45**. Both the *bis*- and mono-co-ordinated amine salts can be isolated by changing the counterion to BPh_4^-.

Another important set of complexes are the vinylidene and acetylene complexes. Otherwise known as carbene complexes, the main application of vinylidene complexes is in olefin metathesis. However, ruthenium vinylidene complexes have also been detected as an intermediate in Trost's reconstitutive condensation reaction (see section 1.4).[12]

In addition to the diazo method employed by Grubbs, above, ruthenium vinylidene complexes can also be synthesised by reacting complex **37** with a chloride scavenger and a terminal alkyne (starting from cationic complex **43** and not employing a scavenger is also possible). Upon deprotonation, a ruthenium acetylide complex is formed (Scheme 12).[31, 35]

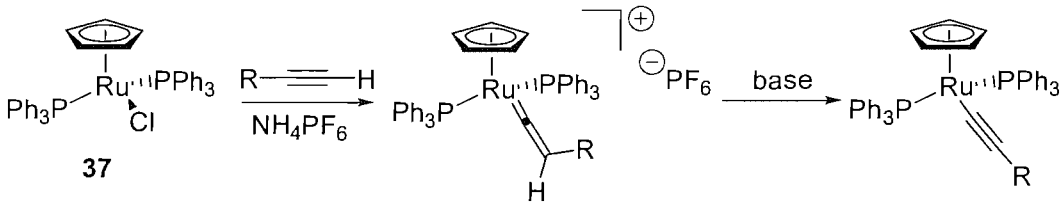

Scheme 12

Acetylide complexes will react with strong electrophiles (e.g. $Me_3O^+BF_4^-$) on the β carbon, generating a cationic vinylidene species. If HPF_6 is used, the intermediate in Scheme 12 is regenerated; otherwise a disubstituted vinylidene species is formed (when $R \neq H$). Acetylide complexes will also react with simple alkyl halides to give disubstituted vinylidene complexes under relatively mild conditions.[35] However, reaction with elemental bromine results in bromovinylidene complexes and, in the case for R = Ph, a bromine atom is substituted in the 4-position on the phenyl ring (Scheme 13).[36]

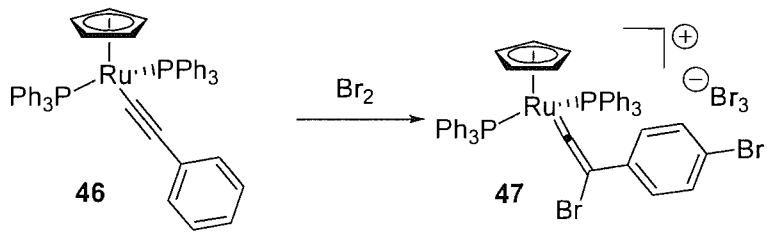

Scheme 13

Vinylidene complexes will also add nucleophiles to the α carbon. A high degree of stereoselectivity is observed upon addition of cyanide to non-symmetrical vinylidene ligands, the stereoselectivity being determined by the steric bulk of the vinylidene groups.[37]

1.34 – Reactions at the Rhodium Centre

Displacement of the carbonyl from Cp-phosphine bidentate rhodium (I) carbonyl complexes is not facile. Indeed, when reacted with PMe_3, complex **48** dissociates the Cp-bound phosphine in preference to the carbonyl (Scheme 14).[38]

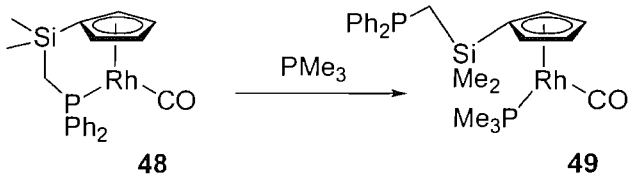

Scheme 14

However, when tethered indenyl-phosphine complex **50** was reacted with P^tBu_3, displacement of the carbonyl did take place (Scheme 15).[10]

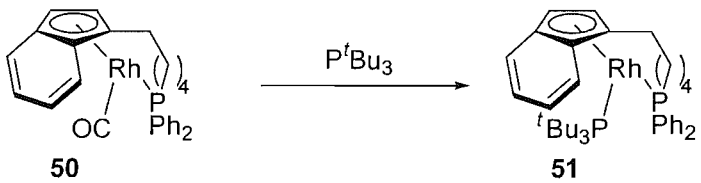

Scheme 15

Instead of carbonyl displacement, Rh^I complexes tend to undergo oxidative addition, especially with iodine and small alkyl halides. Rhodium complex **11** was reacted with I_2 to form the *bis*-iodide rhodium (III) complex **52** (Scheme 16).[10]

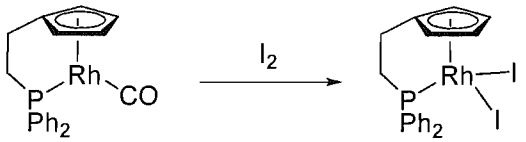

11 **52**

Scheme 16

Tani has investigated the oxidative addition of alkyl halides to bidentate indenyl phosphine rhodium carbonyl complexes.[39] Instead of displacing the carbonyl, as the iodine did above, the alkyl group migrated to the carbonyl, forming a rhodium (III) acetyl complex (Scheme 17).

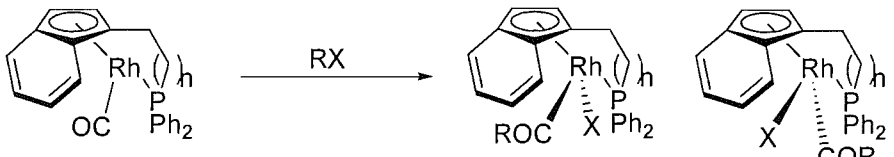

53 - n = 2
54 - n = 3
50 - n = 4

55 - n = 2
56 - n = 3
57 - n = 4

Scheme 17

Reaction	Complex	RX	Yield (%)	(*R*, *S*) : (*R*, *R*)
1	**53**	MeI	90	33 : 67 (34 % d.e.)
2	**53**	EtI	83	4 : 96 (92 % d.e.)
3	**54**	MeI	97	89 : 11 (78 % d.e.)
4	**50**	MeI	92	85 : 15 (70 % d.e.)
5	**50**	EtI	77	98 : 2 (96 % d.e.)

Table 2

Tani found that the size of the alkyl group and the length of the tether both had an influence on the reactivity and the stereochemical outcome. Complex **53** with a 2-carbon tether proved more active than **50** with a 4-carbon tether (reactions 2 and 5, Table 2). However, as the tether length increased, the stereocontrol also increased (reactions 1, 3 and 4, Table 2). Only R = Me or Et successfully formed the acyl complexes, with the smaller methyl group showing greater reactivity, but the larger ethyl group showing greater stereocontrol.

Although there are many more synthetic transformations of rhodium and ruthenium complexes in the literature, this brief review has covered the ones which are of most interest to this project. The remainder of the introduction will concentrate on the 5 reactions which complexes **22** and **27**, and their derivatives, will hopefully catalyse.

1.4 – Reactions Catalysed by Rhodium and Ruthenium Cp-Phosphine Complexes

A recent review of ruthenium-catalysed chemistry, although not comprehensive, showed a large number of reactions catalysed by ruthenium complexes, of which a significant portion were catalyzed by $CpRuCl(PPh_3)_2$ or derivatives thereof.[40] The number of reactions was condensed further to 5, all of which resulted in a chiral product being formed in the hope that enantioinduction, as well as catalytic activity, would be observed.

Harrison tested complex **27** in Trost's 'reconstitutive condensation' reaction, where terminal alkynes and secondary alcohols are combined, affording a chiral ketone (also see section 1.2) (Scheme 18).[12, 17]

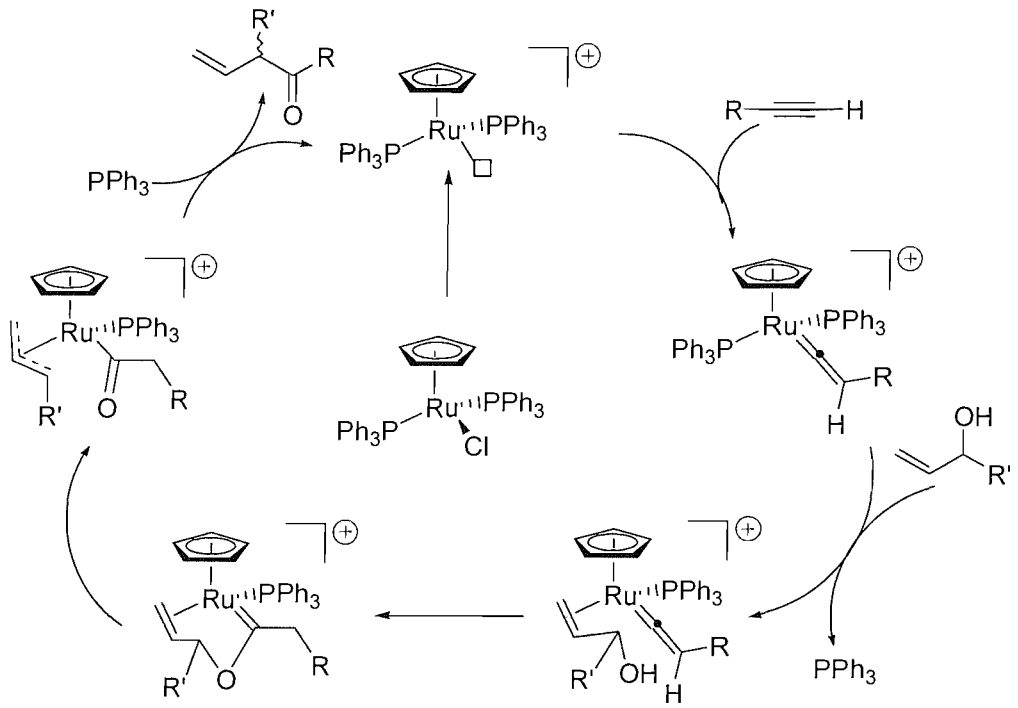

Scheme 18

Unfortunately, when complex **27** was attempted with Trost's conditions, no product was observed. Complete consumption of the alcohol was noted by GC monitoring (despite being in a three-fold excess) which led Harrison to suggest some isomerisation of the allyl alcohol was occurring, in keeping with other aspects of ruthenium chemistry.[41] Further investigation led to the synthesis of the vinylidene complex which Trost postulated was the first step in the catalytic cycle, although this too yielded no product when reacted with the allylic alcohol. Switching the chloride scavenger to NH_4PF_6 reduced the number of byproducts formed, but still no catalytic turnover was observed.

It was thought that the main reason for the reaction not taking place is the presence of the indenyl ligand, instead of a Cp. Trost reported a large decrease in reactivity with large Cp groups and the indenyl ligand in complex **27** can be thought of as a tri-substituted Cp ligand.

The electronic effects of the indenyl ligand could also have had an effect. Although indenyl groups can 'ring-slip' to form η^3 complexes, often leading to an increase in reactivity (see section 1.2), the presence of an indenyl ligand is not always beneficial.[42] The extra benzene ring can act as an 'electron reservoir', donating electron density towards electron-poor ruthenium species, thus deactivating them for catalytic activity.[43]

Harrison postulated some improvements to complex **27** in an attempt to achieve catalysis,[17] but it is unlikely this project will return to this reaction.

1.41 – Hydrogenation

The hydrogenation of unsaturated systems is a classic application of homogeneous catalysis, and numerous catalysts are known which will reduce double bonds enantioselectively. For carbon-carbon double bonds, the catalytic system involves addition of H_2 to a catalyst, co-ordination of the olefin, then reductive elimination of the saturated compound.[44] However, a different mechanism involving the reduction of double bonds by addition of hydride in acidic solution has been reported: this mechanism is selective for polar C=X bonds over C=C bonds (Scheme 19).[45, 46]

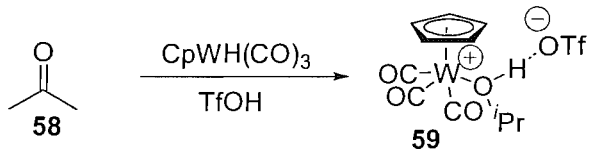

58 **59**

Scheme 19

Ruthenium BINAP complexes are perhaps the most well-known mediators of enantioselective reduction. BINAP complexes offer several advantages: they are chemoselective, preferentially reducing carbonyls over alkenes and nitriles; both enantiomers are easy to prepare, thus allowing access to both enantiomers of the product; the required catalyst loading is often very small and the catalysts offer excellent yields and e.e.'s.[47]

Cp-ruthenium BINAP complexes are also known to reduce carbonyl compounds.[48] Hoke reacted $CpRuCl(PPh_3)_2$ with enantiopure BINAP to form CpRuCl(BINAP) complexes.

However, he postulated that retention of the chloride ligand is essential to retaining the enantioselectivity of the reaction, meaning that loss of the cyclopentadienyl anion is the catalyst activation step.

The specific reaction chosen for catalyst testing is one developed by Norton, who reduced iminium tetrafluoroborate salts to the corresponding ammonium salt both catalytically and stoichiometrically with a Cp-ruthenium hydride complex (Scheme 20).[28]

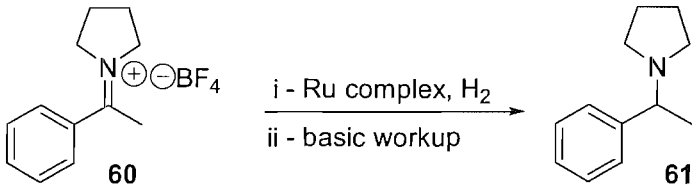

Scheme 20

The iminium cation is generally pre-formed as a crystalline solid by reaction of the ammonium salt with a carbonyl, although *in-situ* formation from the corresponding imine is also possible. Norton's choice of catalyst is a Cp-ruthenium hydride with a chiral bidentate phosphine ligand, incredibly similar to complex **27**. Varying the temperature and pressure of the reaction had no effect on the yield and e.e., indicating that hydride transfer from the metal to the iminium cation is the turnover-limiting step. Although complex **27** contains a chloride ligand rather than a hydride, synthesis of ruthenium hydride species is a well-known reaction (see section 1.32).

1.42 – Transfer hydrogenation

Transfer hydrogenation is a particular variant of hydrogenation where no gaseous hydrogen is involved. Instead, metal-hydride complexes are generated *in-situ* by oxidation of a suitable substrate (usually IPA or formic acid).

Transfer hydrogenation has its roots in the Meerwein-Ponndorf-Verley (MPV) reduction, where ketones are reduced with $Al(O^iPr)_3$ in IPA (Scheme 21).

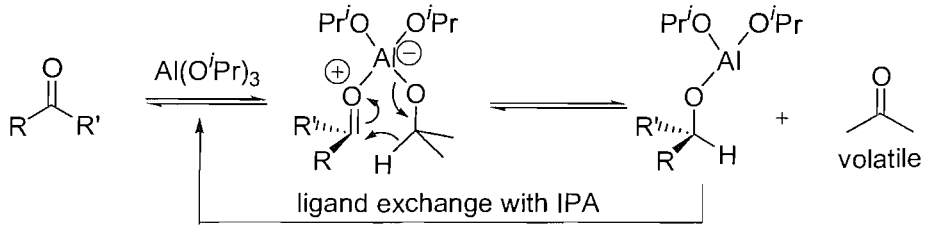

Scheme 21

Although the reaction is actually an equilibrium (the reverse is known as the Oppenhauer oxidation), the reaction is driven by loss of acetone. Attempts to develop an asymmetric version of the MPV reduction succeeded with chiral lanthanide catalysts, although the high catalyst loading required meant that scale-up was impractical.[49]

To this end, attention turned to transition metals; in particular rhodium, ruthenium and iridium. Avecia focused on rhodium (and latterly iridium), whilst Noyori specialised in ruthenium. Both groups hold similar patents: a metal halide (typically chloride) with aromatic ligand (anionic for Avecia, e.g. Cp*; neutral for Noyori, e.g. *p*-cymene) and a chiral bidentate ligand, where one end is a neutral amine. The mechanism is the same for both systems (Scheme 22).[50]

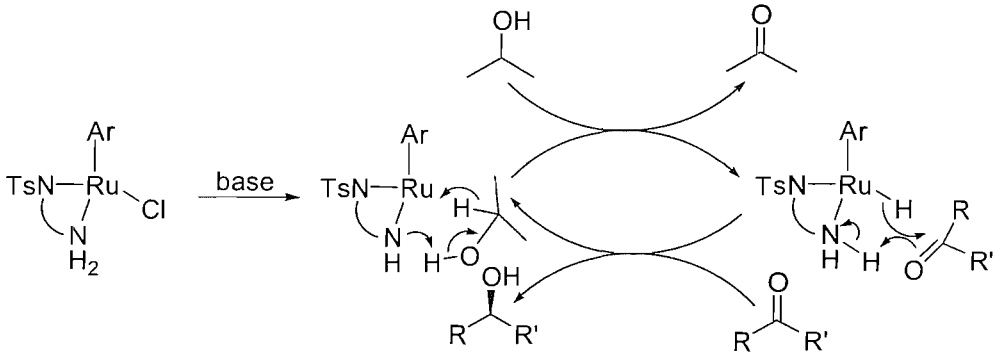

Scheme 22

Much like the MPV reduction, the hydride source is IPA, which is oxidised to acetone. However, the reduction step is not a concerted hydride transfer from IPA to the substrate, but a transfer of hydride from the metal to the ketone, *via* a 6-membered transition state.[51]

Transfer hydrogenation has also been shown to work with imines, although IPA is not a suitable solvent for this reaction. A 5:2 mixture of formic acid:TEA (TEAF) is used instead, where the formic acid is the hydride source, being oxidised to CO_2. If necessary, a polar aprotic solvent can be used to aid dissolution of the substrate.[52]

The specific reaction chosen for catalyst testing is the reduction of acetophenone in IPA. Although complex **27** has no amine ligand, it should be possible to form an amine complex by displacing PPh_3 with an amine (see section 1.31). It should also be possible to use the TEAF system to reduce acetophenone, and an imine derived from acetophenone, e.g. acetophenone anil.

1.43 – Allylic Displacement

One method of effecting an enantioselective reaction is through the enantiofacial selection of a prochiral substrate. Many enantioselective reactions proceed *via* this method, e.g. transfer hydrogenation (see above). The addition of a nucleophile to a π-allyl complex of a transition metal is another such reaction.

Transition metal-allyl complexes offer several advantages for enantioselective syntheses: the ability to produce enantiomerically enriched products from chiral or achiral starting materials, the large variety of nucleophiles which can be used (both carbon and heteroatom nucleophiles) and the ability to form π-allyl complexes from a variety of different substrates (olefins, diolefins and olefins with a leaving group in the allylic position).[53]

Stoichiometric allylic substitution was discovered in the 1960s by Tsuji,[54] although it wasn't until 1970 when catalytic allylic substitution was first reported. In many cases, the products were chiral: these results led to much study into the stereochemistry, mechanism and applications of catalytic allylic substitution.[53]

The majority of transition metal catalysts are palladium based, although catalysts based around ruthenium,[55] nickel,[56] copper[57] and others are known. The most common ligands are bidentate phosphines e.g. DPPE, although P-N bidentate ligands are also widely used.[58]

The reaction chosen for testing is the displacement of 3-acetoxy-1,3-diphenylpropene, with benzylamine,[59] although ethyl 3-(1,3-diphenylpropenyl) carbonate, **62**, is also a suitable starting material (Scheme 23).[55] There are many similarities between Takahashi's ruthenium catalyst and complex **27**, but the majority of the published catalysts for this reaction were tested with the allylic acetate and not the carbonate.

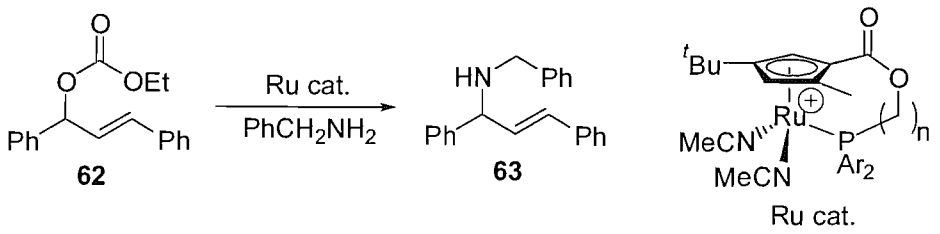

Scheme 23

1.44 – Diels-Alder reaction

The Diels-Alder reaction is possibly the most useful and reliable structural transformation in organic synthesis. It is a widely used method for forming carbon-carbon, carbon-heteroatom and heteroatom-heteroatom bonds *via* a [4 + 2] cycloaddition mechanism, in which a conjugated diene (e.g. 1,3-butadiene) reacts with a dienophile (e.g. ethene). It has been found that the fastest reactions occur with dienes locked in the *cisoid* conformation and when the dienophile is electron-poor.[60]

The reaction can be accelerated by high pressures, and is catalysed by a range of compounds. It was first observed in 1942 by Wasserman that Diels-Alder reactions in acidic media were faster than those not run in acidic media.[61] Ever since 1960, however, Lewis acid catalysed Diels-Alder reactions have been known: Yates and Eaton noted the effect of $AlCl_3$ on the Diels-Alder reaction between anthracene and maleic anhydride.[62]

The traditional Lewis acids (e.g. BCl_3, $AlCl_3$, $TiCl_4$) can give excellent reaction rates at moderate catalyst loadings, provided the dienophile contains oxygen. However, their major disadvantage is their moisture sensitivity, requiring the rigorous exclusion of water from the reactions. Lanthanide Lewis acids (e.g. $Eu(fod)_3$[63]) are much more moisture-stable, though markedly less reactive. To this end, Hollis *et al* turned to transition metal Lewis acid catalysts, which would ideally possess the reactivity of traditional Lewis acids, combined with the stability of lanthanide-based Lewis acids (in addition to a range of other desirable properties).[64]

A few examples of transition metal Lewis acid catalysts had already been reported (Figure 13), including cationic ruthenium complex **66**. All had their drawbacks: **64** was moisture sensitive and tended to polymerise the diene, a fault of **65** as well. However, it indicated that normally electron-rich tungsten (0) complexes could act as Lewis acids, with the right

ligands.[5] Complex **66** was a poor Lewis acid despite the positive charge at the ruthenium metal centre: this was due to the electron-donating properties of the phosphine and the Cp group, thus the complex had a tendency to bind electron-poor olefins and not catalyse the reaction.[65]

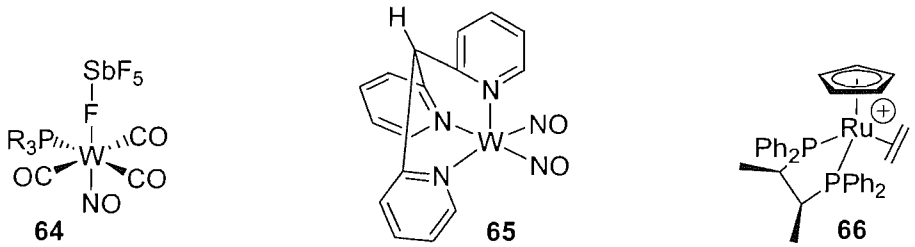

Figure 13

Chiral ruthenium-based Lewis acids analogous to **66** have been reported, in particular [CpRu(biphop-F)(methacrolein)]$^{+}SbF_6^{-}$, where biphop-F is the chiral ligand 1,2-*bis*[*bis*(pentafluorophenyl)phosphanyloxy]-1,2-diphenylethane.[66] It catalyses the reaction between methacrolein and cyclopentadiene (Scheme 24) with an *exo*:*endo* ratio of 97:3, rising to 99.7:0.3 if the Cp ligand is replaced by an indenyl ligand. This reaction is also the reaction of choice for testing complexes in this project.

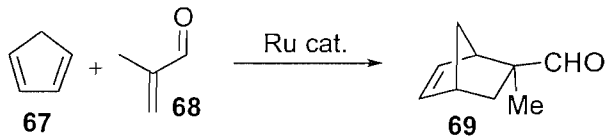

Scheme 24

1.45 – Cyclopropanation of Olefins

The reaction between a diazo compound and an olefin is one that has been used to test many new transition metal complexes for activity (and if the complex is chiral, enantioselectivity). Transition metal-catalysed decomposition of diazo compounds has been known for almost a century,[67] and cyclopropanation is merely one of many reactions that involve the subsequent metal-carbene complex. Other reactions include C-H insertions, cyclopropenations, ylide generation[68] and metathesis (see section 1.3).

Hubert *et al* discovered that dirhodium tetraacetate was a very efficient catalyst for the decomposition of diazo compounds and then the formation of cyclopropanes.[69] Although the catalyst showed no enantioselectivity, it remains in use to this day as a cyclopropanation catalyst.

The first transition metal complex shown to induce an e.e. was discovered by Nozaki in 1966. Complexation of a salicylaldimine ligand to copper II created a complex which gave a 6% e.e. for the reaction between ethyl diazoacetate and styrene.[70] Although there are many transition metal complexes in the literature which claim to catalyse the cyclopropanation of styrene,[68] it was discovered that $CpRuCl(PPh_3)_2$, **37**, and its indenyl analogue were also efficient catalysts for this reaction.[71, 72] Therefore, the reaction between EDA and styrene is the final reaction which will be used to screen complexes **22** and **27** for activity.

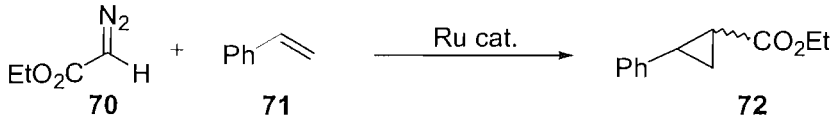

70 **71** **72**

Scheme 25

2.0: SYNTHESIS OF RHODIUM AND RUTHENIUM COMPLEXES

2.1 – Background and Aims

Previous work within the Whitby group led to a short, high-yielding route to ruthenium **27** and rhodium **22** complexes (Scheme 26).[8, 17]

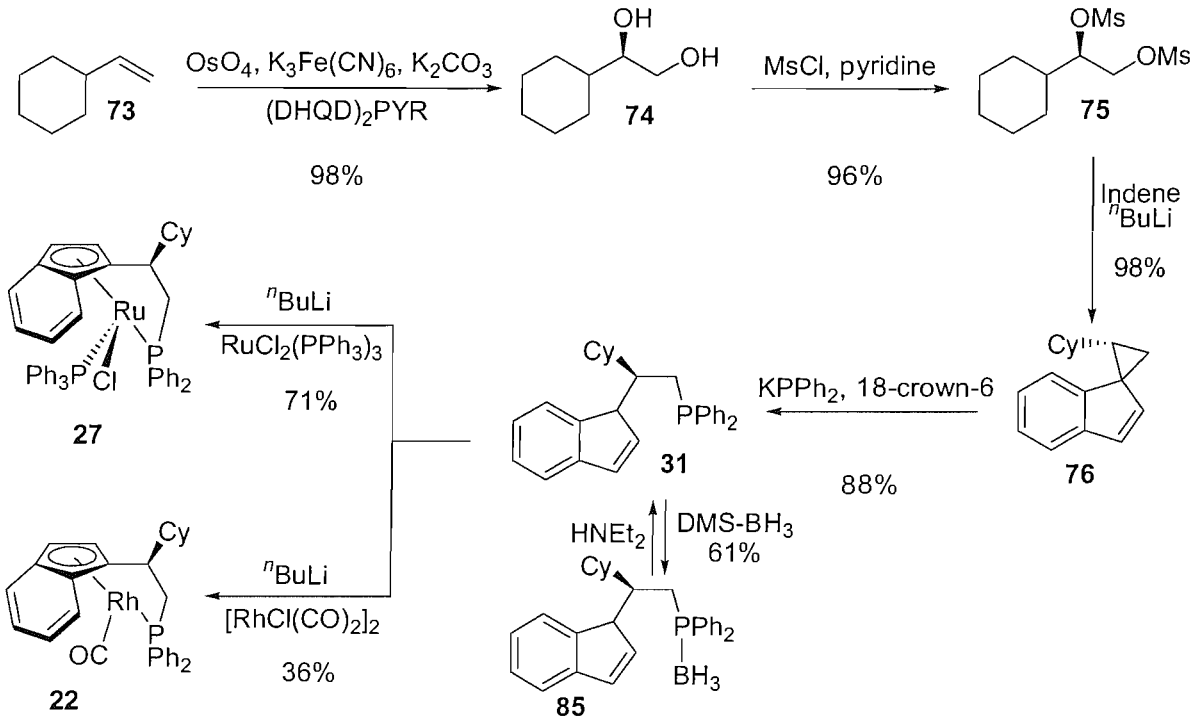

Scheme 26

Starting with vinylcyclohexane, **73**, asymmetric dihydroxylation under Sharpless' conditions,[73] mesylation of the chiral diol and displacement of the mesylates formed an indenyl spirocyclopropane intermediate. The cyclopropane ring was opened with $KPPh_2$ to give the asymmetric indenyl-phosphine ligand **31** in 81% overall yield. Complexation of ligand **31** to $[RhCl(CO)_2]_2$ gave rhodium complex **22** in modest yield and complexation to $RuCl_2(PPh_3)_3$ afforded ruthenium complex **27** in good yield.

With the exception of phosphine **31**, an air-sensitive oil, compounds **73-76**, **23** and **27** are air-stable solids, although purification of the metal complexes was carried out in an inert atmosphere due to uncertainties about their air stability in solution. Harrison looked into protection of the phosphine by formation of the borane adduct in an effort to simplify

handling of the phosphine, but decided not to optimise the route. The yield of the complexation step to rhodium was worryingly low, mainly due to the high cost of the metal. It was hoped that this step would be optimised over the course of the project, but literature precedence for high-yielding complexations of indenyl ligands to rhodium is sparse: indeed, the formation of **23**, the three-carbon tethered analogue of **22,** proceeded in a miserly 16% (Scheme 27).[17]

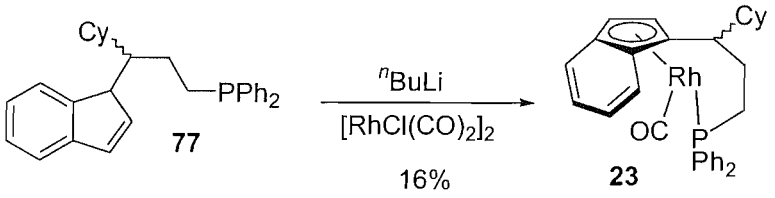

Scheme 27

Once complexes **22** and **27** had been synthesised, it was hoped that slight modifications would allow the easy synthesis of derivatives with the aim of increasing the reactivity (Scheme 28).

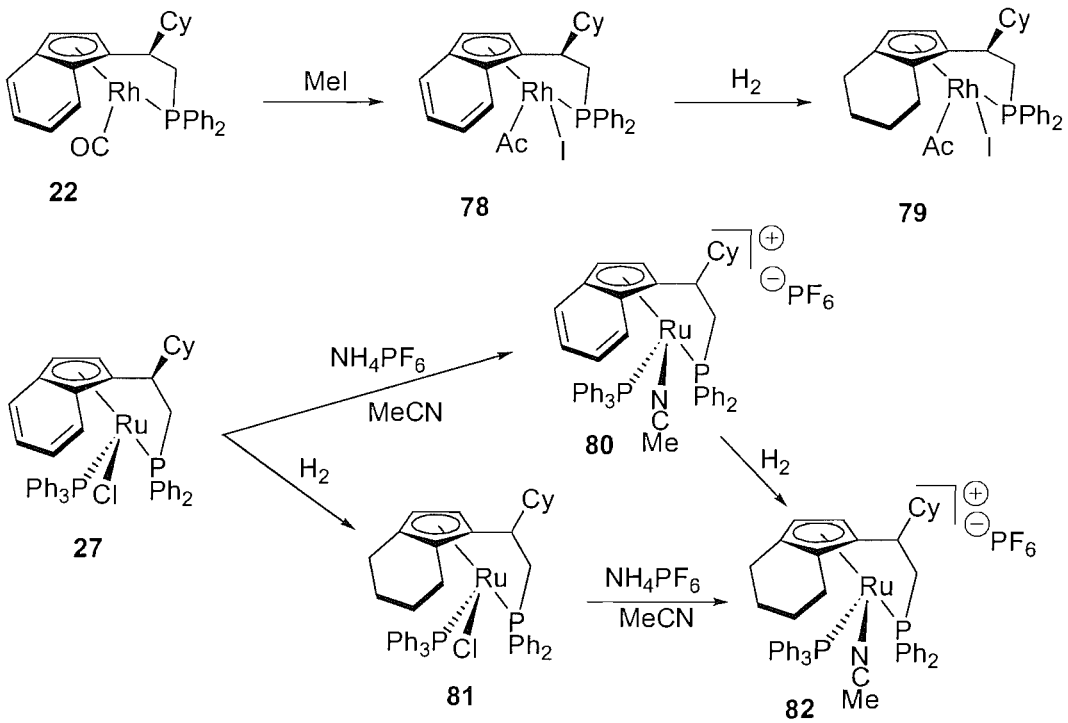

Scheme 28

Hydrogenation of ruthenium complex **27** to the tetrahydroindenyl complex **81** is a known process, but is unoptimised.[17] Formation of cationic ruthenium complexes is a known literature procedure (see section 1.33) and should give cationic ruthenium complexes **80** and **82** in good yield.

2.2 – Bidentate Indenyl-Phosphine Ligand Synthesis

Following the procedure outlined in Scheme 26 above, dihydroxylation of vinylcyclohexane (98% yield), mesylation (96%) and then reaction to form the spirocycle (98%) proceeded as expected. However, isolation of phosphine **31** proved problematic due to its air sensitivity and a yield of 15% was recorded after purification. To avoid wasting valuable enantiopure compound on learning the techniques to effectively purify the phosphine, and also to avoid using complexes **22** and **27** for general activity screening, it was decided to synthesise racemic versions of phosphine ligand **31**. This would also allow the optimisation of the synthesis of rhodium complex **22** with racemic ligand; again, not wasting valuable enantiopure ligand.

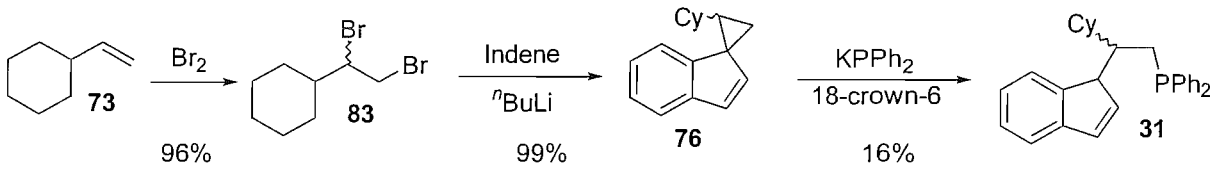

Scheme 29

Slightly modifying the procedure outlined in Scheme 26 gave a more direct route to spirocycle **76**, which proceeded in an excellent 95% overall yield (Scheme 29). However, formation of the phosphine again failed to proceed in good yield. At this point, other methods of purifying the phosphine were looked at, all of which involved protection then purification of the protected phosphine. Three well-known phosphine protection methods were looked at: forming the phosphine oxide,[74] forming the phosphine-borane complex[75] and also forming the phosphine sulfide[76] (Scheme 30).

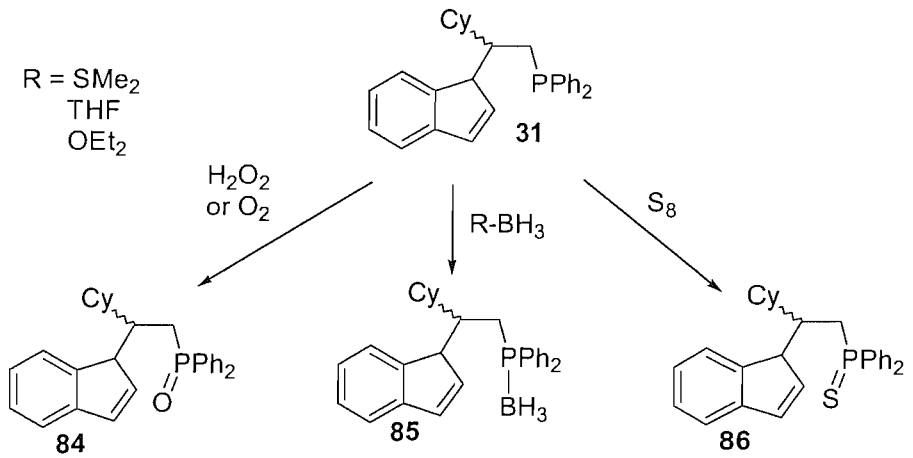

Scheme 30

The first protection method to be looked at was the phosphine oxide, mainly because of the ease of formation – simply expose the phosphine to air! Oxidation with peroxide is another facile method of forming phosphine oxides.[77] Deoxygenation of phosphine oxides is traditionally carried out with trichlorosilane[78] or $LiAlH_4$[79], although here $LiAlH_4$ may reduce the indenyl olefin bond as well. Using AlH_3 removes the need for an aqueous workup, but it does require column chromatography in an inert atmosphere,[80] the difficulties of which were one of the reasons for looking at protecting the phosphine.

Crude phosphine **31** was reacted with H_2O_2 and after 15 minutes, no phosphine was present by TLC. However, upon workup, a disappointing 21% yield of phosphine oxide **84** was isolated. Although optimisation of this reaction was an option, removing the protecting group looked like it would provide more problems, so another method of protecting the phosphine was tried.

The second method to be looked at was the phosphine-borane complex. Reacting the phosphine with a source of borane (THF-BH_3, DMS-BH_3, Et_2O-BH_3 etc.) should furnish the phosphine-borane complex[75] and the deprotection is much easier than the phosphine oxide; merely reaction with a secondary amine.[81] Upon reacting crude phosphine **31** with DMS-BH_3, phosphine-borane complex **85** was isolated in 49% yield as a white, air-stable solid. By quenching the indenyl anion with a stoichiometric amount of water, rather than a large excess, the yield was upped to 91%. Due to the success of this route, no investigations into the phosphine sulfide were carried out.

Harrison synthesised phosphine-borane **85** directly from spirocycle **76** with the use of lithium diphenylphosphide-borane in 61% yield (Scheme 31).[17] Although many attempts to repeat this result were carried out, the maximum isolated yield was 16%.

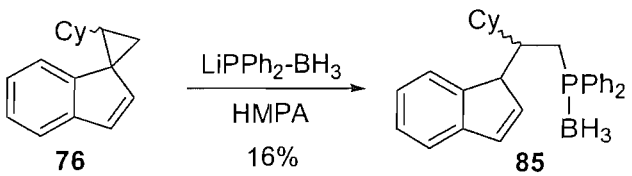

76 **85**

Scheme 31

The $LiPPh_2$-BH_3 was initially synthesised from PPh_3-BH_3, in accordance with the procedure devised by Brisset *et al*,[81] whereby lithium metal is reacted with PPh_3-BH_3. A byproduct of this reaction is PhLi, which has to be destroyed before use – this is accomplished by adding 1

equivalent of ^{t}BuCl. It is conceivable that if the reaction of PPh_3-BH_3 with lithium did not go to completion, an excess of ^{t}BuCl could also have destroyed some of the $LiPPh_2 \cdot BH_3$, accounting for the low yields. To test this theory, $HPPh_2$-BH_3 was reacted with 1 equivalent of ^{n}BuLi, and the $LiPPh_2$-BH_3 formed by this method was reacted with spirocycle **76**. No increase in the isolated yield was seen. Increasing the concentration of the $LiPPh_2$-BH_3 also had no effect on the yield, so this route was abandoned in favour of the established $KPPh_2$ route outlined above.

Once a reliable, high-yielding route to phosphine-borane **85** had been established, enantiopure **85** was synthesised from spirocycle **76** in 91% yield. Chiral complex **85** had been synthesised in 84% overall yield from vinylcyclohexane: asymmetric dihydroxylation and mesylation of the resulting diol, then reaction with indenyl lithium furnished spirocycle **76**, which was ring-opened with $KPPh_2$ and protected with DMS-BH_3. Racemic **85** was synthesised in 87% overall yield from vinylcyclohexane: bromination of vinylcyclohexane and reaction with indenyl lithium yielded racemic spirocycle **76**.

Deprotection of the protected phosphine was carried out by refluxing the phosphine-borane in a large excess of $HNEt_2$, with TLC monitoring. After reflux for 16 hours, no phosphine-borane was detected, so the $HNEt_2$ was removed *via* vacuum transfer, leaving a yellow oil. Although phosphine **31** is supposed to be white, the yellow colouration came from trace impurities in the $HNEt_2$ and no purification of the phosphine was carried out. The yield of the reaction was not measured; rather the phosphine was used directly in the synthesis of the metal complexes.

2.3 – Synthesis of Rhodium Complex 22

Following the procedure outlined by Harrison,[17] phosphine **31** was deprotonated and reacted with $[RhCl(CO)_2]_2$. After workup and purification, rhodium complex **22** was isolated in 9% yield (Scheme 32).

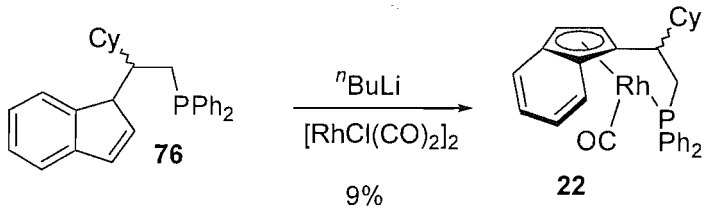

Scheme 32

Despite repeated attempts at optimisation, the isolated yield never increased above 18%. Varying solvent, temperature, time and even the rhodium metal source did not bring about a high-yielding reaction (summary of results in Table 3).

Reaction	Solvent	Temp. (°C)	Time (h)	Rh source	Yield (%)[a]
1	THF	RT	16	$[RhCl(CO)_2]_2$	25
2	THF	65	16	$[RhCl(CO)_2]_2$	26
3	THF	RT	60	$[RhCl(CO)_2]_2$	27
4	Toluene	RT	16	$[RhCl(CO)_2]_2$	18
5	Toluene	110	16	$[RhCl(CO)_2]_2$	20
6	MeOH	RT	16	$[RhCl(CO)_2]_2$	9
7	MeOH	70	16	$[RhCl(CO)_2]_2$	11
8	DME	RT	60	$RhCl_3 \cdot 3H_2O$	-
9	DME	85	60	$RhCl_3$	-
10	THF	RT	16	$[RhCl(COD)]_2$	<5
11	THF	RT	16	$[RhCl(C_2H_4)_2]_2$	-
12	THF	RT	16	[RhCl(norbornadiene)]$_2$	<5
13	THF	RT	16	$RhCl(PPh_3)_3$	<5

a - crude yield, calculated by integration of Cp peaks in ^1H NMR against an internal standard

Table 3 – attempted synthesis of rhodium indenyl complexes

Unfortunately, a crude yield of 25% (reaction 1) under the initial conditions only yielded 15% after purification. The established conditions for purification were flash chromatography

on alumina (neutral, Brockmann Grade III) in an inert atmosphere. Switching to chromatography in air slightly increased the amount of material lost, whilst switching to silica resulted in the loss of almost all the complex.

Reluctantly, mainly due to time pressures, the optimisation of the synthesis of rhodium complex **22** was abandoned, as was the synthesis of novel derivatives of **22**. The small amount of material already synthesised was sufficient for activity testing: should complex **22** prove active, optimisation could be attempted again.

2.4 – Synthesis of Ruthenium Complexes

Following the procedure outlined by Harrison,[17] phosphine **31** was deprotonated and reacted with $RuCl_2(PPh_3)_3$. It was discovered that chromatography under argon was unnecessary for complex **27**, which resulted in a yield of 82% (Scheme 33). Use of the chiral phosphine ligand resulted in the synthesis of the chiral version of **27** in 71% yield.

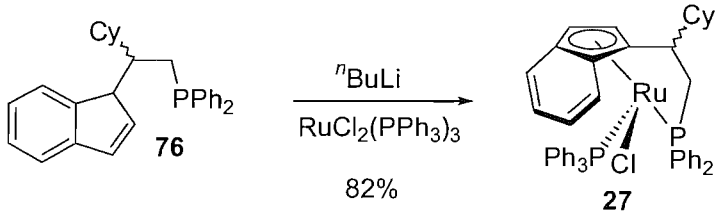

Scheme 33

Harrison found non-optimised conditions for the hydrogenation of ruthenium indenyl complex **27** to tetrahydroindenyl complex **81**, using 1800 psi H_2 and 10 mol% PtO_2 in DCM at 65 °C for 3 days (Scheme 34).[17] It was hoped that cationic indenyl complex **80** would reduce to cationic tetrahydroindenyl complex **82** under milder conditions, but literature precedent for the reduction of indenyl rings attached to late transition metals was sparse.[82]

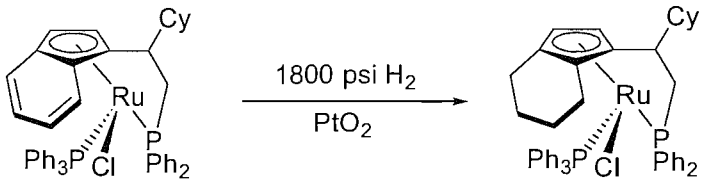

Scheme 34

Cationic indenyl complex **80** was synthesised by refluxing NH_4PF_6 and neutral indenyl complex **27** in MeCN (Scheme 35). Crystallisation by slow diffusion of ether into a concentrated MeCN solution of **80** allowed full analysis: the crystals grown were of X-ray quality (Appendix II). The chiral cationic complex, starting from chiral **27**, was also synthesised.

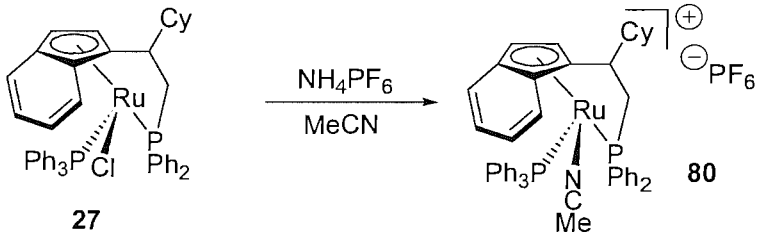

Scheme 35

For the reduction of **80** to **82**, various H_2 pressures ranging from atmospheric pressure up to 50 bar were tried at RT with 10 mol% PtO_2 catalyst for 2½ days, but only slight reduction was observed at 50 bar. Heating the reaction to 65 °C saw increased reduction product, but also the presence of two new products (one major and one minor) in the $^{31}P\{^1H\}$ NMR spectrum (Scheme 36). Leaving the reaction for increased amounts of time merely decreased the amount of **82** present and increased the amount of the minor impurity product.

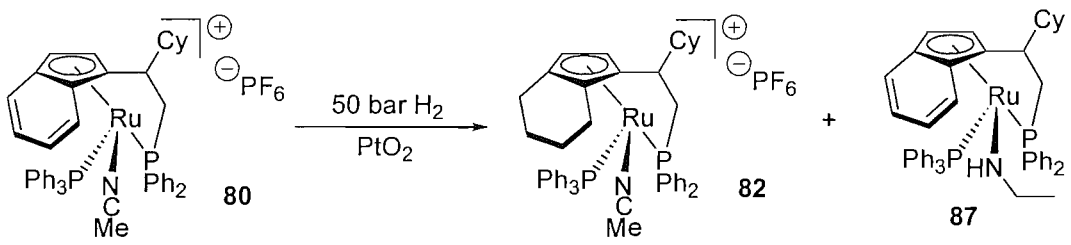

Scheme 36

It was thought that reduction of the acetonitrile ligand to the corresponding neutral ethylamine complex **87** was one of the possible impurities and indeed, a peak at 818.5 in the ES^+ MS was observed. This peak corresponds to the indenyl ethylamine complex **87** and none of the corresponding tetrahydroindenyl ethylamine complex was observed, indicating that once the neutral indenyl ethylamine complex is formed, it is inert to hydrogenation under these conditions. A peak corresponding to complex **82** $(M\text{-}PF_6\text{-}MeCN)^+$ was observed and a small impurity peak at 811.6, probably corresponding to the minor reduction impurity.

To be sure that the ethylamine complex was the byproduct of the reduction of **80**, direct synthesis of the ethylamine complex was attempted. Stirring diethylamine and complex **80** in TEA afforded neutral complex **87** (Scheme 37). Unfortunately, complex **87** was unstable to column chromatography and resisted all attempts at crystallisation, so full characterisation was not achieved. However, the presence of two doublets in the $^{31}P\{^1H\}$ spectrum at 51.95 and 53.28 ppm (J = 20.2 Hz), corresponding to the doublets from the reduction of complex **80**, indicated that ethylamine complex **87** was a byproduct of the reduction of **80**.

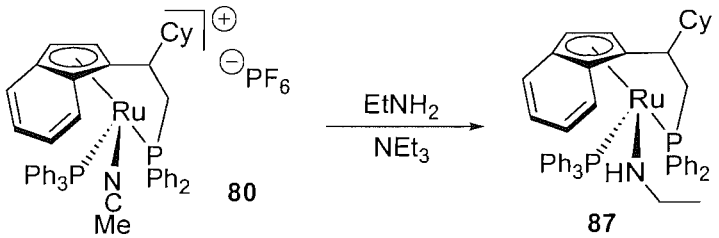

Scheme 37

Purification of tetrahydroindenyl cationic complex **82** was attempted, but no TLC system could be found which separated the compounds (MeOH streaked the compound up an alumina plate, whilst MeCN and DCM afforded no separation – no other solvents moved the compounds). Crystallisation also failed to afford a pure product, so other methods of purification were investigated.

One attempt involved taking the products of the reduction of **80** and treating them with chloride ions, in an attempt to reform neutral complex **81**. Literature precedent is again sparse, so a trial of complex **80** was stirred with brine in DCM. This failed to yield neutral complex **27**, as did stirring complex **80** in a mixture of concentrated HCl and DCM. However, Lindsay *et al* used tetra-^{n}butylammonium chloride in refluxing acetone to form a neutral ruthenium complex from the cationic hexafluorophosphate species.[83] In the absence of tetra-^{n}butylammonium chloride, tetraethylammonium chloride was tried instead. After refluxing with complex **80** for 2 days in dry acetone, complex **27** was isolated in 81% yield (Scheme 38). These conditions were applied to the crude product of the reduction of complex **80** and after purification, complex **81** was isolated in 42% yield. However, it was decided that synthesising complex **82** *via* the reduction of complex **27** would be a more economic and faster method.

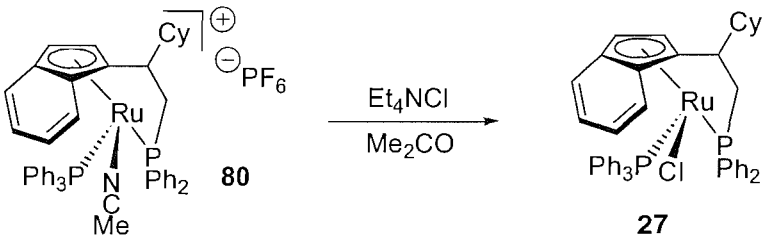

Scheme 38

Submitting **27** to the known conditions afforded tetrahydroindenyl complex **81** in 33% yield, along with a significant impurity. After purification, complex **81** was crystallised by slow diffusion of pentane into a benzene solution and the crystals formed were suitable for X-ray analysis (Appendix III). Reducing the pressure to 1600 psi made no difference to the yield, but lowering the pressure further did reduce the yield.

Park found that (Ind)Ru(PPh_3)$_2$ reacted with certain chlorinated solvents (DCM and chloroform in particular).[84] It was therefore not an unreasonable assumption that the unknown impurities in the $^{31}P\{^{1}H\}$ spectra of the reduced complexes were products of the reaction between the solvent (DCM) and complex **27**. Switching the solvent to DME

eliminated the impurity in the $^{31}P\{^{1}H\}$ spectrum and the yield for the reduction of **27** to **81** increased to 55%, with no sign of any impurity.

Another route to cationic tetrahydroindenyl complex **82** was to take complex **81** and NH_4PF_6 in refluxing MeCN (Scheme 39). This went in 65% yield and cationic tetrahydroindenyl complex **82** was crystallised by slow diffusion of ether into a MeCN solution. X-ray analysis of the crystals was obtained (Appendix IV).

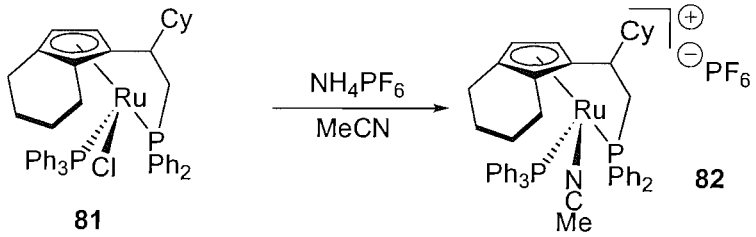

Scheme 39

The reduction of cationic indenyl complex **80** to cationic tetrahydroindenyl complex **82** was attempted again, this time in DME. Only two reduced products were observed: ethylamine complex **87** and tetrahydroindenyl complex **82**. However, isolation again proved to be a problem and separating the two complexes (plus unreduced complex **27**) *via* reforming the neutral species did not improve on the previous 42% yield.

2.5 – Conclusions

Adaptation of the existing route to spirocycle **76** gave easy access to a racemic version of ligand **31**. An easy method of handling air-sensitive phosphine **31** *via* protection with BH_3 has also been optimised. This led to the syntheses of racemic ruthenium complexes **27** and **80-82**, all of which have been synthesised in sufficient quantity to allow testing of their catalytic properties. Should any complexes prove active, chiral versions of complexes **27** and **80** have also been synthesised in excellent yield to test for enantioinduction.

The attempted reduction of cationic indenyl ruthenium complex **80** to tetrahydroindenyl complex **82** failed to go cleanly. Reduction of the acetonitrile ligand was a competing side-reaction and the resulting ethylamine complex **87** was inseparable from complex **82**. Unfortunately, characterisation of this novel compound was not possible due to its instability to chromatography.

The optimisation of the synthesis of rhodium complex **22** was not possible, due to the low reactivity of the indenyl phosphine ligand with various rhodium sources. Enough complex was synthesised to allow testing of its catalytic properties, but the derivatives **78** and **79** were not synthesised. Whilst this was a major setback, enough indenyl-phosphine metal complexes had been synthesised to allow testing for catalytic activity, the results of which will be discussed in chapter 3.

3.0: CATALYTIC STUDIES OF RHODIUM AND RUTHENIUM COMPLEXES

In addition to complexes **22**, **27** and **80-82**, the analogues of **27** and **80** with one extra carbon in the tether (**28**, **92**) were donated by P. Wright for catalytic testing (Figure 14).

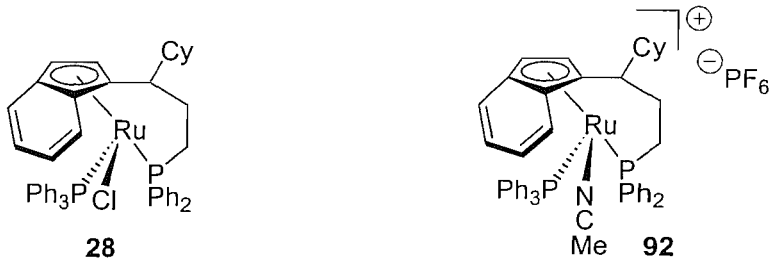

Figure 14

3.1 – Hydrogenation

The first reaction chosen for catalytic activity testing was the hydrogenation of iminium salts under Norton's conditions (see section 1.41).[28] The iminium salt was generated *in-situ* from the corresponding imine (Scheme 40) and a summary of the results are in Table 4.

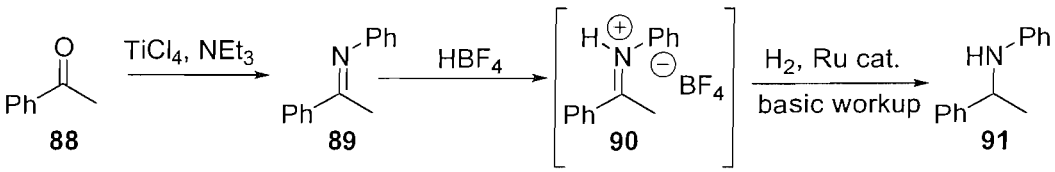

Scheme 40

Reaction	Complex	Temp. (°C)	Yield (%)[a]
1	27	50	11
2	80	50	9
3	27	RT	10
4	80	RT	9
5	81	RT	<5
6	82	RT	<5
7	28[b]	RT	<5
8	92[b]	RT	<5
9	93	RT	-

a - yield calculated by GC
b – complexes supplied by P. Wright

Table 4 – the hydrogenation of iminium salts

The reactions were all run for 60 hours and the pressure was kept constant at 6 bar, mainly because Norton observed no difference when the pressure was increased. No increase in yield was observed when the temperature was raised, and the reactions were all poor-yielding. Although rerunning the reactions with chiral versions of **27** and **80** is possible, the e.e from a 10% reduction would not be very reliable.

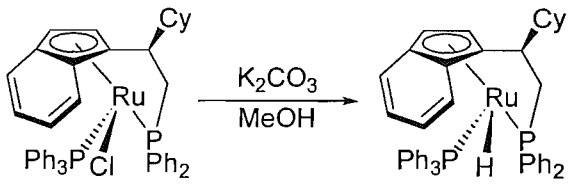

27 **93**

Scheme 41

Complex **93** is the crude ruthenium hydride species, formed by displacement of the chloride from complex **27** (Scheme 41). Although ^{1}H NMR showed a 'filled-in doublet' and another doublet at -15 ppm, characteristic of Cp-ruthenium hydride species,[29] the $^{31}P\{^{1}H\}$ NMR showed a large singlet at 70 ppm, in addition to the expected two doublets. Hydride **93** could not be purified by chromatography, sublimation or crystallisation and was unstable to light and air, decomposing if left exposed for more than 12 hours. The nature of the impurity was indeterminable – the singlet in the $^{31}P\{^{1}H\}$ NMR shows a single phosphorus environment is present, but no trace of PPh_3 or uncomplexed indenyl-phosphine was seen in the spectrum. The downfield shift also implies an electron-deficient phosphine, but it did not correspond to triphenylphosphine oxide or the indenyl-phosphine oxide. Although the crude product was tried in reaction 9, no reduction was observed.

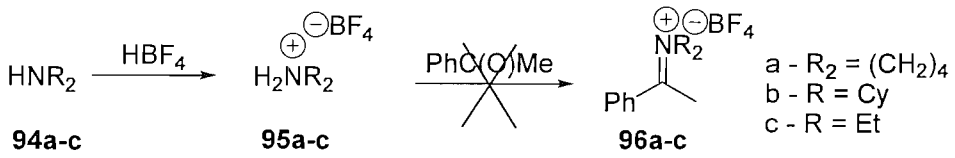

94a-c **95a-c** **96a-c**

Scheme 42

Another method of forming the iminium salt is to react an amine with HBF_4 and then a carbonyl (Scheme 42). Norton mainly used this method, so HBF_4 was added to pyrrolidine, forming a clear oil (**95a**). Despite repeated attempts, crystallisation was not achieved – a soft solid was formed, but condensation with acetophenone failed to yield iminium salt **96a**. Switching to dicyclohexylamine did give a white crystalline solid (**95b**), but the amine was too hindered to react with acetophenone. The last attempt was with diethylamine – although this did also form a soft solid (**95c**), condensation with acetophenone failed again. It is not known why the condensation step repeatedly failed – the use of 4Å molecular sieves and Dean and Stark traps were employed with refluxing toluene to remove water, but no condensation was observed. Reluctantly, due to time pressure, this line of investigation was abandoned.

3.2 – Transfer Hydrogenation

The reduction of acetophenone *via* transfer hydrogenation was the second reaction chosen to test complexes for catalytic activity. Although none of the complexes have amine ligands attached, they were initially tried in IPA with KOH as base and a little reduction was observed. When the conditions were varied, it was found that the best conditions were in the presence of an excess of cyclohexylamine and NaO^{i}Pr as base (Table 5).

Reaction	Complex	Base	Solvent	Additive	Yield (%)[a]
1	27	KOH	IPA	-	<5
2	80	KOH	IPA	-	10
3	80	KOH	IPA	-	-
4	81	KOH	IPA	-	9
5	82	KOH	IPA	-	5
6	82	KOH	IPA	-	-
7[b]	28	KOH	IPA	-	21
8[b]	92	KOH	IPA	-	-
9[b]	92	KOH	IPA	-	-
10	80	NaO^{i}Pr	IPA	-	10
11	80	NaO^{i}Pr	IPA	1 eq. O_2	25
12	80	NaO^{i}Pr	MeOH	-	-
13	80	NaO^{i}Pr	IPA	$CyNH_2$	72
14[b]	28	NaO^{i}Pr	IPA	-	5
15[b]	28	NaO^{i}Pr	IPA	1 eq. O_2	19
16[b]	28	NaO^{i}Pr	MeOH	-	-
17[b]	28	NaO^{i}Pr	IPA	$CyNH_2$	43

a - yield calculated by GC
b – complexes supplied by P. Wright

Table 5 – transfer hydrogenation of acetone

All reactions were run overnight in an inert atmosphere at 60 °C, to remove any acetone formed.

The other transfer hydrogenation system of triethylamine/formic acid was also tried, but no reduction was observed with any catalysts. It was also tried with acetophenone anil, **89**, but again, no reduction was observed – the only products detectable by GC were acetophenone and aniline.

The best conditions found with the racemic catalysts were chosen to test the chiral catalysts. Chiral variants of complexes **28** and **80** were reacted with NaO^{i}Pr in the presence of an excess of cyclohexylamine and oxygen and the e.e. measured on a chiral GC. Unfortunately, despite many repeat measurements, the reduction product was racemic. It is possible that loss

of the indenyl ring is the step which forms the catalytically active species – this would result in the loss of the chirality at the metal centre and a racemic product.

In an attempt to synthesise a closer analogue of the more common transfer hydrogenation catalysts, and in an attempt to explain the effectiveness of adding an excess of cyclohexylamine in the above series of reactions, displacement of the PPh_3 ligand with an amine was attempted. When complex **27** was refluxed in pyridine, free PPh_3 was observed in the $^{31}P\{^1H\}$ NMR, along with many other products. The lack of a clean displacement of PPh_3 was in accordance with the attempt to synthesise the ethylamine complex **87** (section 2.4) where many products were obtained and the complex was unstable to chromatography.

With no prospect of synthesising a pure ruthenium amine complex by displacement, it was decided that this reaction offered no hope of gaining an e.e. and studies were halted.

3.3 – Allylic Displacement

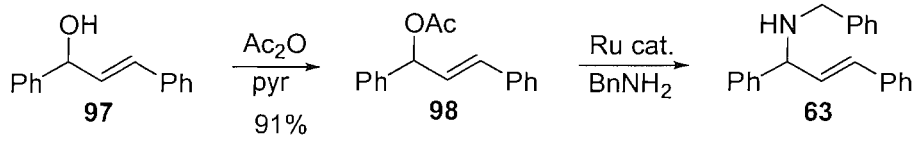

Scheme 42

The displacement of an allylic acetate by a nucleophile was the third reaction chosen for catalytic testing. Most examples in the literature use 3-acetoxy-1,3-diphenylpropene as a starting material (see section 1.43), which is synthesised by reducing chalcone with $LiAlH_4$ and acetylating (Scheme 42). Unfortunately, when allylic acetate **62** and benzylamine were reacted in the presence of ruthenium catalysts **27**, **28**, **80-82** and **92**, no reaction was observed. Even upon heating to 60 °C, no loss of starting material was observed by GC, although free PPh_3 was detected by GC.

Takahashi used an allylic carbonate instead of an allylic acetate for his displacement reaction.[55]

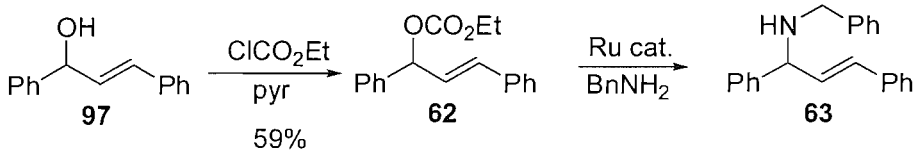

Scheme 43

The allylic carbonate **98** was synthesised by reaction of allylic alcohol **97** with ethyl chloroformate (Scheme 43). Upon reaction with benzylamine at 60 °C with catalysts **27**, **28**, **80-82** and **92**, free PPh_3 was again observed by GC but no loss of starting material was seen by GC. The presence of free PPh_3 can be explained by Rigo's observation that PPh_3 will dissociate from $(Ind)RuCl(PPh_3)_2$ at 65 °C[71] and should not be taken as evidence of the formation of an allylic ruthenium intermediate. Although a stronger nucleophile was not tried in these reactions, there was no evidence to suggest the formation of an allylic metal intermediate, which would not change with the use of a stronger nucleophile. On the basis of this complete lack of activity, it was decided to abandon this course of investigation.

3.4 – Diels-Alder Reaction

The Diels-Alder reaction between cyclopentadiene and methacrolein is a simple reaction which offers 4 possible product diastereomers, all of which are separable by chiral GC (Scheme 24, section 1.44).

Freshly cracked cyclopentadiene and methacrolein were mixed in DCM with the rhodium and ruthenium complexes at -18 °C, along with a non-catalysed reaction to take into account any background reaction that may occur. After GC showed no sign of reaction after 48 hours, the temperature was raised to 40 °C. Again, no reaction was observed and there was no trace of the Cp peak on the GC, indicating that it had evaporated before any reaction could take place.

To try and counter this problem, the diene was switched to 1,3-cyclohexadiene which is much less volatile than cyclopentadiene (Scheme 44). Unfortunately, it is also much less reactive and no reaction was observed with methacrolein.

Attempts were made to synthesise a more Lewis acidic ruthenium complex by oxidative addition of iodine, but the reaction produced a complex mix of products. Insufficient rhodium complex remained to try the oxidative addition of MeI to **22** and produce a Rh^{III} complex, which would be more Lewis acidic than the Rh^{I} complex. With time rapidly running out, no further studies into creating a more Lewis acidic ruthenium complex were undertaken and this line of research was abandoned.

3.5 – Cyclopropanation

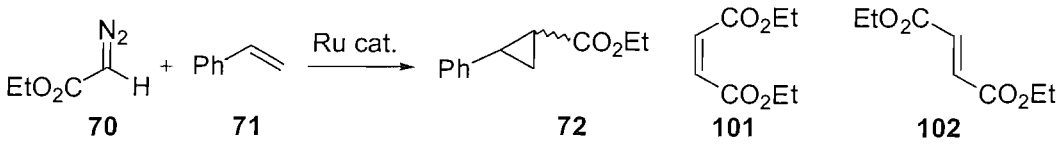

70 **71** **72** **101** **102**

Scheme 45

The cyclopropanation of styrene was the final reaction chosen to test the complexes for catalytic activity (Scheme 45). There are many examples in the literature of complexes that catalyse this reaction, so hopes were high that activity would be seen. Initial studies looked promising: after dissolving complexes **27**, and **80-82** in styrene at 40 °C, EDA was added over a 4 hour period and the reactions were monitored by GC. The ratio of **72** to byproducts **101** (diethylmaleate) and **102** (diethylfumarate) was encouraging. However, work by P. Wright had shown that complex **28** was inactive in this reaction and the ratio of products seen was a result of a background reaction. When EDA was added to styrene without any complex present, the same ratio of product peaks was seen, indicating that the complexes were inactive in this reaction. This is at odds with the variety of reactions in the literature (see section 1.45) which claim to have complexes which catalyse this reaction – the substantial background reaction does raise questions about the level of activity of the literature complexes.

The carbene intermediate is similar to Grubbs' olefin metathesis catalysts, so metathesis was attempted. 4,4-*bis*(methoxymethyl)-1,6-heptadiene was dissolved in chlorobenzene with complex **27** and a catalytic amount of trimethylsilyldiazomethane was added at 60 °C. After overnight heating, no cyclised product was seen by GC. However, when norbornylene was used instead of a diene, polynorbornylene was produced after overnight heating (Scheme 46).

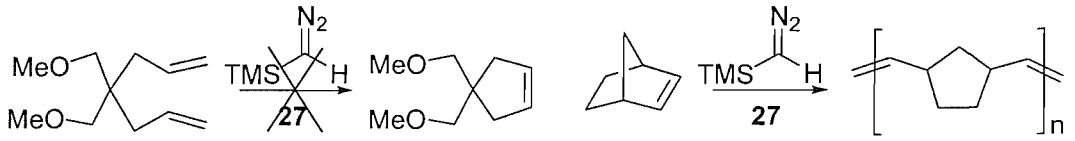

103 **104** **105** **106**

Scheme 46

This time, when a background reaction was run, no ROMP was seen without the presence of **27**. An attempt was made to synthesise the metal-carbene species formed by the decomposition of EDA, but the $^{31}P\{^{1}H\}$ spectrum showed many products and no carbene signal could be found in the ^{13}C spectrum. It is not known why the ROMP succeeded whilst the cyclopropanation proved inactive, but no further studies were undertaken in this area.

3.6 – Stoichiometric Reactions

Due to the failure of the complexes to produce a non-racemic product in any of the above 5 reactions, a couple of stoichiometric reactions were carried out on complex **27**. The first was the formation of the phenylacetylide complex by chloride displacement – it was hoped that the chiral environment around the metal would influence the product formed upon addition of a nucleophile. The second was a series of phosphine displacements, in an attempt to determine whether displacement was an associative or dissociative process.

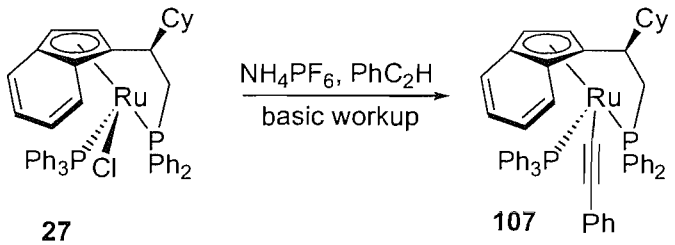

27 **107**

Scheme 47

Several literature methods were known for synthesising acetylide complexes (see section 1.32). Phenylacetylene and ammonium hexafluorophosphate were added to complex **27** and the resulting solution was filtered through basic alumina.[31] A complex mix of products resulted and further attempts at chromatography were unsuccessful, although the molecular ion of the acetylide complex was observed by ES^+ MS in the crude reaction mixture. A different method of synthesising the acetylide complex was tried; lithium phenylacetylide was reacted with complex **27** – again, a complex mix of products was obtained which did not separate *via* chromatography. Unfortunately, a lack of time precluded any further efforts at synthesising the acetylide complex.

Complex **27** was also reacted with various phosphines, in order to see whether displacement of PPh_3 occurred. Although there was no reaction with tricyclohexylphosphine, when **27** and the phosphine were refluxed in toluene, displacement occurred with tri-^{n}butylphosphine, methyldiphenylphosphine and dimethylphenylphosphine. X-ray structures of the methyldiphenylphosphine (Appendix V) and dimethylphenylphosphine (Appendix VI) complexes were obtained, both of which show the phosphine occupying the same position that the PPh_3 ligand was. This indicates the thermodynamic product was formed in these displacements, and also that the displacement is probably a dissociative process, as inversion of configuration at the metal centre might have been seen if it was an associative process.

3.7 – Conclusions

Catalytic studies of complexes **22**, **27** and **80-82** have been carried out on a variety of reactions. Although activity was noted for the transfer hydrogenation of acetophenone, no e.e. was recorded, possibly because the catalytically active species had no chiral environment at the metal centre. No other reactions recorded catalytic activity, although the ROMP of norbornylene was successful with TMS-diazomethane as an initiator.

Stoichiometric transformations of complex **27** were undertaken: although the phenylacetylide complex could not be isolated, displacement of the PPh_3 ligand was successful. X-ray structures of the displacement products indicated that phosphine displacement went *via* a dissociative mechanism.

3.8 – Future Work

Although the overall lack of catalytic activity is a big disappointment, the transfer hydrogenation result is encouraging. Work is ongoing into amine analogues of rhodium and ruthenium complexes **22** and **27**, which would be a much closer analogue of the known transfer hydrogenation catalysts (Figure 15).

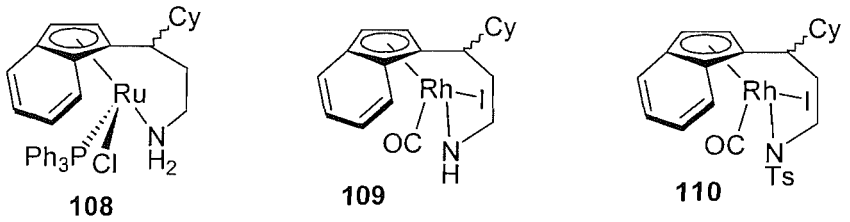

108 **109** **110**

Figure 15

Increasing the Lewis acidity of the ruthenium complexes might result in an active catalyst for the Diels-Alder reaction, as might performing an oxidative addition on rhodium complex **22**. The positive result gained from the ROMP of norbornylene indicates that olefin metathesis may also be achievable with suitable modification of **27**.

4.0: EXPERIMENTAL

INSTRUMENTATION AND EXPERIMENTAL TECHNIQUES

Unless otherwise stated, all reactions and manipulations involving organometallic complexes were carried out under an argon atmosphere using standard Schlenk, syringe and vacuum line techniques. Reaction flasks, syringes and needles were dried in a hot oven (>160 °C) for 12 hours prior to use and allowed to cool in a sealed desiccator over silica gel.

Unless otherwise indicated, materials were obtained from commercial sources and used without further purification. Specific purifications were carried out according to standard methods.[85] ^{n}Butyllithium was purchased from Aldrich as a 2.5 M solution in hexanes. Potassium diphenylphosphide (0.5 M solution in THF) was purchased from Aldrich. OsO_4 was purchased as a solid from Aldrich and made up into a 0.04 M solution in ^{t}BuOH, stabilised with 2 mol% ^{t}BuOOH.

Diethyl ether, THF, benzene and toluene were freshly distilled from dark purple solutions of sodium/benzophenone ketyl under an argon atmosphere. Chlorinated solvents, TEA, diethylamine and HMPA were distilled from, and stored over, CaH_2. Petrol refers to the fraction of petroleum ether which boils between 40°C and 60°C.

$[Rh\text{-}\mu Cl(CO)_2]_2$[86] and $[Rh\text{-}\mu Cl(COD)]_2$[87] were synthesised from $RhCl_3{\cdot}3H_2O$ according to literature procedures in 75% and 77% yield respectively. All other rhodium sources were obtained commercially. $RuCl_2(PPh_3)_3$ was synthesised from $RuCl_3{\cdot}2.5H_2O$ according to a literature procedure in 96% yield.[88] Borane complexes of di- and tri-phenylphosphine were obtained by reacting a solution of the free phosphine in THF with DMS-borane in 88% and 94% yield respectively after recrystallisation from Et_2O.[75]

Proton nuclear magnetic resonance (^{1}H NMR), carbon-13 nuclear magnetic resonance ($^{13}C\{^{1}H\}$ NMR) spectra, phosphorus-31 ($^{31}P\{^{1}H\}$ NMR) spectra and fluorine-19 ($^{19}F\{^{1}H\}$ NMR) spectra were recorded on Bruker AM300, AC300, AV300 or DPX400 spectrometers.

NMR spectra of organic compounds were recorded using $CDCl_3$ as the solvent, stored over anhydrous K_2CO_3. Unless otherwise stated, the NMR spectra of organometallic compounds were recorded in C_6D_6, stored over 4Å molecular sieves. Coupling constants (*J*) are expressed in Hertz (Hz), approximated to the nearest 0.5Hz. Chemical shifts are quoted in parts per million (δ) downfield from tetramethylsilane and are referenced to the residual solvent signal.[89] $^{31}P\{^1H\}$ and $^{19}F\{^1H\}$ spectra were referenced to external H_3PO_4 and $CFCl_3$ standards respectively.

When reporting splitting patterns, the following abbreviations are used: (s) singlet, (d) doublet, (t) triplet, (q) quartet, (m) multiplet, (br) broad and (fs) fine splitting. ^{13}C spectra are reported as C, CH, CH_2 and CH_3 depending on the number of attached protons (0, 1, 2, 3 respectively); this being determined by DEPT experiments. 2D COSY spectra (H-H and H-C correlation) were routinely used to conclusively assign signals from ^1H and ^{13}C spectra and have not been specifically documented.

Thin layer chromatography (TLC) was performed using aluminium plates coated with Merck 60H-F_{254} silica gel, except for organometallic compounds when Polygram Alox N/UV_{254} plates coated in 0.2mm Al_2O_3 was used. TLC was used both to monitor the progress of reactions and to assess the purity of compounds. Visualisation of compounds was achieved by illumination under ultra-violet light (254nm), by the use of sulphuric acid stain (5% w/v in MeOH) or by iodine (SiO_2). Column chromatography of organic compounds was performed on silica 60 (230-400 mesh) under slight positive pressure and column chromatography of organometallic compounds was performed on Al_2O_3 (neutral, commercial Brockman grade I deactivated with 6% w/v water), under argon if necessary.

Mass spectra, including accurate masses, were recorded on a VG Analytical 70-250-SE double focussing mass spectrometer using Electron Impact (EI) at 70eV in DCM. Electrospray (ES^+) were recorded on a VG Platform quadropole spectrometer in acetonitrile. M/z signals are reported as values in atomic mass units followed by the peak intensity relative to the base peak. All ruthenium compounds showed the expected ruthenium isotope pattern.

Infra-red spectra were recorded on a Perkin Elmer 1600 FT-IR spectrometer as films between NaCl plates or as a powder. Absorptions are given in wavenumbers (cm^{-1}) and peaks are described as 's' (strong), 'm' (medium), 'w' (weak) and may be compounded by 'br' (broad).

Optical rotations were measured in an AA-100 Polarimeter (Optical Activity Ltd.).

Elemental analyses were performed by MEDAC Ltd., Egham, Surrey.

Melting points were determined on a Kofler hotstage.

Gas chromatography was carried out on a Hewlett Packard 6890 system with autosampler, passing through a 30 m 5% phenyl methyl siloxane column with He as the carrier gas.

- Method A: 80-250 °C at 25 °C/min, then held at 250 °C for 4.2 minutes
- Method B: 40 °C for 2 minutes, then 40-100 °C at 10 °C/min, then 25 °C/min to 200 °C
- Method C: 60 °C for 2 minutes, then 60-130 °C at 10 °C/min, then 25 °C/min to 180 °C, hold 2 minutes

Chiral GC was carried out on a Hewlett Packard 6890 system with autosampler, passing through a 25 m FS-Hydrodex β-3p column.

- Method D: 110 °C for 20 minutes, then to 150 °C at 10 °C/min, hold 2 minutes

***Rac*-1-cyclohexyl-1,2-dibromoethane (83)**[90]

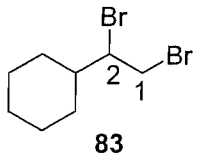

83

A solution of bromine (5.1 mL, 99.8 mmol) in DCM (50 mL) was dropped into a solution of vinylcyclohexane (12.4 mL, 91.0 mmol) in DCM (100 mL), gradually forming a pale yellow solution. When the solution turned permanently deep yellow, one drop of vinylcyclohexane was then added, returning the solution to a pale yellow colour. Solvents were removed *in vacuo* and the crude yellow oil was Kugelrohr distilled at 140°C (1.0 mmHg), affording 23.52 g (96% yield) of the title compound as a pale yellow oil. Compound data was identical to that in the literature.[90]

δ_H (300 MHz, $CDCl_3$): 4.17 (1H, ddd, J = 9.0, 5.0, 3.5 Hz, H2), 3.72-3.87 (2H, m, H1), 1.56-1.93 (6H, m, Cy), 1.08-1.44 (5H, m, Cy) ppm.

***Rac*-Spiro-[(2-cyclohexylcyclopropane)-1,1'-indene] (76)**[17]

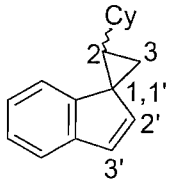

76

A solution of indene (5.8 mL, 50.0 mmol) in THF (50 mL) was cooled to -78 °C and ^{n}BuLi (15.8 mL of a 2.5 M solution in hexanes, 39.4 mmol) was added dropwise in the dark. The solution was stirred at -78 °C for 15 minutes, then warmed to RT and stirred for 90 minutes. After this time, the solution was cooled to 0 °C and a solution of dibromide **83** (4.42 g, 16.40 mmol) in THF (25 mL) was added dropwise over 2 minutes. The solution was stirred at 0°C for 15 minutes then warmed to RT overnight.

After 20 hours, TLC showed no dibromide remaining, so the reaction was quenched with water (50 mL), diluted with Et_2O (50 mL) and more water (50 mL). The aqueous layer was extracted into Et_2O (3 * 30 mL), then the combined organic layers were washed with satd. $NaHCO_3$ solution (50 mL), dried ($MgSO_4$) and concentrated *in vacuo*. The resulting dark brown liquid was purified by flash chromatography (100% petrol), yielding the title

compound contaminated by a small amount of indene. The indene was removed by evaporation under vacuum (1.0 mmHg) for 8 hours at RT, affording 3.64 g of the title compound in 99% yield as a clear oil in a 1:1 mixture of diastereoisomers. Compound data was identical to that in the literature.[17]

δ_H (300 MHz, $CDCl_3$): 7.00-7.40 (4H, m, indene Ar), 6.96 (½H, d, J = 6.0 Hz, H2' of diastereoisomer 1), 6.82 (½H, d, J = 6.0 Hz, H2' of diastereoisomer 2), 6.42 (½H, d, J = 6.0 Hz, H3' of diastereoisomer 1), 6.17 (½H, d, J = 6.0 Hz, H3' of diastereoisomer 2), 1.94-2.03 (1H, m, Cy), 1.00-1.87 (10H, m, Cy), 0.80-1.00 (3H, m, H2 + H3) ppm.
GC R_T (Method A): 6.32 mins

***Rac*-2-cyclohexyl-2-(3'*H*-1'-indenyl)ethyl diphenylphosphine (31)**[17]

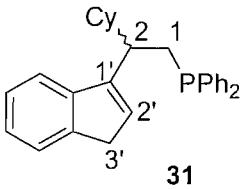

31

To a solution of spirocycle **76** (1.23 g, 5.50 mmol) and 18-crown-6 (29 mg, 2 mol%) in THF (40 mL) at 0 °C was added $KPPh_2$ (11.00 mL of a 0.5 M solution in THF, 5.50 mmol). The solution was stirred at 0 °C for 15 minutes then at RT for 60 hours.

After 60 hours, G.C. showed no spirocycle starting material remaining (Method A), so the reaction was quenched with degassed EtOH (10 mL) and approximately half the solvents were removed *via* vacuum transfer under an Ar atmosphere. The remainder was filtered through a 3 cm plug of silica, washing through with THF (3 * 10 mL) and concentrated by vacuum transfer. The resulting yellow oil was purified by flash chromatography under slight argon pressure (100% hexane then 97:3 hexane:EtOAc) affording 345 mg of the title compound as a cloudy, air-sensitive oil in 15% yield. Compound data was identical to that in the literature.[17]

δ_H (300 MHz, $CDCl_3$): 7.56-7.64 (2H, m, Ar), 7.31-7.44 (6H, m, Ar), 7.00-7.26 (6H, m, Ar), 5.94 (1H, br s, H1'), 3.12-3.24 (1H, m, H2), 2.69-2.93 (3H, m, H2' + H1) 2.52-2.62 (1H, ddd, J = 13.5, 10.0, 2.0 Hz, H1), 0.83-1.79 (11H, m, Cy) ppm.
δ_P (121.5 MHz, $CDCl_3$): -17.9 (s) ppm.

***Rac*-[2-cyclohexyl-2-(3'*H*-1'-indenyl)ethyl]diphenylphosphine oxide (84)**

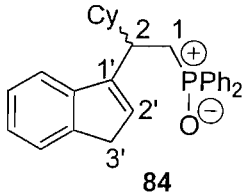

84

To a solution of crude phosphine **31** (max. 9 mmol) in DCM (20 mL) was added H_2O_2 (0.90 mL of a 35% w/w solution in water, 9 mmol). After 5 minutes, TLC showed no free phosphine present, so the aqueous layer was extracted into DCM (3 * 10 mL) and the combined organic layers were washed with brine, dried (Na_2CO_3), filtered and concentrated *in vacuo*. The resulting yellow liquid was purified by flash chromatography (100% Et_2O), yielding a white solid which was recrystallised from Et_2O, yielding 803 mg of the title compound as a white, air-stable solid in 21% yield.

MP: 130-132 °C

δ_H (300 MHz, $CDCl_3$): 7.56-7.64 (2H, m, Ar), 7.00-7.44 (12H, m, Ar), 5.94 (1H, br s, H-2'), 3.12-3.24 (1H, m, H-2), 2.52-2.93 (4H, m, H-3' + H-1), 0.83-1.79 (11H, m, Cy) ppm.

δ_C (75.5 MHz, $CDCl_3$): 131.81, 131.67, 131.22, 131.20, 131.12, 131.03, 130.91, 130.82, 129.16, 128.94, 128.83, 128.08, 127.96, 127.05, 126.03, 124.67, 124.04, 120.40, 42.50, 38.55, 37.83, 33.51, 31.60, 31.53, 30.94, 26.86, 26.79 ppm.

δ_P (121.5 MHz, $CDCl_3$): 31.20 (s) ppm.

IR (NaCl, thin film): 3051 (m), 2984 (w), 2305 (w), 1421 (m), 1265 (s), 896 (m), 739 (s) cm^{-1}

LRMS (EI^+): m/z = 427.3 ($[M+H]^+$, 82%), 490.3 (44), 528.4 (100), 875.3 (47)

HRMS (ES^+): submitted, awaiting analysis

Lithium diphenylphosphide-borane[81]

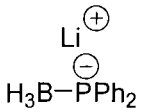

Method i: To a solution of triphenylphosphine-borane complex (450 mg, 1.63 mmol) in THF (5 mL) was added, under a counterflow of argon, very small pieces of lithium metal (24.80 mg, 3.59 mmol), which was stirred overnight. After 16 hours, there was very little lithium remaining and the solution had turned deep orange, so the liquid was transferred to a flask

containing ^{t}BuCl (0.2 mL, 1.6 mmol) and refluxed for 5 minutes. The resulting yellow solution was used without further purification.

Method ii: ^{n}BuLi (0.9 mL of a 2.5 M solution in hexanes, 2.25 mmol) was added dropwise to a solution of diphenylphosphine-borane complex (400 mg, 2.00 mmol) in THF (5 mL) at 0 °C, until the solution was permanently yellow. The solution was stirred at RT for 15 minutes and then used without further purification.

<u>*Rac*-[2-cyclohexyl-2-(3'*H*-1'-indenyl)ethyl]diphenylphosphine-borane (85)</u>[17]

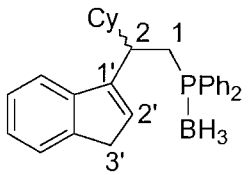

85

Method i: To a solution of $LiPPh_2$-BH_3 in THF at 0 °C was added HMPA (0.2 mL, 1.0 mmol) and a solution of spirocycle **76** (224 mg, 1.0 mmol) in THF (1 mL). The solution was stirred at 0 °C for 15 minutes then at RT for 60 hours. After this time, the reaction was quenched by the addition of ice-water (5 mL) and then extracted into EtOAc (3 * 5 mL). The combined organic layers were washed with brine (5 mL), dried ($MgSO_4$) and concentrated *in vacuo*. The resulting dark green liquid was then purified by flash chromatography (9:1 petrol:EtOAc), affording 55 mg of the title compound in 16% yield as a white solid.

Method ii: To a solution of spirocycle **76** (1.50 g, 6.69 mmol) and 18-crown-6 (35 mg, 2 mol%) in THF (30 mL) at 0°C, was added $KPPh_2$ (14.7 mL of a 0.5 M solution in THF, 7.35 mmol) dropwise. The reaction was stirred at 0°C for 15 minutes then at RT for 60 hours. After this time, the reaction was quenched with water (0.15 mL, 8.3 mmol) and DMS-borane (3.0 mL, 30.0 mmol) was added dropwise. The reaction was stirred at 0 °C for 1 hour, after which time no starting material remained by TLC. The reaction was quenched by the addition of ice-water (25 mL) and then extracted into EtOAc (3 * 25 mL). The combined organic layers were washed with brine (25 mL), dried ($MgSO_4$) and concentrated *in vacuo*. The resulting dark green liquid was then purified by flash chromatography (9:1 petrol:EtOAc), affording 2.59 g of the title compound in 91% yield as a white solid. Compound data was identical to that in the literature.[17]

MP: 123-125 °C (EtOAc) (Lit. 124-126 °C)[17]

δ_H (300 MHz, $CDCl_3$): 7.00-7.64 (14H, m, Ar), 5.94 (1H, br s, H2'), 3.12-3.24 (1H, dddd, *J* = 13.0, 10.0, 7.5, 2.5 Hz, H2), 2.69-2.93 (3H, m, H2' + H1) 2.52-2.62 (1H, ddd, *J* = 14.0, 9.5, 3.0 Hz, H1), 1.88 (3H, s, BH_3), 0.83-1.79 (11H, m, Cy) ppm.

δ_P (121.5 MHz, $CDCl_3$):-16.94 (d, *J* = 60.5 Hz) ppm.

***Rac*-(η^5:η^1-indenyl-CH(Cy)-CH_2PPh_2)Rh(CO) (22)**[17]

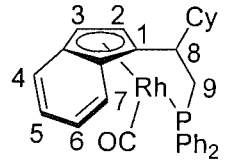

22

Phosphine-borane complex **85** (200 mg, 0.47 mmol) was dissolved in $HNEt_2$ (5 mL) and refluxed for 3 hours. After 3 hours, TLC showed phosphine-borane was still present, so the $HNEt_2$ was removed *in vacuo* and fresh $HNEt_2$ (5 mL) was added. The reaction was refluxed overnight and TLC now showed no sign of phosphine-borane. $HNEt_2$ was removed *in vacuo* and the resultant phosphine (yellow oil) was dissolved in THF (10 mL) and cooled to -78 °C. ^{n}BuLi (0.2 mL of a 2.5 M solution in hexanes, 0.5 mmol) was added dropwise in the dark, the reaction was stirred at -78 °C for 15 minutes then for 2 hours at RT.

After this time, the solution was cooled to -78 °C and added dropwise to a solution of $[RhCl(CO)_2]_2$ (88 mg, 0.20 mmol) in THF (10 mL) at -78 °C. The reaction was stirred at -78 °C for 15 minutes then overnight at RT. After this time, solvents were removed *in vacuo* and the product purified by flash chromatography (3:7 toluene:petrol → 100% toluene) on alumina under slight argon pressure, affording 41 mg of the title compound in 18% yield as a yellow powder. Compound data was identical to that in the literature.[17]

MP: decomposes 165 °C (diffusion of hexane into an Et_2O solution) (Lit. 168 °C (dec.))[17]

δ_H (300 MHz, C_6D_6): 7.55-7.79 (4H, m, Ar), 7.19-7.35 (5H, m, Ar), 7.05-7.15 (4H, m, Ar), 6.99 (1H, d, *J* = 7.5 Hz, Ar), 6.22 (1H, dd, *J* = 3.0, 3.0 Hz, H3), 6.14 (1H, dd, *J* = 3.0, 2.5 Hz, H2), 3.28 (1H, dddd, *J* = 13.5, 13.5, 4.5, 2.5 Hz, H9), 2.95 (1H, ddd, *J* = 13.5, 13.5, 7.0 Hz, H9), 2.59 (1H, dddd, *J* = 13.5, 9.0, 4.5, 4.5 Hz, H8), 0.77-1.72 (11H, m, Cy) ppm.

δ_P (121.5 MHz, C_6D_6): 57.19 (d, *J* = 212 Hz), 53.66 (d, *J* = 212 Hz) ppm.

***Rac*-(η^5:η^1-indenyl-CH(Cy)-CH_2PPh_2)RuCl(PPh_3) (27)**[17]

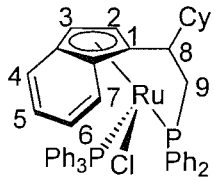

27

Phosphine-borane complex **85** (2.12 g, 4.24 mmol) was dissolved in $HNEt_2$ (20 mL) and refluxed for 3 hours. TLC showed phosphine-borane still remaining, so the $HNEt_2$ was removed *in vacuo* and fresh $HNEt_2$ added (20 mL). The reaction was refluxed overnight and TLC now showed no sign of phosphine-borane. $HNEt_2$ was removed *in vacuo* and the resultant phosphine (pale yellow oil) was dissolved in toluene (20 mL) and cooled to -78 °C. ^{n}BuLi (1.7 mL of a 2.5 M solution in hexanes, 4.24 mmol) was added dropwise with the exclusion of light, the reaction was stirred at -78 °C for 15 minutes and then for 2 hours at room temperature.

After 2 hours, the solution was cooled to -78 °C and added dropwise to a suspension of $RuCl_2(PPh_3)_3$ (4.07 g, 4.24 mmol) in toluene (60 mL) at -78 °C. The reaction was stirred at -78 °C for 15 minutes then gently warmed to reflux overnight. After this time, the solvents were removed *in vacuo* and the product purified by flash chromatography (4:6 Et_2O:petrol → 100% Et_2O) on alumina, affording 2.42 g of the title compound in 71% yield as a brown powder and a single metal-centred diastereoisomer. Compound data was identical to that in the literature.[17]

MP: 165-166 °C (diffusion of pentane into a benzene solution) (Lit. 165-167 °C)[17]

δ_H (300 MHz, C_6D_6): 8.19 (2H, 2d, J = 9.0, 10.0Hz, Ar), 7.74 (5H, br m, Ar), 7.04-7.34 (8H, m, Ar), 6.87-6.98 (11H, m, Ar), 6.75 (1H, t + fs, J = 7.0Hz, Ar), 6.62 (2H, t + fs, J = 7.0Hz, Ar), 4.94 (1H, d, J = 1.0 Hz, H3), 3.36 (1H, ddd, J = 16.0, 12.0, 4.5 Hz, H9), 2.72 (1H, ddd, J = 16.0, 12.0, 4.5 Hz, H9), 2.27-2.39 (1H, dddd, J = 13.0, 8.5, 4.5, 4.5 Hz, H8), 2.13 (1H, s+fs, H2), 1.21-1.64 (5H, m, Cy), 0.79-0.91 (6H, m, Cy) ppm.

δ_P (121.5 MHz, C_6D_6): 47.90 (d, J = 26.5 Hz), 38.91 (d, J = 26.5 Hz) ppm.

***Rac*-[(η^5:η^1-indenyl-CH(Cy)-CH_2PPh_2)Ru(MeCN)(PPh_3)]$^+$[PF_6]$^-$ (80)**

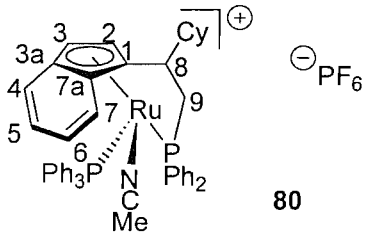

80

Indenyl ruthenium complex **27** (2.00 g, 2.47 mmol) and NH_4PF_6 (484 mg, 2.97 mmol) were dissolved in dry MeCN (100 mL) and refluxed for 16 hours. After this time, the solution was cooled, filtered through celite and concentrated *in vacuo*, yielding a red solid. The product was recrystallised from a slow diffusion of Et_2O into an acetonitrile solution, affording 2.31 g of the title compound in 98% yield as a dark red crystalline solid. The X-ray structure has been obtained (see Appendix II).

MP: decomposes 200 °C

δ_H (300 MHz, CD_3CN): 7.22-7.45 (13H, m, Ar), 6.94-7.14 (13H, m, Ar), 6.86 (2H, td, J = 8.0, 2.0 Hz, Ar), 6.76 (1H, d+fs, J = 8.5 Hz, Ar), 5.11 (1H, d, J = 2.0 Hz, H3), 4.26 (1H, d, J = 2.0 Hz, H2), 3.50 (1H, td, J = 13.5, 5.0 Hz, H9), 3.05 (1H, td, J = 13.5, 5.0 Hz, H9), 2.72-2.85 (1H, m, H8), 1.79-1.91 (2H, m, Cy), 1.40-1.71 (7H, m, Cy + CH_3CN), 0.79-1.23 (5H, m, Cy) ppm.

δ_C (75.5 MHz, CD_3CN): 134.83 (3C, d, J = 43.5 Hz, ^{i}Ph (PPh_3)), 134.53 (2C, d, J = 37.5Hz, ^{i}Ph (PPh_2)), 132.81 (6CH, d, J = 11.0 Hz, ^{o}Ph (PPh_3)), 131.90 (2CH, d, J = 10.0 Hz, ^{o}Ph (PPh_2)), 131.67 (2CH, d, J = 10.0 Hz, ^{o}Ph (PPh_2)), 129.87 (CH, s, C4/7), *129.21 (CH, Ar), *128.23 (CH, Ar), *128.15 (CH, Ar), *128.02 (CH, Ar), *127.71 (CH, Ar), *127.58 (CH, Ar), 126.07 (CH, C5/6), 124.73 (CH, C5/6), 121.61 (CH, C4/7), 117.01 (C, CH_3CN), 109.96 (C, s+fs, C3a), 100.27 (C, d, J = 7.0 Hz, C7a), 95.11 (C, d, J = 8.0 Hz, C1), 80.15 (CH, C3), 64.72 (CH, C2), 50.30 (CH_2, d, J = 7.0 Hz, C9), 42.03 (CH, d, J = 20.0 Hz, C8), 38.91 (CH, s, Cy), 32.62 (CH_2, s, Cy), 30.55 (CH_2, s, Cy), 25.70 (CH_2, s, Cy), 25.48 (CH_2, s, Cy), 25.42 (CH_2, s, Cy), 3.25 (CH_3, s, CH_3CN) ppm.

δ_P (121.5 MHz, CD_3CN): 49.85 (d, J = 25.2 Hz), 47.68 (d, J = 25.0 Hz) ppm.

δ_F (282.4 MHz, CD_3CN): -72.88 (d, J = 708.0 Hz) ppm.

IR (NaCl, thin film): 3049 (m), 2917 (s), 2851 (w), 2368 (m), 1484 (s), 1434 (s), 1093 (w), 838(m), 746 (w), 696 (s) cm^{-1}

LRMS (ES^+): m/z = 773.5 ((M-MeCN-PF_6)$^+$, 100%)

HRMS (ES^+): (M-MeCN-PF_6)$^+$ $C_{47}H_{45}P_2Ru$ requires *m/z* = 773.2034 found 773.2031

Anal. Calc'd for $C_{49}H_{48}NP_3F_6Ru$: C, 61,38; H, 5.05; N, 1.46. Found: C, 61.20; H, 4.97; N, 1.56.

* = Unable to assign signals, determine integrals and *J* values due to overlapping peaks.

Rac-(η^5:η^1-(4,5,6,7-tetrahydroindenyl)CH(Cy)-CH_2PPh_2)RuCl(PPh_3) (81)[17]

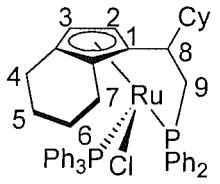

81

A solution of indenyl ruthenium complex **27** (172 mg, 0.21 mmol) in DME (10 mL) was injected into an argon-filled stainless-steel hydrogenation bomb containing PtO_2 (5.0 mg, 10 mol%). The bomb was purged with H_2, then pressurised to 1600psi, heated to 65 °C and stirred for 2½ days. After this time, the bomb was cooled, depressurised and the contents filtered through celite. Solvent was removed *in vacuo* and the resultant yellow-brown solid was purified by flash chromatography (Al_2O_3, 4:6 Et_2O:petrol → 100% Et_2O), affording 99 mg of the title compound as a yellow solid in 57% yield.

Crystals were obtained by slow diffusion of pentane into a benzene solution of the complex and an X-ray of the structure was obtained (Appendix III). Compound data was identical to that in the literature.[17]

MP: 158-159 °C (Lit. 157-159 °C)[17]

δ_H (300 MHz, C_6D_6): 78.67 (2H, dd, *J* = 10.0, 8.5 Hz, Ar), 7.67-7.91 (5H, br s, Ar), 7.38 (2H, t, *J* = 7.0 Hz, Ar), 7.19-7.26 (3H, m, Ar), 7.01-7.13 (10H, br s, Ar), 6.87 (1H, t+fs, *J* = 7.5 Hz, Ar), 6.76 (2H, td, *J* = 7.5, 1.5 Hz, Ar), 4.53 (1H, d, *J* = 1.5 Hz, H3), 3.39 (1H, ddd, *J* = 12.0, 12.0, 5.0 Hz, H9), 3.28 (1H, ddd, *J* = 11.0, 11.0, 5.5 Hz, H4/5/6/7), 2.70 (1H, ddd, *J* = 12.0, 12.0, 5.0 Hz, H9), 2.68-2.76 (2H, m, H4/5/6/7), 2.47-2.55 (1H, m, H4/5/6/7), 2.39 (1H, d, *J* = 2.0 Hz, H2), 2.28-2.39 (2H, m, H4/5/6/7), 2.05 (1H, ddd, *J* = 13.5, 9.0, 4.5 Hz, H8), 0.70-1.92 (13H, m, Cy + H4/5/6/7) ppm.

δ_P (121.5 MHz, C_6D_6): 43.27 (d, *J* = 39.2 Hz), 36.72 (d, *J* = 39.2 Hz) ppm.

***Rac*-[(η^5:η^1-(4,5,6,7-tetrahydroindenyl)CH(Cy)-CH_2PPh_2)RuCl(PPh_3)]$^+$[PF6]$^-$ (82)**

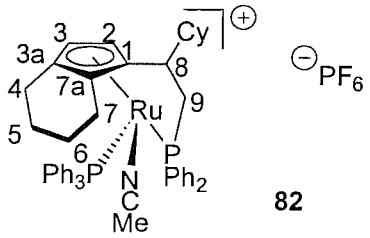

82

Ruthenium complex **81** (110 mg, 0.14 mmol) and NH_4PF_6 (27 mg, 0.16 mmol) were dissolved in dry MeCN (10 mL) and refluxed for 16 hours. After this time, the solution was cooled, filtered through celite and concentrated *in vacuo*, yielding an orange solid. The product was crystallised from slow diffusion of Et_2O into an acetonitrile solution, affording 110 mg of the title compound in 61% yield as an orange crystalline solid. The X-ray structure has been obtained (see Appendix IV).

MP: decomposes 195 °C

δ_H (300 MHz, CD_3CN): 7.28-7.54 (15H, m, Ar), 6.86-7.17 (10H, m, Ar), 4.51 (1H, d, J = 2.0 Hz, H3), 4.20 (1H, d, J = 2.0 Hz, H2), 3.46 (1H, td, J = 6.0, 14.0 Hz, H9), 2.94 (1H, td, J = 6.0, 14.0 Hz, H8), 1.84-2.38 (11H, m, H9 + CH_3CN + Cy + H4/5/6/7), 1.47-1.78 (7H, m, Cy + H4/5/6/7), 0.92-1.26 (5H, m, Cy) ppm.

δ_C (75.5 MHz, CD_3CN): 136.66 (3C, d, J = 40.0 Hz, ^{i}Ph (PPh_3)), 136.25 (2C, d, J = 42.0 Hz, ^{i}Ph (PPh_2)), 134.88 (6C, d, J = 11.5 Hz, ^{o}Ph (PPh_3)), 133.79 (2C, d, J = 10.0 Hz, ^{o}Ph (PPh_2)), 133.58 (2C, d, J = 10.0 Hz, ^{o}Ph (PPh_2)), *130.99 (CH, Ar), *130.49 (CH, Ar), *130.37 (CH, Ar), *130.22 (CH, Ar), *130.10 (CH, Ar), *129.72 (CH, Ar), *129.59 (CH, Ar), 119.09 (C, CH_3CN), 97.32 (C, s+fs, C3a), 96.02 (C, s+fs, C7a), 95.73 (C, s, C1), 86.02 (CH, s, C3), 59.41 (CH, s, C2), 52.06 (CH_2, d, J = 33.0 Hz, C9), 43.98 (CH, d, J = 18.5 Hz, C8), 39.85 (CH, s, Cy), 34.17 (CH_2, s, Cy/C4/5/6/7), 32.38 (CH_2, s, Cy/C4/5/6/7), 27.44 (CH_2, s, Cy/C4/5/6/7), 27.28 (CH_2, s, Cy/C4/5/6/7), 27.13 (CH_2, s, Cy/C4/5/6/7), 23.91 (CH_2, s, Cy/C4/5/6/7), 23.74 (CH_2, s, Cy/C4/5/6/7), 23.00 (CH_2, s, Cy/C4/5/6/7), 22.39 (CH_2, s, Cy/C4/5/6/7), 2.10 (CH_3, s, CH_3CN) ppm.

δ_P (121.5 MHz, CD_3CN): 43.58 (d, J = 34.1 Hz), 50.04 (d, J = 34.1 Hz) ppm.

δ_F (282.4 MHz, CD_3CN): -72.27 (d, J = 706.0 Hz) ppm.

IR (NaCl, thin film): 3055 (s), 2987 (s), 2306 (s), 1422 (m), 1265 (w), 896 (s), 846 (w), 739 (m) cm^{-1}

LRMS (ES^+): m/z = 777.5 ($(M\text{-}MeCN\text{-}PF_6)^+$, 100%)

HRMS (ES^+): $(M\text{-}PF_6)^+$ $C_{49}H_{52}NP_2Ru$ requires *m/z* = 818.2613 found 818.2638

Anal. Calc'd for $C_{49}H_{52}NP_3F_6Ru$: C, 61.12; H, 5.44; N, 1.45. Found: C, 60.90; H, 5.48; N, 1.54.

* = Unable to assign signals, determine integrals and *J* values due to overlapping peaks.

***Rac*-(η^5:η^1-indenyl-CH(Cy)-CH_2PPh_2)RuCl(P^nBu_3) (111)**

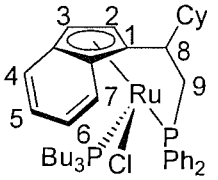

111

To a solution of ruthenium complex **27** (100 mg, 0.12 mmol) in toluene (10 mL) was added tributylphosphine (0.1 mL, 0.37 mmol) and the solution was refluxed for 16 hours. After this time, solvents were removed *in vacuo* and the resulting solid purified by flash chromatography (Al_2O_3, 4:6 Et_2O:petrol → 100% Et_2O) affording 65 mg of the title compound as a brown solid in 70% yield. The compound was recrystallised by slow diffusion of Et_2O into a C_6H_6 solution.

MP: 194-195 °C

δ_H (300 MHz, C_6D_6): 8.24 (2H, s + fs, Ar), 7.56 (2H, s + fs, Ar), 7.21-7.43 (5H, m, Ar), 6.94-7.09 (5H, m, Ar), 5.25 (1H, s, H3), 3.65-3.76 (2H, m, H2 + H9), 2.92 (1H, dd + fs, *J* = 12.5, 13.0 Hz, H9), 2.45 (1H, br s, H8), 1.91-2.04 (3H, m, Cy), 1.66-1.76 (2H, m, Cy), 1.47-1.62 (8H, m, P-CH_2 + Cy), 1.29-1.43 (12H, m, CH_2 (^{n}Bu)), 0.97-1.05 (11H, CH_3 (^{n}Bu) + Cy), 0.69-0.91 (2H, m, Cy) ppm.

δ_C (75.5 MHz, C_6D_6): 143.01 (2C, d, *J* = 26.0 Hz, ^{i}Ph), 135.49 (4CH, d, *J* = 10.0 Hz, ^{o}Ph), 132.10 (4CH, d, *J* = 8.0 Hz, ^{m}Ph), 129.03 (CH, s, C4/5/6/7), 128.86 (CH, s, C4/5/6/7), 128.42 (2CH, d, *J* = 9.0 Hz, ^{p}Ph), 122.38 (CH, s, C4/5/6/7), 121.68 (CH, s, C4/5/6/7), 110.64 (C, s, C3a/7a), 103.12 (C, s, C3a/7a), 95.28 (C, d, *J* = 10.0 Hz, C1), 70.47 (CH, d, *J* = 10.0 Hz, C3), 63.28 (CH, s, C2), 52.60 (CH_2, d, *J* = 33.0 Hz, C9), 43.46 (CH, d, *J* = 18.5 Hz, C8), 37.58 (CH, s, Cy), 33.90 (CH_2, s, Cy), 31.81 (CH_2, s, Cy), 28.88 ($3CH_2$, d, *J* = 24.0 Hz, Bu), 27.20 ($3CH_2$, s, Bu), 27.03 (CH_2, s, Cy), 26.81 (CH_2, s, Cy), 26.65 (CH_2, s, Cy), 25.30 ($3CH_2$, d, *J* = 12.5 Hz, Bu), 14.59 ($3CH_3$, s, Bu) ppm.

δ_P (121.5 MHz, C_6D_6): 33.15 (d, *J* = 31.0 Hz), 38.43 (d, *J* = 31.0 Hz) ppm.

IR (Powder): 3049 (w), 2916 (m), 2851 (m), 1586 (w), 1483 (w), 1433 (s), 1184 (w), 1093 (s), 884 (s), 737 (s), 719 (s) cm^{-1}

LRMS (ES$^+$): m/z = 748.5 (M^+, 100%)

HRMS (ES$^+$): $(M)^+$ $C_{41}H_{57}ClP_2Ru$ requires *m/z* = 748.2663 found 748.2658

Anal. Calc'd for $C_{41}H_{57}ClP_2Ru$: C, 65.80; H, 7.68. Found: C, 65.75; H, 7.72.

***Rac*-(η^5:η^1-indenyl-CH(Cy)-CH_2PPh_2)RuCl($PMePh_2$) (112)**

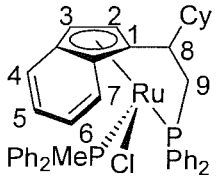

112

To a solution of ruthenium complex **27** (100 mg, 0.12 mmol) in toluene (10 mL) was added methyldiphenylphosphine (0.1 mL, 0.37 mmol) and the solution was refluxed for 16 hours. After this time, solvents were removed *in vacuo* and the resulting solid purified by flash chromatography (Al_2O_3, 4:6 Et_2O:petrol → 100% Et_2O) affording 87 mg of the title compound as a brown solid in 94% yield. The compound was recrystallised by slow diffusion of Et_2O into a C_6H_6 solution and the X-ray structure has been obtained (Appendix V).

MP: decomposes 225-226 °C

δ_H (300 MHz, C_6D_6): 7.98 (4H, ddd, *J* = 27.5, 9.0, 7.0 Hz, Ar), 6.75-7.28 (20H, m, Ar), 4.83 (1H, s, H3), 3.14-3.24 (1H, m, H8), 3.03 (1H, s, H2), 2.16 (2H, d, *J* = 7.0 Hz, H9), 1.17-1.46 (8H, m, Cy), 0.72-0.96 (4H, m, Cy + CH_3), 0.38-0.58 (2H, m, Cy) ppm.

δ_C (75.5 MHz, C_6D_6): 143.02 (C, d, *J* = 40.0 Hz, ^{i}Ph), 141.85 (C, d, *J* = 43.5 Hz, ^{i}Ph), 140.97 (C, d, *J* = 29.0 Hz, ^{i}Ph), 139.47 (C, d, *J* = 26.0 Hz, ^{i}Ph), 134.08 (4CH, d, *J* = 10.0 Hz, ^{o}Ph), 133.00 (4CH, d, *J* = 11.0 Hz, ^{o}Ph), 130.76 (4CH, d, *J* = 9.0 Hz, ^{m}Ph), 130.47 (4CH, d, *J* = 9.0 Hz, ^{m}Ph), 128.75 (2CH, d, *J* = 10.5 Hz, ^{p}Ph), 128.30 (CH, s, C4/5/6/7), 127.73 (2CH, d, *J* = 7.0 Hz, ^{p}Ph), 127.51 (CH, s, C4/5/6/7), 121.81 (CH, s, C4/5/6/7), 120.53 (CH, s, C4/5/6/7), 107.54 (C, s, C3a/7a), 103.32 (C, s, C3a/7a), 93.52 (C, d, *J* = 11.0 Hz, C1), 73.01 (CH, s, C3), 65.93 (CH, s, C2), 51.02 (CH_2, d, *J* = 33.0 Hz, C9), 42.95 (CH, d, *J* = 19.0 Hz, C8), 37.74 (CH, s, Cy), 33.80 (CH_2, s, Cy), 31.67 (CH_2, s, Cy), 26.82 (CH_2, s, Cy), 26.62 (CH_2, s, Cy), 26.52 (CH_2, s, Cy), 15.37 (CH_3, s, Me) ppm.

δ_P (121.5 MHz, C_6D_6): 38.89 (d, *J* = 27.5 Hz), 39.99 (d, *J* = 27.5 Hz) ppm.

IR (Powder): 3046 (w), 2923 (s), 2857 (m), 1449 (w), 1433 (m), 1089 (m), 1036 (w), 900 (w), 875 (w), 798 (w), 727 (s) cm^{-1}

LRMS (ES$^+$): m/z = 746.3 (M^+, 100%)

HRMS (ES$^+$): $(M)^+$ $C_{42}H_{43}ClP_2Ru$ requires *m/z* = 746.1557 found 746.1566

Anal. Calc'd for $C_{42}H_{43}ClP_2Ru$: C, 67.60; H, 5.81. Found: C, 67.73; H, 5.88.

***Rac*-(η^5:η^1-indenyl-CH(Cy)-CH_2PPh_2)RuCl(PMe_2Ph) (113)**

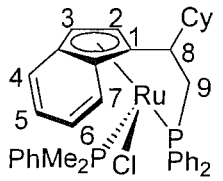

113

To a solution of ruthenium complex **27** (200 mg, 0.25 mmol) in toluene (10 mL) was added dimethylphenylphosphine (0.4 mL of a 4.0 M solution in toluene, 0.75 mmol) and the solution was refluxed for 16 hours. After this time, solvents were removed *in vacuo* and the resulting solid purified by flash chromatography (Al_2O_3, 4:6 Et_2O:petrol → 100% Et_2O) affording 152 mg of the title compound as a brown solid in 90% yield. The compound was recrystallised by cooling a CD_3CN solution to -18 °C and the X-ray structure has been obtained (Appendix VI).

MP: decomposes 144-145 °C

δ_H (300 MHz, C_6D_6): 8.16 (2H, d, *J* = 7.0 Hz, Ar), 7.82 (2H, t, *J* = 7.5 Hz, Ar), 7.57 (2H, s + fs, Ar), 7.01-7.38 (11H, m, Ar), 6.90 (2H, br s, Ar), 4.40 (1H, br s, H3), 3.67 (1H, br d, *J* = 8.5 Hz, H8), 3.56 (1H, s, H2), 2.55 (1H, t, *J* = 12.5 Hz, H9), 2.39 (1H, ddd, *J* = 22.5, 93.5, 4.5 Hz, H9), 1.77 (2H, dd, *J* = 23.5, 13.5, Cy), 1.50-1.61 (3H, m, Cy), 1.44 (3H, 6, *J* = 8.0 Hz, P-Me), 1.35 (3H, d, *J* = 7.5 Hz, P-Me), 1.13-1.31 (2H, m, Cy), 1.01-1.13 (2H, m, Cy), 0.77-0.89 (1H, m, Cy), 0.59-0.69 (1H, m, Cy) ppm.

δ_C (75.5 MHz, C_6D_6): 145.27 (C, d, *J* = 38.0 Hz, ^{i}Ph), 141.32 (C, d, *J* = 28.0 Hz, ^{i}Ph), 138.69 (C, d, *J* = 25.5 Hz, ^{i}Ph), 134.49 (2CH, d, *J* = 10.5 Hz, ^{o}Ph), 131.42 (2CH, d, *J* = 9.0 Hz, ^{o}Ph), *129.82 (CH, Ar), *129.76 (CH, Ar), *129.32 (CH, Ar), 129.00 (CH, s, C4/5/6/7), 128.78 (CH, s, C4/5/6/7), *128.57 (CH, Ar), *128.49 (CH, Ar), *128.25 (CH, Ar), *128.20 (CH, Ar), *128.16 (CH, Ar), 121.74 (CH, s, C4/5/6/7), 121.14 (CH, s, C4/5/6/7), 112.76 (C, s, C3a/7a), 101.51 (C, s + fs, C3a/7a), 95.54 (C, d, *J* = 12.0 Hz, C1), 72.35 (CH, d, *J* = 11.0 Hz, C3), 66.55 (CH, s, C2), 51.21 (CH_2, d, *J* = 33.0 Hz, C9), 42.90 (CH, d, *J* = 18.5 Hz, C8), 37.26 (CH, d, *J* = 4.8 Hz, Cy), 33.62 (CH_2, s, Cy), 31.44 (CH_2, s, Cy), 26.63 (CH_2, s, Cy), 26.38 (CH_2, s, Cy), 26.28 (CH_2, s, Cy), 16.97 ($2CH_3$, d, *J* = 28.0 Hz, P-Me) ppm.

δ_P (121.5 MHz, C_6D_6): 24.13 (d, *J* = 34.4 Hz), 39.26 (d, *J* = 34.4 Hz) ppm.

IR (Powder): 3047 (w), 2924 (m), 2853 (w), 1477 (w), 1432(s), 1275 (w), 1099 (w), 942 (m), 904 (s), 885 (m), 856 (w), 835 (w), 736 (s) cm^{-1}

LRMS (ES^+): m/z = 684.3 (M^+, 100%)

HRMS (ES^+): $(M)^+$ $C_{37}H_{41}ClP_2Ru$ requires *m/z* = **sub.** found **sub.**

Anal. Calc'd for $C_{37}H_{41}ClP_2Ru$: C, 64.95; H, 6.04. Found: C, 64.86; H, 6.12.

* = Unable to assign signals, determine integrals and *J* values due to overlapping peaks.

(*R*)-1-cyclohexyl-1,2-ethanediol (74)[73]

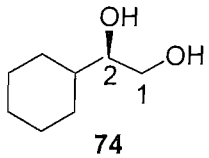

74

To a stirred solution of ^{t}BuOH (100 mL) and water (100 mL) was added $K_3Fe(CN)_6$ (19.76 g, 60.00 mmol), anhydrous K_2CO_3 (8.29 g, 60.00 mmol), $(DHQD)_2PYR$ (0.26 mg, 0.30 mmol) and OsO_4 (7.5 mL of a 0.04 M solution in ^{t}BuOH, 0.30 mmol). The solution was cooled to 0 °C and vinylcyclohexane (2.74 mL, 20.00 mmol) was added. The solution was stirred for 24 hours, after which time GC (Method B) showed no trace of starting material. The reaction was quenched with $Na_2S_2O_5$ (30 g) and diluted with DCM (200 mL). The aqueous layer was extracted into DCM (3 * 200 mL) and the combined organic layers were dried ($MgSO_4$), filtered and concentrated *in vacuo*. The resulting crude liquid was purified by flash chromatography (9:1 Et_2O:petrol), affording 2.81g of the title compound as a cream solid in 98% yield. Compound data was identical to that in the literature.[73]

MP: 36-37 °C (Lit. 38-39 °C)[73]

$[\alpha]_D^{20}$ = +3.58 (c = 1.73, $CHCl_3$) (Lit. +3.56, $CHCl_3$)[73]

δ_H (300 MHz, $CDCl_3$): 3.67-3.75 (1H, m, H2), 3.40-3.57 (2H, m, H1), 2.20 (2H, br s, OH), 1.59-1.92 (5H, m, Cy), 1.34-1.47 (1H, m, Cy), 0.96-1.29 (5H, m, Cy) ppm.

(*R*)-1-cyclohexyl-1,2-di(methanesulfonyl)ethane (75)[17]

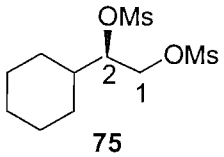

75

A solution of diol **74** (2.12 g, 14.70 mmol) in DCM (100 mL) was cooled to -30 °C. TEA (7.2 mL, 51.5 mmol) and methanesulfonyl chloride (2.9 mL, 36.8 mmol) were added dropwise and the reaction was stirred at -30 °C for 3 hours. TLC showed no sign of starting material, so the solution was filtered cold, washing through with cold DCM (2 * 25 mL). The filtrate was washed with water and extracted into DCM (3 * 25 mL). The combined organic layers were dried ($MgSO_4$) and concentrated in vacuo, affording 4.22 g of the title compound as a white solid in 96% crude yield. Compound data was identical to that in the literature.[17]

MP: 115-116 °C (DCM) (Lit. 114-116 °C)[17]

$[\alpha]_D^{25}$ = -17.1 (c = 1, $CHCl_3$) (Lit. -17.2, $CHCl_3$)[17]

δ_H (300 MHz, $CDCl_3$): 4.67 (1H, ddd, *J* = 6.5, 6.5, 2.5 Hz, H2), 4.47 (1H, dd, *J* = 12.0, 2.5 Hz, H1), 4.35 (1H, dd, *J* = 12.0, 6.5 Hz, H1), 3.12 (3H, s, Ms), 3.09 (3H, s, Ms), 1.65-1.91 (6H, m, Cy), 1.03-1.37 (5H, m, Cy) ppm.

***trans*-Spiro-[(2-cyclohexylcyclopropane)-1,1'-indene)] (76)**[17]

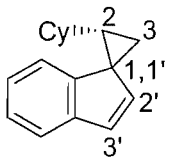

76

A solution of indene (0.5 mL, 3.8 mmol) in THF (10 mL) was cooled to -78 °C and ^{n}BuLi (1.5 mL of a 2.5 M solution in hexanes, 3.75 mmol) was added dropwise in the dark. The solution was stirred at -78 °C for 15 minutes then warmed to RT and stirred for 90 minutes. After this time, the solution was cooled to 0 °C and a solution of dimesylate **75** (476 mg, 1.59 mmol) in THF (15 mL) was added dropwise over 2 minutes. The solution was stirred at 0 °C for 15 minutes then warmed to RT overnight.

Workup was as above, yielding the title compound contaminated by a small amount of indeed. The indene was removed by evaporation under vacuum (1.0 mmHg) for 8 hours at

RT, affording 350 mg of the title compound in 98% yield as a clear oil and a 3:1 mixture of diastereoisomers.

Spectral data was identical to the racemic compound prepared from dibromide **83**, with the exception that the signals corresponding to the olefinic protons (H2' and H3') were in a 3:1 ratio as opposed to a 1:1 ratio.

[(2*R*)-2-cyclohexyl-2-(3'*H*-1'-indenyl)ethyl]diphenylphosphine-borane (85)[17]

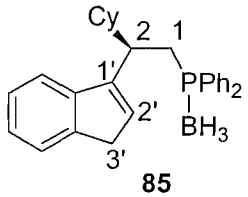

85

Synthesis, workup and spectral data were identical to that given above. The compound was synthesised in 91% yield, MP as above, optical rotation as per the literature.[17]

***Chiral*-(η^5:η^1-indenyl-CH(Cy)-CH_2PPh_2)RuCl(PPh_3) (27)**[17]

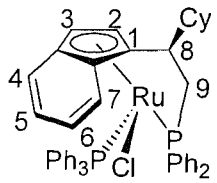

27

Synthesis, workup and spectral data were identical to that given above. The compound was synthesised in 71% yield, MP and optical rotation as per the literature.[17]

***Chiral*-[(η^5:η^1-indenyl-CH(Cy)-CH_2PPh_2)Ru(MeCN)(PPh_3)]$^+$[PF_6]$^-$ (80)**

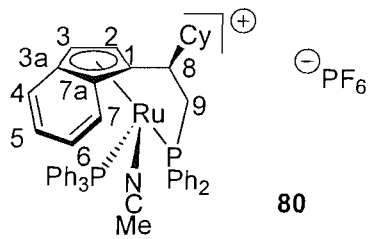

80

Synthesis, workup and spectral data were identical to that given above. The compound was synthesised in 95% yield, MP = 196 °C (dec.), $[\alpha]_D^{23}$ = -0.90 (c = 0.5, CH_3CN)

***Rac*-1-phenylethanol (114)**[91]

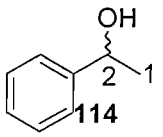

114

$NaBH_4$ (84 mg, 2.2 mmol) was added to a solution of acetophenone (240 mg, 2.0 mmol) in IPA (10 mL) and the solution was stirred for 30 minutes. At this point, TLC showed no starting material remaining, so water (10 mL) was added to quench the reaction, then the product was extracted into Et_2O (3 * 10 mL). The combined organic layers were dried (Na_2CO_3), filtered and solvents removed *in vacuo*, affording 296 mg of an orange liquid. The product was not purified further, but was analysed by GC to determine the retention time. Compound data was identical to that in the literature.[91]

δ_H (300 MHz, $CDCl_3$): 7.16-7.33 (5H, m, Ph), 4.81 (1H, q, J = 6.5 Hz, H2), 1.63 (1H, br s, OH), 1.42 (3H, d, J = 6.5 Hz, H1) ppm.
GC R_T (Method C): 6.17 mins
GC R_T (Method D): 12.77, 14.05 mins

***Rac*-*N*-(1-phenylethylidene)aniline (89)**[92]

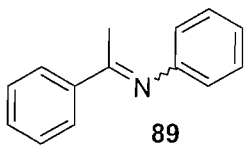

89

To a solution of acetophenone (1.2 mL, 10.0 mmol), aniline (1.1 mL, 12.0 mmol) and TEA (2.8 mL, 20.0 mmol) at 0 °C in DCM (35 mL), was added $TiCl_4$ (0.6 mL, 5.0 mmol). The reaction was stirred at 0 °C for 30 minutes, then at RT for 7 hours. After this time, satd. K_2CO_3 solution (30 mL) was added, then the solution was filtered and the aqueous layer extracted into DCM (3 * 10 mL). The combined organic layers were washed with brine (20 mL), dried (Na_2CO_3), filtered and concentrated *in vacuo*. The resulting brown solid was recrystallised from hot EtOH, affording 1.33 g of the title compound as a yellow solid in 68% yield. Compound data was identical to that in the literature.[92]

MP: 37-38°C (Lit. 39-40 °C)[92]

δ_H (300 MHz, $CDCl_3$): 7.84-8.07 (2H, m, Ar), 6.91-7.49 (6H, m, Ar), 6.67-6.82 (2H, m, Ar), 2.18 (3H, s, CH_3) ppm.

GC R_T (Method A): 5.63 mins

***Rac*-*N*-phenyl-*α*-methylbenzylamine (91)**[92]

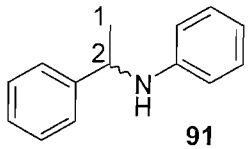

91

To a solution of imine **89** (60 mg, 0.31 mmol) and $NaBH_4$ (58 mg, 1.55 mmol) in IPA (10 mL) was added acetic acid (neat, 1 drop). The reaction was stirred for 1 hour, after which time GC showed complete consumption of imine. The reaction was quenched with water (10 mL), then the aqueous layer was extracted into Et_2O (3 * 10 mL). The combined organic layers were dried (Na_2CO_3), filtered and concentrated *in vacuo*, affording 60 mg of the title compound in 99% yield as a brown liquid. The product was not purified further, but was analysed by GC (Method A) to determine its retention time. Compound data was identical to that in the literature.[92]

δ_H (300 MHz, $CDCl_3$): 7.11-7.33 (5H, m, Ar), 7.01 (2H, t, J = 7.5 Hz, Ar), 6.56 (1H, t, J = 7.5 Hz, Ar), 6.43 (2H, d + fs, J = 8.0 Hz, Ar), 4.41 (1H, q, J = 7.0 Hz Hz, H2), 3.86 (1H, v br s, NH), 1.43 (3H, d, J = 7.0 Hz Hz, H1) ppm.

GC R_T (Method A): 5.53 mins

***Rac*-1,3-diphenyl-3-propenol (97)**[59]

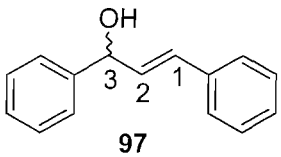

97

To a solution of $LiAlH_4$ (243 mg, 6.4 mmol) in THF (15 mL) at 0 °C was added a solution of chalcone (2.00 g, 9.6 mmol) in THF (10 mL) dropwise and the reaction was stirred at 0 °C. After 1 hour, TLC showed no starting material remaining, so the reaction mixture was quenched with 2N H_2SO_4 (10 mL) and extracted into Et_2O (3 * 15 mL). The combined organic layers were dried (Na_2CO_3), filtered and concentrated *in vacuo* to give a clear,

viscous oil. The crude product was purified by flash chromatography (9:1 petrol:EtOAc) affording 1.29 g of the title compound in 64% yield as a clear liquid. Compound data was identical to that in the literature.[59]

δ_H (300 MHz, $CDCl_3$): 7.12-7.42 (10H, m, Ph), 6.61 (1H, d, J = 16.0 Hz, H1), 6.31 (1H, dd, J = 16.0, 6.5 Hz, H2), 5.31 (1H, d, J = 6.5 Hz, H3), 1.99 (1H, br s, OH) ppm.

***Rac*-3-acetoxy-1,3-diphenylpropene (98)**[59]

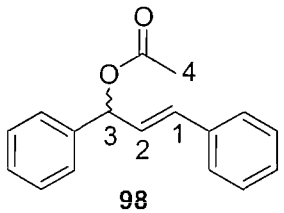

98

A solution of Ac_2O (0.9 mL, 10.0 mmol) and alcohol **97** (1.29 g, 6.13 mmol) in dry pyridine (10 mL) was refluxed for 1 hour. After this time, the reaction mixture was cooled, poured onto 1N HCl (50 mL) and extracted with Et_2O (3 * 25 mL). The combined organic layers were washed with 1N HCl (50 mL) and saturated Na_2CO_3 solution (50 mL), then dried (Na_2CO_3), filtered and concentrated *in vacuo*, affording 1.40 g of the title compound in 91% yield as a yellow liquid. Compound data was identical to that in the literature.[59]

δ_H (300 MHz, $CDCl_3$): 7.12-7.36 (10H, m, Ph), 6.55 (1H, d, J = 15.5 Hz, H1), 6.37 (1H, d, J = 7.0 Hz, H3), 6.26 (1H, dd, J = 15.5, 7.0 Hz, H2), 2.05 (3H, s, H4) ppm.
GC R_T (Method A): 6.48 mins

***Rac*-Ethyl-3-(1,3-diphenylpropenyl) carbonate (62)**[55]

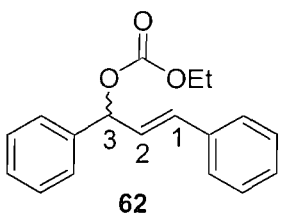

62

To a solution of alcohol **97** (1.11 g, 5.30 mmol), dry pyridine (1.6 mL, 20.0 mmol) and a catalytic amount of DMAP in THF (5 mL) at 0 °C was added ethyl chloroformate (1.3 mL, 17.0 mmol) and the solution was stirred at RT. After 16 hours, water (15 mL) was added to quench and the aqueous was extracted with Et_2O (3 * 20 mL). The combined organic layers

were washed with 1N HCl (3 * 20 mL), saturated Na_2CO_3 solution (20 mL), water (20 mL), then dried (Na_2CO_3), filtered and concentrated *in vacuo*. The crude product was purified by flash chromatography (9:1 petrol:EtOAc), affording 804 mg of the title compound as a clear oil in 54% yield. Compound data was identical to that in the literature.[55]

δ_H (300 MHz, $CDCl_3$): 7.12-7.36 (10H, m, Ph), 6.55 (1H, d, J = 15.5 Hz, H1), 6.37 (1H, d, J = 7.0 Hz, H3), 6.26 (1H, dd, J = 15.5, 7.0 Hz, H2), 4.11 (2H, q, J = 7.5 Hz, Et), 1.22 (3H, t, J = 7.5 Hz, Et) ppm.
GC R_T (Method A): 6.76 mins

General procedures and specific details of the catalytic studies are listed in Appendix I.

5.0: REFERENCES

1) Schafer, A.; Karl, E.; Zsolnai, L.; Huttner, G.; Brintzinger, H. H., *J. Organomet. Chem.* **1987,** 328, 87-89.
2) Cesarotti, E.; Kegan, H. B.; Goddard, R.; Krüger, C., *J. Organomet. Chem.* **1978,** 162, 297-309.
3) Komatsuzaki, N.; Uno, M.; Kikuchi, H.; Takahashi, S., *Chem. Lett.* **1996,** 677-678.
4) Willoughby, C. A.; Buchwald, S., *J. Am. Chem. Soc.* **1994,** 116, 8952-8965.
5) Jaquith, J. B.; Gaun, J.; Wang, S.; Collins, S., *Organometallics* **1995,** 14, 1079-1081.
6) Morken, J. P.; Diduik, M. T.; Hoveyda, A. H., *J. Am. Chem. Soc.* **1993,** 115, 6997-6998.
7) Bell, L.; Whitby, R. J., *Tetrahedron Lett.* **1996,** 37, 7139-7142.
8) Brookings, D. C. Ph.D. Thesis. University of Southampton, 1999.
9) Butenschön, H., *Chem. Rev.* **2000,** 100, 1527-1564.
10) Lee, I.; Dahan, F.; Maisonnat, A.; Poilblanc, R., *Organometallics* **1994,** 13, 2743-2750.
11) Davies, S. G.; Scott, F., *J. Organomet. Chem.* **1980,** 188, C41-42.
12) Trost, B. M.; Vidal, B.; Thommen, M., *Chem. Eur. J.* **1999,** 5, 1055-1069.
13) Kataoka, Y.; Saito, Y.; Nagata, K.; Kitamura, K.; Shibahara, A.; Tani, K., *Chem. Lett.* **1995,** 833-834.
14) Ciruelos, S.; Englert, U.; Salzer, A.; Bolm, C.; Maischak, A., *Organometallics* **2000,** 19, 2240-2242.
15) Habib, A.; Tanke, R. S.; Holt, E. M.; Crabtree, R. H., *Organometallics* **1989,** 8, 1225-1231.
16) Schumann, H.; Stenzel, O.; Dechert, S.; Girgsdies, F.; Halterman, R. L., *Organometallics* **2001,** 20, 2215-2225.
17) Harrison, S. A. Ph.D. Thesis. University of Southampton, 2002.
18) Kaulen, C.; Pala, C.; Hu, C. H.; Ganter, C., *Organometallics* **2001,** 20, 1614-1619.
19) Bitterwolf, T. E.; Leonard, M. B.; Horine, P. A.; Shade, J. E.; Rheingold, A. L.; Staley, D. J.; Yap, G. P. A., *J. Organomet. Chem.* **1995,** 512, 11-20.
20) Schwab, P.; Grubbs, R. H.; Ziller, J. W., *J. Am. Chem. Soc.* **1996,** 118, 100-110.
21) Dias, E. L.; Nguyen, S. T.; Grubbs, R. H., *J. Am. Chem. Soc.* **1997,** 119, 3887-3897.
22) Palma-Ramirez, P.; Cole-Hamilton, D. J.; Pogorzelec, P.; Campora, J., *Polyhedron* **1990,** 9, 1107-1112.

23) Wong, W. K.; Chiu, K. W.; Wilkinson, G.; Howes, A. J.; Hursthouse, M. B., *Polyhedron* **1985,** 4, 603-614.

24) Douglas, P. G.; Shaw, B. L., *J. Chem. Soc. A* **1970**, 1556-1557.

25) Ashok, R. F. N.; Gupta, M.; Arulsamy, K. S.; Agarwala, U. C., *Inorg. Chim. Acta.* **1985,** 98, 161-167.

26) Abbenhuis, R. A. T. M.; del Rio, I.; Bergshoef, M. M.; Boersma, J.; Veldman, N.; Spek, A. L.; van Koten, G., *Inorg. Chem.* **1998,** 37, 1749-1758.

27) Wilczewski, T.; Bochenska, M.; Biernat, J. F., *J. Organomet. Chem.* **1981,** 215, 87-96.

28) Magee, M. P.; Norton, J. R., *J. Am. Chem. Soc.* **2001,** 123, 1778-1779.

29) Lemke, F. R., *J. Am. Chem. Soc.* **1994,** 116, 11183-11184.

30) Crochet, P.; Demerseman, B.; Rocaboy, C.; Schleyer, D., *Organometallics* **1996,** 15, 3048-3061.

31) Bruce, M. I.; Wallis, R. C., *Aust. J. Chem.* **1979,** 32, 1471-1485.

32) Ashworth, T. V.; Chalmers, A. A.; Singleton, E.; Swanepoel, H. E., *J. Chem. Soc. Chem. Commun.* **1982**, 214-215.

33) Bruce, M. I.; Hinterding, P.; Tiekink, E. R. T.; Skelton, B. W.; White, A. H., *J. Organomet. Chem.* **1993,** 450, 209-218.

34) Prasad, R.; Mishra, L.; Agarwala, U. C., *Indian J. Chem.* **1991,** 30A, 162-165.

35) Abbott, S.; Davies, S. G.; Warner, P., *J. Organomet. Chem.* **1983,** 246, C65-68.

36) Bruce, M. I.; Humphrey, M. G.; Koutsantonis, G. A., *J. Organomet. Chem.* **1985,** 296, C47-50.

37) Davies, S. G.; Smallridge, A. J., *J. Organomet. Chem.* **1991,** 413, 313-319.

38) Lefort, L.; Crane, T. W.; Farwell, M. D.; Baruch, D. M.; Kaeuper, J. A.; Lachicotte, R. J.; Jones, W. D., *Organometallics* **1998,** 17, 3889-3899.

39) Kataoka, Y. S. A.; Saito, Y.; Yamagata, T.; Tani, K., *Organometallics* **1998,** 17, 4338-4340.

40) Naota, T.; Takaya, H.; Murahashi, S.-I., *Chem. Rev.* **1998,** 98, 2599-2660.

41) Trost, B. M.; Kulawiec, R. J., *J. Am. Chem. Soc.* **1993,** 115, 2027-2036.

42) del Zotto, A.; Baratta, W.; Sandri, M.; Verardo, G.; Rigo, P., *Eur. J. Inorg. Chem.* **2004**, 524-529.

43) Gamasa, M. P.; Gimeno, J.; GonzalezBernardo, C.; MartinVaca, B. M.; Monti, D.; Bassetti, M., *Organometallics* **1996,** 15, 302-308.

44) Landis, C. R.; Branch, T. W., *Inorg. Chim. Acta.* **1998,** 270, 285-297.

45) Gaus, P. L.; Kao, S. C.; Youngdahl, K.; Darensbourg, M. Y., *J. Am. Chem. Soc.* **1985,** 107, 2428-2434.

46) Gibson, D. H.; El-Omrani, Y. S., *Organometallics* **1985,** 4, 1473-1475.

47) Kitamura, M.; Ohkuma, T.; Inoue, S.; Sayo, N.; Kumobayashi, H.; Akutagawa, S.; Ohta, T.; Takaya, H.; Noyori, R., *J. Am. Chem. Soc.* **1988,** 110, 629-631.

48) Hoke, J. B.; Hollis, L. S.; Stern, E. W., *J. Organomet. Chem.* **1992,** 455, 193-196.

49) Evans, D. A.; Nelson, S. G.; Gagné, S. G.; Muci, A. R., *J. Am. Chem. Soc.* **1993,** 115, 9800-9801.

50) Yamakawa, M.; Yamada, I.; Noyori, R., *Angew. Chem. Int. Ed.* **2001,** 40, 2818-2821.

51) Yamakawa, M.; Ito, H.; Noyori, R., *J. Am. Chem. Soc.* **2000,** 122, 1466-1478.

52) Uematsu, N.; Fujii, A.; Hashiguchi, S.; Ikariya, T.; Noyori, R., *J. Am. Chem. Soc.* **1996,** 118, 4916-4917.

53) Consiglio, G.; Waymouth, R. M., *Chem. Rev.* **1989,** 89, 257-276.

54) Tsuji, J.; Takahashi, H.; Morikawa, M., *Tetrahedron Lett.* **1965,** 6, 4387-2388.

55) Matsushima, Y.; Onitsuka, K.; Kondo, T.; Mitsudo, T.; Takahashi, S., *J. Am. Chem. Soc.* **2001,** 123, 10405-10406.

56) Nomura, N.; Rajanbabu, T. V., *Tetrahedron Lett.* **1997,** 38, 1713-1716.

57) Baruah, J. B.; Samuelson, A. G., *New J. Chem.* **1994,** 18, 961-971.

58) Constantineux, T.; Brunel, J. M.; Labande, A.; Buono, G., *Syn. Lett.* **1998,** 1, 49-50.

59) Leung, W.; Cosway, S.; Jones, R. H. V.; McCann, H.; Wills, M., *J. Chem. Soc. Perkin Trans. 1* **2001**, 2588-2594.

60) Fringuelli, F.; Taticchi, A., *Dienes in the Diels-Alder Reaction*. ed.; Wiley-Interscience: 1990; 'Vol.' p.

61) Wasserman, A., *J. Chem. Soc.* **1942**, 618-621.

62) Yates, P.; Eaton, P., *J. Am. Chem. Soc.* **1960,** 82, 4436-4437.

63) Bednarski, M.; Danishefsky, S., *J. Am. Chem. Soc.* **1983,** 105, 3716-3717.

64) Hollis, T. K.; Odenkirk, W.; Robinson, N. P.; Whelan, J.; Bosnich, B., *Tetrahedron* **1993,** 49, 5415-5430.

65) Faller, J. W.; Smart, C. J., *Tetrahedron Lett.* **1989,** 30, 1189-1192.

66) Kündig, E. P.; Saudan, C. M.; Alezra, V.; Viton, F.; Bernardinelli, G., *Angew. Chem. Int. Ed.* **2001,** 40, 4481-4485.

67) Silberrad, O.; Roy, C. S., *J. Chem. Soc.* **1906,** 89, 179-182.

68) Doyle, M. P.; Forbes, D. C., *Chem. Rev.* **1998,** 98, 911-935.

69) Paulissenen, R.; Reimlinger, H.; Hayez, E.; Hubert, A. J.; Teyssie, P. H., *Tetrahedron Lett.* **1973,** 14, 2233-2236.

70) Nozaki, H.; Moriuti, S.; Takaya, H.; Noyori, R., *Tetrahedron Lett.* **1966,** 7, 5239-5244.

71) Baratta, W.; del Zotto, A.; Rigo, P., *Organometallics* **1999,** 18, 5091-5096.

72) Tutusaus, O.; Delfosse, S.; Demonceau, A.; Noels, A. F.; Núñez, R.; Viñas, C.; Teixidor, F., *Tetrahedron Lett.* **2002,** 43, 983-987.

73) Crispino, G. A.; Jeong, K.-S.; Kolb, H. C.; Wang, Z.-M.; Xu, D.; Sharpless, K. B., *J. Org. Chem.* **1993,** 58, 3785-3786.

74) Buss, A. D.; Warren, S., *J. Chem. Soc. Perkin Trans. 1* **1985**, 2307-2325.

75) Imamoto, T.; Oshiki, T.; Onozawa, T.; Kusumoto, T.; Sato, K., *J. Am. Chem. Soc.* **1990,** 112, 5244-5252.

76) Piettre, S. R., *Tetrahedron Lett.* **1996,** 37, 4707-4710.

77) Goodwin, N. J.; Henderson, W.; Nicholson, B. J.; Sarfo, J. K.; Fawcett, J.; Russell, D. R., *J. Chem. Soc. Dalton Trans.* **1997**, 4377-4384.

78) Naumann, K.; Zon, G.; Mislow, K., *J. Am. Chem. Soc.* **1969,** 91, 7012-7023.

79) Imamoto, T.; Kikuchi, S.-I.; Miura, T.; Wada, Y., *Org. Lett.* **2001,** 3, 87-90.

80) Griffin, S.; Heath, L.; Wyatt, P., *Tetrahedron Lett.* **1998,** 39, 4405-4406.

81) Brisset, H.; Gourdel, Y.; Pellon, P.; Le Corre, M., *Tetrahedron Lett.* **1993,** 34, 4523-4526.

82) Gansow, O. A.; Burke, A. R.; Vernon, W. D., *J. Am. Chem. Soc.* **1976,** 98, 5817-5826.

83) Lindsay, C.; Cesarotti, E.; Adams, H.; Bailey, N. A.; White, C., *Organometallics* **1990,** 9, 2594-2602.

84) Park, J. H.; Koh, J. H.; Park, J., *Organometallics* **2001,** 20, 1892-1894.

85) Armarego, W. L. F.; Perrin, D. D., *Purification of Laboratory Chemicals*. 4th ed.; Butterworth-Heinemann: 1997; 'Vol.' p.

86) McCleverty, J. A.; Wilkinson, G., *Inorg. Synth.* **1966,** 8, 211-212.

87) Potgeiter, H. H., *J. Organomet. Chem.* **1989,** 366, 369-376.

88) Wilkinson, G.; Hallman, P. S.; Stephenson, T. A., *Inorg. Synth.* **1970,** 12, 237-239.

89) Gottleib, H. E.; Kotlyar, V.; Nudelman, A., *J. Org. Chem.* **1997,** 62, 7512-7515.

90) Hubert, A. J., *J. Chem. Soc.* **1965**, 6669-6674.

91) Lee, D.; Huh, E. A.; Kim, M.-J.; Jung, H. M.; Koh, J. H.; Park, J., *Org. Lett.* **2000,** 2, 2377-2379.

92) Periasamy, M.; Srinivas, G.; Bharathi, P., *J. Org. Chem.* **1999,** 64, 4204-4205.

APPENDICES

Appendix I	**Specific details of the catalytic studies**	**1-1**
Appendix II	**X-Ray structure of ruthenium complex 80**	**2-1**
Appendix III	**X-Ray structure of ruthenium complex 81**	**3-1**
Appendix IV	**X-Ray structure of ruthenium complex 82**	**4-1**
Appendix V	**X-Ray structure of ruthenium complex 112**	**5-1**
Appendix VI	**X-Ray structure of ruthenium complex 113**	**6-1**

Many thanks to Susanne Huth for running and solving the X-Ray structures

General Procedure for the hydrogenation reaction:

Catalyst (3 mg), imine **89** (40 mg), HBF_4 (10 μL) and DCM (3 mL) were placed in a stainless-steel hydrogenation bomb under an inert atmosphere. The bomb was purged with hydrogen and pressurised to 6 bar, then stirred for 60 hours at RT. After this time, the reaction was analysed by GC (Method A). Two more reactions, with complexes **27** and **80**, were performed at 50 °C. See Table 4 (section 3.1) for results.

General Procedure for the transfer hydrogenation reactions:

IPA system: To a solution of catalyst (3 mg) in IPA (4 mL) was added base, acetophenone and any other additives. The reactions were stirred with GC monitoring (Method C). See Table 5 (section 3.2) for results.

General Procedure for the allylic displacement reaction:

To a solution of catalyst (3 mg) in THF (2 mL) was added the allylic acetate, followed by benzylamine at RT. The reactions were monitored by GC (Method A).

No.	Catalyst	**98**	$PhCH_2NH_2$	No.	Catalyst	**62**	$PhCH_2NH_2$
1	27	19 mg	9 mg	7	27	20 mg	10 mg
2	80	19 mg	9 mg	8	80	20 mg	10 mg
3	81	19 mg	9 mg	9	81	20 mg	10 mg
4	82	19 mg	9 mg	10	82	20 mg	10 mg
5	28[a]	19 mg	9 mg	11	28[a]	20 mg	10 mg
6	92[a]	19 mg	9 mg	12	92[a]	20 mg	10 mg

a – complexes supplied by P. Wright

Table 6 – Allylic Displacement Details

General Procedure for the Diels-Alder reaction:

To a solution of catalyst (3 mg) in DCM (1 mL) was added methacrolein and either cyclopentadiene or 1,3-cyclohexadiene. The reactions were shaken, then cooled to -18 °C and monitored by GC (Method C). After 48 hours, the reactions were heated to 40 °C.

No.	Catalyst	Cyclopentadiene*	MA*	No.	Catalyst	1,3-hexadiene	MA*
1	27	0.3 mL	0.3 mL	9	27	15 mg	0.3 mL
2	80	0.25 mL	0.25 mL	10	80	13 mg	0.25 mL
3	81	0.3 mL	0.3 mL	11	81	15 mg	0.3 mL
4	82	0.25 mL	0.25 mL	12	82	13 mg	0.25 mL
5	28[a]	0.3 mL	0.3 mL	13	28[a]	16 mg	0.3 mL
6	92[a]	0.25 mL	0.25 mL	14	92[a]	13 mg	0.25 mL
7	22	0.3 mL	0.3 mL	15	22	21 mg	0.3 mL
8	-	0.3 mL	0.3 mL	16	-	15 mg	0.3 mL

** - 0.64 M solution in DCM*
a – complexes supplied by P. Wright

Table 7 – Diels-Alder Reaction Details

General Procedure for the cyclopropanation of styrene:

To a solution of catalyst (3 mg) in styrene (1 mL) at 40 °C was added 1 mL of a 1:1 mix of styrene and EDA over a 4 hour period. The reaction was monitored by GC (Method A). A blank reaction where 1 mL of a 1:1 mix of styrene and EDA was added to styrene (1 mL) at 40 °C over a 4 hour period was also performed.

University of Southampton · Department of Chemistry

EPSRC National Crystallography Service

Table 1. Crystal data and structure refinement.

Identification code	**03sot0165 (DCP 070/1)**	
Empirical formula	$C_{49}H_{48}F_6NP_3Ru$	
Formula weight	958.86	
Temperature	120(2) K	
Wavelength	0.71073 Å	
Crystal system	Triclinic	
Space group	*P*–1	
Unit cell dimensions	a = 11.5522(9) Å	α = 105.232(5)°
	b = 12.4256(5) Å	β = 96.698(10)°
	c = 16.8434(17) Å	γ = 111.231(7)°
Volume	2113.3(3) Å^3	
Z	2	
Density (calculated)	1.507 Mg / m^3	
Absorption coefficient	0.548 mm^{-1}	
F(000)	984	
Crystal	Cut block; dark red	
Crystal size	0.36 × 0.22 × 0.20 mm^3	
θ range for data collection	3.02 – 27.50°	
Index ranges	$-15 \le h \le 14$, $-16 \le k \le 16$, $-21 \le l \le 21$	
Reflections collected	39295	
Independent reflections	9615 [R_{int} = 0.0281]	
Completeness to θ = 27.50°	99.3 %	
Absorption correction	Multiscans	
Max. and min. transmission	0.8983 and 0.8271	
Refinement method	Full-matrix least-squares on F^2	
Data / restraints / parameters	9615 / 0 / 734	
Goodness-of-fit on F^2	1.059	
Final R indices [$F^2 > 2\sigma(F^2)$]	$R1$ = 0.0301, $wR2$ = 0.0722	
R indices (all data)	$R1$ = 0.0354, $wR2$ = 0.0753	
Extinction coefficient	0.0023(3)	
Largest diff. peak and hole	0.807 and –0.767 e Å^{-3}	

Diffractometer: *Nonius KappaCCD* area detector (ϕ scans and ω scans to fill *asymmetric unit* sphere). **Cell determination:** DirAx (Duisenberg, A.J.M.(1992). J. Appl. Cryst. 25, 92-96.) **Data collection:** Collect (Collect: Data collection software, R. Hooft, Nonius B.V., 1998). **Data reduction and cell refinement**: *Denzo* (Z. Otwinowski & W. Minor, *Methods in Enzymology* (1997) Vol. **276**: *Macromolecular Crystallography*, part A, pp. 307–326; C. W. Carter, Jr. & R. M. Sweet, Eds., Academic Press). **Absorption correction**: *SORTAV* (R. H. Blessing, Acta Cryst. A**51** (1995) 33–37; R. H. Blessing, J. Appl. Cryst. **30** (1997) 421–426). **Structure solution**: *SHELXS97* (G. M. Sheldrick, Acta Cryst. (1990) A**46** 467–473). **Structure refinement**: *SHELXL97* (G. M. Sheldrick (1997), University of Göttingen, Germany). **Graphics:** Cameron - A Molecular Graphics Package. (D. M. Watkin, L. Pearce and C. K. Prout, Chemical Crystallography Laboratory, University of Oxford, 1993).

Special details:

APPENDIX II: X-RAY STRUCTURE OF RUTHENIUM COMPLEX **80**

Table 2. Atomic coordinates [$\times 10^4$], equivalent isotropic displacement parameters [$Å^2 \times 10^3$] and site occupancy factors. U_{eq} is defined as one third of the trace of the orthogonalized U^{ij} tensor.

Atom	*x*	*y*	*z*	U_{eq}	*S.o.f.*
C1	2285(2)	3239(2)	2480(1)	16(1)	1
C2	3575(2)	3375(2)	2744(1)	17(1)	1
C3	3882(2)	3704(2)	3641(1)	19(1)	1
C3A	2819(2)	3829(2)	3954(1)	18(1)	1
C4	2627(2)	4224(2)	4785(1)	23(1)	1
C5	1501(2)	4272(2)	4865(1)	28(1)	1
C6	502(2)	3943(2)	4148(2)	30(1)	1
C7	637(2)	3578(2)	3340(1)	22(1)	1
C7A	1827(2)	3531(2)	3225(1)	15(1)	1
C8	1530(2)	2811(2)	1576(1)	17(1)	1
C9	1623(2)	1635(2)	1091(1)	18(1)	1
C10	1914(2)	3780(2)	1126(1)	20(1)	1
C11	3305(2)	4215(2)	1058(1)	24(1)	1
C11'	1609(2)	4858(2)	1541(2)	26(1)	1
C12'	1951(3)	5807(2)	1088(2)	35(1)	1
C12	3640(3)	5171(2)	610(2)	32(1)	1
C13	3345(3)	6243(2)	1047(2)	37(1)	1
C14	−270(2)	−372(2)	1437(1)	17(1)	1
C15	−1147(2)	−6(2)	1086(1)	18(1)	1
C16	−2453(2)	−721(2)	896(1)	24(1)	1
C17	−2896(2)	−1805(2)	1059(1)	27(1)	1
C18	−2039(2)	−2181(2)	1417(2)	32(1)	1
C19	−737(2)	−1470(2)	1608(2)	29(1)	1
C20	2145(2)	−368(2)	1120(1)	19(1)	1
C21	1441(2)	−1478(2)	472(1)	26(1)	1
C22	2062(3)	−2040(2)	−35(2)	34(1)	1
C23	3374(3)	−1513(2)	96(2)	35(1)	1
C24	4079(3)	−425(2)	746(2)	31(1)	1
C25	3471(2)	146(2)	1255(1)	23(1)	1
C26	2548(2)	−497(2)	3798(1)	14(1)	1
C27	1862(2)	−1467(2)	3052(1)	17(1)	1
C28	1077(2)	−2605(2)	3072(1)	22(1)	1
C29	966(2)	−2781(2)	3844(2)	24(1)	1
C30	1658(2)	−1834(2)	4588(2)	24(1)	1
C31	2452(2)	−698(2)	4568(1)	19(1)	1
C32	4822(2)	802(2)	3335(1)	15(1)	1
C33	5018(2)	−262(2)	3242(1)	20(1)	1
C34	6083(2)	−354(2)	2982(2)	26(1)	1
C35	6980(2)	619(2)	2837(1)	26(1)	1
C36	6798(2)	1683(2)	2930(1)	24(1)	1
C37	5719(2)	1767(2)	3169(1)	21(1)	1
C38	4212(2)	1942(2)	4830(1)	15(1)	1
C39	5499(2)	2339(2)	5200(1)	21(1)	1
C40	5992(2)	3073(2)	6044(1)	26(1)	1
C41	5207(2)	3393(2)	6524(1)	25(1)	1
C42	3923(2)	2997(2)	6165(1)	22(1)	1
C43	3432(2)	2286(2)	5319(1)	18(1)	1
C44	−5(2)	118(2)	3612(1)	21(1)	1
C45	−1012(2)	−812(2)	3810(2)	31(1)	1
N1	807(2)	801(2)	3443(1)	17(1)	1
P1	1444(1)	590(1)	1716(1)	15(1)	1
P2	3475(1)	1003(1)	3720(1)	12(1)	1
Ru1	2303(1)	1872(1)	3094(1)	12(1)	1
P3	2654(1)	−4722(1)	−2226(1)	26(1)	1
F1	3279(2)	−4539(1)	−3003(1)	43(1)	1
F2	1536(2)	−4422(2)	−2625(1)	63(1)	1
F3	1844(1)	−6141(1)	−2763(1)	44(1)	1
F4	3747(2)	−5085(2)	−1885(1)	56(1)	1
F5	3482(2)	−3323(2)	−1720(1)	65(1)	1

F6 1996(3) −4930(2) −1477(1) 80(1) 1

Table 3. Bond lengths [Å] and angles [°].

C1–C7A	1.429(3)	C16–H16	0.93(3)
C1–C2	1.438(3)	C17–C18	1.380(3)
C1–C8	1.513(3)	C17–H17	0.95(3)
C1–Ru1	2.2147(18)	C18–C19	1.386(3)
C2–C3	1.422(3)	C18–H18	0.86(3)
C2–Ru1	2.1878(19)	C19–H19	0.93(3)
C2–H2	0.96(2)	C20–C25	1.393(3)
C3–C3A	1.434(3)	C20–C21	1.395(3)
C3–Ru1	2.2038(18)	C20–P1	1.828(2)
C3–H3	0.97(2)	C21–C22	1.387(3)
C3A–C4	1.427(3)	C21–H21	0.96(3)
C3A–C7A	1.444(3)	C22–C23	1.379(4)
C3A–Ru1	2.2954(18)	C22–H22	0.92(3)
C4–C5	1.344(3)	C23–C24	1.381(4)
C4–H4	0.96(2)	C23–H23	0.94(3)
C5–C6	1.425(3)	C24–C25	1.384(3)
C5–H5	0.93(3)	C24–H24	0.91(3)
C6–C7	1.363(3)	C25–H25	0.91(3)
C6–H6	0.91(3)	C26–C27	1.393(3)
C7–C7A	1.431(3)	C26–C31	1.394(3)
C7–H7	0.93(3)	C26–P2	1.8304(19)
C7A–Ru1	2.2833(18)	C27–C28	1.388(3)
C8–C9	1.523(3)	C27–H27	0.94(2)
C8–C10	1.547(3)	C28–C29	1.387(3)
C8–H8	1.00(2)	C28–H28	0.94(3)
C9–P1	1.846(2)	C29–C30	1.379(3)
C9–H9A	0.97(2)	C29–H29	0.94(3)
C9–H9B	0.99(2)	C30–C31	1.389(3)
C10–C11'	1.522(3)	C30–H30	0.92(3)
C10–C11	1.527(3)	C31–H31	0.91(2)
C10–H10	1.00(2)	C32–C37	1.390(3)
C11–C12	1.528(3)	C32–C33	1.392(3)
C11–H11A	1.01(2)	C32–P2	1.8263(19)
C11–H11B	0.96(3)	C33–C34	1.386(3)
C11'–C12'	1.528(3)	C33–H33	0.93(3)
C11'–H11C	0.99(2)	C34–C35	1.380(3)
C11'–H11D	0.96(3)	C34–H34	0.93(3)
C12'–C13	1.518(4)	C35–C36	1.384(3)
C12'–H12C	0.98(3)	C35–H35	0.95(3)
C12'–H12D	0.93(3)	C36–C37	1.385(3)
C12–C13	1.519(4)	C36–H36	0.95(3)
C12–H12A	0.94(2)	C37–H37	0.94(2)
C12–H12B	0.96(3)	C38–C39	1.391(3)
C13–H13A	1.04(3)	C38–C43	1.394(3)
C13–H13B	1.00(3)	C38–P2	1.8287(19)
C14–C15	1.384(3)	C39–C40	1.389(3)
C14–C19	1.395(3)	C39–H39	0.93(3)
C14–P1	1.8286(19)	C40–C41	1.378(3)
C15–C16	1.391(3)	C40–H40	0.93(3)
C15–H15	0.92(2)	C41–C42	1.383(3)
C16–C17	1.371(3)	C41–H41	0.97(3)

APPENDIX II: X-RAY STRUCTURE OF RUTHENIUM COMPLEX **80**

C42–C43	1.385(3)
C42–H42	0.95(3)
C43–H43	0.93(2)
C44–N1	1.137(3)
C44–C45	1.455(3)
C45–H45A	0.87(5)
C45–H45B	0.91(4)
C45–H45C	0.94(5)
N1–Ru1	2.0216(17)
P1–Ru1	2.2990(6)
P2–Ru1	2.3311(5)
P3–F6	1.5775(18)
P3–F5	1.5786(17)
P3–F4	1.5823(16)
P3–F2	1.5923(17)
P3–F1	1.5944(16)
P3–F3	1.6032(15)

C7A–C1–C2	107.54(17)
C7A–C1–C8	126.13(17)
C2–C1–C8	126.28(18)
C7A–C1–Ru1	74.11(10)
C2–C1–Ru1	69.92(11)
C8–C1–Ru1	119.44(12)
C3–C2–C1	108.02(17)
C3–C2–Ru1	71.72(11)
C1–C2–Ru1	71.94(11)
C3–C2–H2	125.8(14)
C1–C2–H2	125.9(14)
Ru1–C2–H2	126.4(15)
C2–C3–C3A	108.98(17)
C2–C3–Ru1	70.51(11)
C3A–C3–Ru1	74.92(11)
C2–C3–H3	125.7(14)
C3A–C3–H3	125.3(14)
Ru1–C3–H3	122.5(14)
C4–C3A–C3	133.37(19)
C4–C3A–C7A	119.80(19)
C3–C3A–C7A	106.74(17)
C4–C3A–Ru1	128.44(14)
C3–C3A–Ru1	67.97(10)
C7A–C3A–Ru1	71.17(10)
C5–C4–C3A	118.6(2)
C5–C4–H4	121.0(14)
C3A–C4–H4	120.4(14)
C4–C5–C6	122.0(2)
C4–C5–H5	118.3(16)
C6–C5–H5	119.6(16)
C7–C6–C5	122.0(2)
C7–C6–H6	118.3(17)
C5–C6–H6	119.7(17)
C6–C7–C7A	117.9(2)
C6–C7–H7	122.8(15)
C7A–C7–H7	119.2(15)
C1–C7A–C7	131.71(18)
C1–C7A–C3A	108.67(17)
C7–C7A–C3A	119.61(18)
C1–C7A–Ru1	68.89(10)
C7–C7A–Ru1	125.50(13)
C3A–C7A–Ru1	72.08(10)
C1–C8–C9	108.28(15)
C1–C8–C10	114.44(16)
C9–C8–C10	112.08(16)
C1–C8–H8	106.7(12)
C9–C8–H8	108.5(12)
C10–C8–H8	106.6(12)
C8–C9–P1	111.91(14)
C8–C9–H9A	111.8(13)
P1–C9–H9A	111.7(13)
C8–C9–H9B	109.2(13)
P1–C9–H9B	103.2(13)
H9A–C9–H9B	108.7(18)
C11'–C10–C11	110.85(17)
C11'–C10–C8	110.98(17)
C11–C10–C8	113.86(17)
C11'–C10–H10	106.8(14)
C11–C10–H10	107.4(14)
C8–C10–H10	106.5(14)
C10–C11–C12	111.99(19)
C10–C11–H11A	109.0(13)
C12–C11–H11A	108.2(13)
C10–C11–H11B	108.0(16)
C12–C11–H11B	107.5(16)
H11A–C11–H11B	112(2)
C10–C11'–C12'	111.5(2)
C10–C11'–H11C	109.2(13)
C12'–C11'–H11C	108.8(13)
C10–C11'–H11D	108.1(15)
C12'–C11'–H11D	112.8(15)
H11C–C11'–H11D	106(2)
C13–C12'–C11'	111.2(2)
C13–C12'–H12C	106.4(18)
C11'–C12'–H12C	108.1(18)
C13–C12'–H12D	109.3(18)
C11'–C12'–H12D	109.9(18)
H12C–C12'–H12D	112(3)
C13–C12–C11	110.8(2)
C13–C12–H12A	108.6(13)
C11–C12–H12A	107.5(13)
C13–C12–H12B	110.2(16)
C11–C12–H12B	110.9(16)
H12A–C12–H12B	109(2)
C12'–C13–C12	110.5(2)
C12'–C13–H13A	109.5(16)
C12–C13–H13A	108.6(16)
C12'–C13–H13B	111.5(18)
C12–C13–H13B	108.8(18)
H13A–C13–H13B	108(2)
C15–C14–C19	117.95(18)
C15–C14–P1	121.04(15)
C19–C14–P1	120.95(15)
C14–C15–C16	121.09(19)
C14–C15–H15	121.8(15)
C16–C15–H15	117.1(15)
C17–C16–C15	120.2(2)
C17–C16–H16	122.4(16)
C15–C16–H16	117.4(16)
C16–C17–C18	119.6(2)
C16–C17–H17	120.6(16)
C18–C17–H17	119.8(16)
C17–C18–C19	120.3(2)
C17–C18–H18	120(2)

C19–C18–H18	120(2)	C40–C39–C38	120.1(2)
C18–C19–C14	120.8(2)	C40–C39–H39	119.1(15)
C18–C19–H19	120.2(18)	C38–C39–H39	120.8(15)
C14–C19–H19	118.9(18)	C41–C40–C39	120.4(2)
C25–C20–C21	118.9(2)	C41–C40–H40	119.7(17)
C25–C20–P1	116.19(15)	C39–C40–H40	119.9(17)
C21–C20–P1	124.26(17)	C40–C41–C42	120.10(19)
C22–C21–C20	119.9(2)	C40–C41–H41	120.3(15)
C22–C21–H21	121.1(15)	C42–C41–H41	119.6(15)
C20–C21–H21	118.9(15)	C41–C42–C43	119.8(2)
C23–C22–C21	120.6(2)	C41–C42–H42	119.8(15)
C23–C22–H22	120.8(19)	C43–C42–H42	120.4(15)
C21–C22–H22	118.5(19)	C42–C43–C38	120.71(19)
C22–C23–C24	119.7(2)	C42–C43–H43	118.9(14)
C22–C23–H23	119.9(17)	C38–C43–H43	120.4(14)
C24–C23–H23	120.3(17)	N1–C44–C45	176.5(2)
C23–C24–C25	120.2(2)	C44–C45–H45A	108(3)
C23–C24–H24	122.0(18)	C44–C45–H45B	107(2)
C25–C24–H24	117.8(19)	H45A–C45–H45B	117(4)
C24–C25–C20	120.6(2)	C44–C45–H45C	111(3)
C24–C25–H25	121.8(16)	H45A–C45–H45C	106(4)
C20–C25–H25	117.6(16)	H45B–C45–H45C	108(4)
C27–C26–C31	118.58(18)	C44–N1–Ru1	174.03(16)
C27–C26–P2	118.34(15)	C20–P1–C14	104.95(9)
C31–C26–P2	123.02(15)	C20–P1–C9	98.12(9)
C28–C27–C26	120.90(19)	C14–P1–C9	104.59(9)
C28–C27–H27	118.5(14)	C20–P1–Ru1	125.10(6)
C26–C27–H27	120.6(14)	C14–P1–Ru1	116.44(6)
C29–C28–C27	119.8(2)	C9–P1–Ru1	104.20(6)
C29–C28–H28	119.8(15)	C32–P2–C38	102.31(9)
C27–C28–H28	120.4(15)	C32–P2–C26	102.93(9)
C30–C29–C28	119.90(19)	C38–P2–C26	102.43(9)
C30–C29–H29	120.6(16)	C32–P2–Ru1	121.43(6)
C28–C29–H29	119.5(16)	C38–P2–Ru1	109.59(6)
C29–C30–C31	120.4(2)	C26–P2–Ru1	115.81(6)
C29–C30–H30	119.9(18)	N1–Ru1–C2	162.05(7)
C31–C30–H30	119.8(18)	N1–Ru1–C3	137.87(7)
C30–C31–C26	120.42(19)	C2–Ru1–C3	37.77(7)
C30–C31–H31	119.1(14)	N1–Ru1–C1	125.68(7)
C26–C31–H31	120.5(14)	C2–Ru1–C1	38.14(7)
C37–C32–C33	118.75(18)	C3–Ru1–C1	63.17(7)
C37–C32–P2	118.89(15)	N1–Ru1–C7A	99.93(7)
C33–C32–P2	122.28(15)	C2–Ru1–C7A	62.26(7)
C34–C33–C32	120.3(2)	C3–Ru1–C7A	61.92(7)
C34–C33–H33	118.5(16)	C1–Ru1–C7A	37.01(7)
C32–C33–H33	121.1(16)	N1–Ru1–C3A	105.26(7)
C35–C34–C33	120.4(2)	C2–Ru1–C3A	62.41(7)
C35–C34–H34	120.5(16)	C3–Ru1–C3A	37.10(7)
C33–C34–H34	119.1(16)	C1–Ru1–C3A	62.29(7)
C34–C35–C36	119.8(2)	C7A–Ru1–C3A	36.75(7)
C34–C35–H35	120.1(16)	N1–Ru1–P1	89.65(5)
C36–C35–H35	120.0(16)	C2–Ru1–P1	93.68(5)
C35–C36–C37	119.9(2)	C3–Ru1–P1	131.09(6)
C35–C36–H36	122.3(15)	C1–Ru1–P1	81.01(5)
C37–C36–H36	117.8(15)	C7A–Ru1–P1	107.71(5)
C36–C37–C32	120.80(19)	C3A–Ru1–P1	142.57(5)
C36–C37–H37	119.2(14)	N1–Ru1–P2	85.78(5)
C32–C37–H37	120.0(14)	C2–Ru1–P2	110.23(5)
C39–C38–C43	118.96(18)	C3–Ru1–P2	91.79(5)
C39–C38–P2	123.60(15)	C1–Ru1–P2	148.33(5)
C43–C38–P2	117.43(14)	C7A–Ru1–P2	146.54(5)

C3A–Ru1–P2	109.86(5)	F5–P3–F1	88.65(10)
P1–Ru1–P2	105.243(19)	F4–P3–F1	89.42(10)
F6–P3–F5	92.69(12)	F2–P3–F1	88.48(10)
F6–P3–F4	91.64(12)	F6–P3–F3	89.25(11)
F5–P3–F4	91.77(11)	F5–P3–F3	178.01(11)
F6–P3–F2	90.40(12)	F4–P3–F3	87.71(9)
F5–P3–F2	91.09(11)	F2–P3–F3	89.36(10)
F4–P3–F2	176.40(12)	F1–P3–F3	89.42(9)
F6–P3–F1	178.27(13)		

Symmetry transformations used to generate equivalent atoms:

Table 4. Anisotropic displacement parameters [$Å^2 \times 10^3$]. The anisotropic displacement factor exponent takes the form: $-2\pi^2[h^2a^{*2}U^{11} + \cdots + 2\,h\,k\,a^*\,b^*\,U^{12}]$.

Atom	U^{11}	U^{22}	U^{33}	U^{23}	U^{13}	U^{12}
C1	18(1)	11(1)	20(1)	8(1)	5(1)	5(1)
C2	15(1)	13(1)	22(1)	7(1)	5(1)	3(1)
C3	14(1)	10(1)	27(1)	6(1)	−1(1)	1(1)
C3A	21(1)	9(1)	19(1)	3(1)	0(1)	4(1)
C4	33(1)	15(1)	18(1)	4(1)	2(1)	9(1)
C5	43(1)	24(1)	21(1)	6(1)	13(1)	18(1)
C6	31(1)	29(1)	38(1)	12(1)	17(1)	20(1)
C7	21(1)	19(1)	28(1)	8(1)	3(1)	11(1)
C7A	18(1)	10(1)	19(1)	5(1)	2(1)	6(1)
C8	15(1)	17(1)	19(1)	7(1)	2(1)	6(1)
C9	19(1)	17(1)	18(1)	7(1)	3(1)	5(1)
C10	23(1)	17(1)	18(1)	7(1)	1(1)	7(1)
C11	27(1)	20(1)	24(1)	8(1)	7(1)	7(1)
C11'	30(1)	21(1)	29(1)	12(1)	6(1)	11(1)
C12'	48(2)	26(1)	40(1)	19(1)	11(1)	20(1)
C12	35(1)	30(1)	30(1)	18(1)	10(1)	6(1)
C13	45(2)	23(1)	42(1)	19(1)	7(1)	9(1)
C14	17(1)	15(1)	13(1)	3(1)	0(1)	3(1)
C15	19(1)	18(1)	16(1)	4(1)	5(1)	7(1)
C16	18(1)	29(1)	22(1)	5(1)	4(1)	11(1)
C17	17(1)	28(1)	25(1)	4(1)	3(1)	−1(1)
C18	27(1)	22(1)	37(1)	14(1)	−1(1)	−4(1)
C19	23(1)	23(1)	33(1)	14(1)	−6(1)	2(1)
C20	25(1)	20(1)	15(1)	7(1)	3(1)	13(1)
C21	34(1)	20(1)	23(1)	6(1)	0(1)	14(1)
C22	59(2)	25(1)	21(1)	3(1)	4(1)	26(1)
C23	59(2)	40(1)	27(1)	17(1)	20(1)	38(1)
C24	35(1)	46(1)	30(1)	21(1)	16(1)	27(1)
C25	27(1)	28(1)	18(1)	8(1)	6(1)	14(1)
C26	12(1)	14(1)	19(1)	6(1)	4(1)	7(1)
C27	17(1)	17(1)	19(1)	6(1)	3(1)	8(1)
C28	17(1)	16(1)	29(1)	5(1)	2(1)	6(1)
C29	19(1)	18(1)	38(1)	14(1)	10(1)	5(1)
C30	24(1)	24(1)	30(1)	16(1)	12(1)	10(1)
C31	20(1)	18(1)	20(1)	7(1)	6(1)	9(1)
C32	13(1)	18(1)	14(1)	4(1)	2(1)	7(1)
C33	19(1)	20(1)	24(1)	9(1)	7(1)	9(1)
C34	25(1)	26(1)	33(1)	10(1)	11(1)	17(1)
C35	21(1)	36(1)	26(1)	11(1)	11(1)	16(1)
C36	19(1)	29(1)	29(1)	16(1)	11(1)	9(1)
C37	19(1)	20(1)	27(1)	11(1)	7(1)	9(1)
C38	18(1)	13(1)	15(1)	6(1)	2(1)	6(1)

C39	20(1)	21(1)	22(1)	6(1)	2(1)	10(1)
C40	22(1)	24(1)	24(1)	4(1)	−5(1)	7(1)
C41	35(1)	16(1)	16(1)	1(1)	−1(1)	8(1)
C42	31(1)	16(1)	18(1)	6(1)	9(1)	9(1)
C43	19(1)	15(1)	20(1)	6(1)	5(1)	5(1)
C44	16(1)	20(1)	28(1)	9(1)	7(1)	9(1)
C45	21(1)	30(1)	48(2)	21(1)	16(1)	8(1)
N1	15(1)	17(1)	19(1)	6(1)	4(1)	8(1)
P1	14(1)	12(1)	15(1)	5(1)	1(1)	4(1)
P2	12(1)	12(1)	13(1)	4(1)	3(1)	4(1)
Ru1	11(1)	11(1)	15(1)	4(1)	2(1)	4(1)
P3	26(1)	26(1)	32(1)	14(1)	9(1)	13(1)
F1	52(1)	33(1)	44(1)	16(1)	24(1)	10(1)
F2	41(1)	64(1)	113(2)	54(1)	23(1)	36(1)
F3	26(1)	27(1)	69(1)	18(1)	5(1)	2(1)
F4	32(1)	50(1)	83(1)	32(1)	−10(1)	14(1)
F5	105(2)	28(1)	40(1)	−2(1)	−2(1)	17(1)
F6	136(2)	82(1)	76(1)	53(1)	79(2)	69(2)

APPENDIX II: X-RAY STRUCTURE OF RUTHENIUM COMPLEX **80**

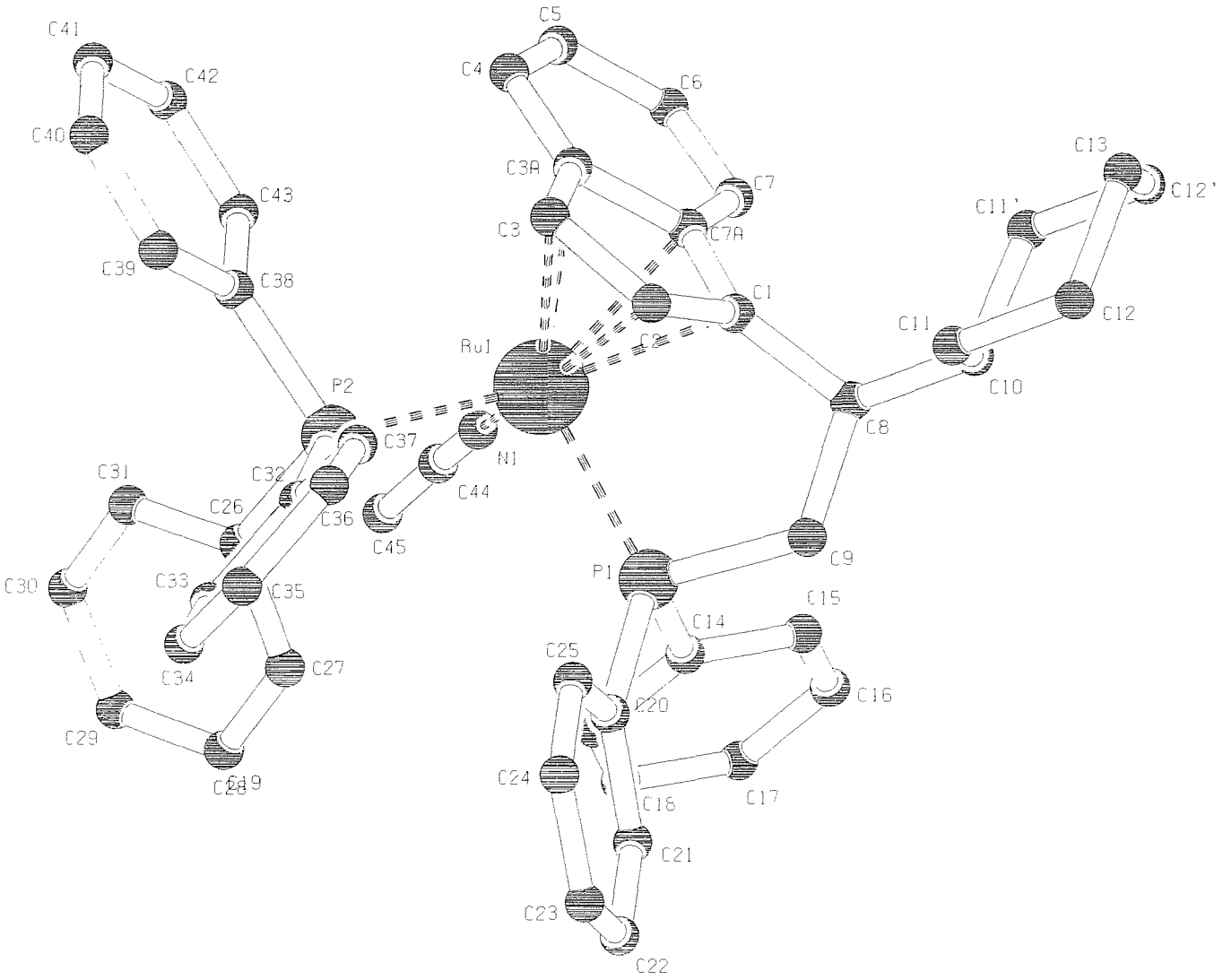

University of Southampton · Department of Chemistry

EPSRC National Crystallography Service

Table 1. Crystal data and structure refinement.

Identification code	**03sot0178 (DCP099/1)**	
Empirical formula	$C_{53}H_{54}ClP_2Ru$	
Formula weight	889.42	
Temperature	120(2) K	
Wavelength	0.71073 Å	
Crystal system	Orthorhombic	
Space group	$Pna2_1$	
Unit cell dimensions	a = 17.914(2) Å	α = 90°
	b = 10.939(2) Å	β = 90°
	c = 22.184(5) Å	γ = 90°
Volume	4347.2(14) Å^3	
Z	4	
Density (calculated)	1.359 Mg / m^3	
Absorption coefficient	0.532 mm^{-1}	
F(000)	1852	
Crystal	Plate; orange	
Crystal size	0.16 × 0.08 × 0.02 mm^3	
θ range for data collection	2.92 – 27.47°	
Index ranges	$-23 \le h \le 22$, $-13 \le k \le 14$, $-28 \le l \le 28$	
Reflections collected	56108	
Independent reflections	9792 [R_{int} = 0.0991]	
Completeness to θ = 27.47°	99.5 %	
Absorption correction	Semi-empirical from equivalents	
Max. and min. transmission	0.9894 and 0.9197	
Refinement method	Full-matrix least-squares on F^2	
Data / restraints / parameters	9792 / 1 / 515	
Goodness-of-fit on F^2	1.133	
Final R indices [$F^2 > 2\sigma(F^2)$]	$R1$ = 0.0652, $wR2$ = 0.1476	
R indices (all data)	$R1$ = 0.0802, $wR2$ = 0.1546	
Absolute structure parameter	0.04(5)	
Extinction coefficient	0.0023(4)	
Largest diff. peak and hole	0.964 and −0.908 e Å^{-3}	

Diffractometer: *Nonius KappaCCD* area detector (ϕ scans and ω scans to fill *asymmetric unit* sphere). **Cell determination:** DirAx (Duisenberg, A.J.M.(1992). J. Appl. Cryst. 25, 92-96.) **Data collection:** Collect (Collect: Data collection software, R. Hooft, Nonius B.V., 1998). **Data reduction and cell refinement**: *Denzo* (Z. Otwinowski & W. Minor, *Methods in Enzymology* (1997) Vol. **276**: *Macromolecular Crystallography*, part A, pp. 307–326; C. W. Carter, Jr. & R. M. Sweet, Eds., Academic Press). **Absorption correction**: *SORTAV* (R. H. Blessing, Acta Cryst. A**51** (1995) 33–37; R. H. Blessing, J. Appl. Cryst. **30** (1997) 421–426). **Structure solution**: *SHELXS97* (G. M. Sheldrick, Acta Cryst. (1990) A**46** 467–473). **Structure refinement**: *SHELXL97* (G. M. Sheldrick (1997), University of Göttingen, Germany). **Graphics:** Cameron - A Molecular Graphics Package. (D. M. Watkin, L. Pearce and C. K. Prout, Chemical Crystallography Laboratory, University of Oxford, 1993).

Special details:
The system was found to have higher symmetry than the data suggested. The symmetry was changed using the Addsym module of Platon.

APPENDIX III: X-RAY STRUCTURE OF RUTHENIUM COMPLEX **81**

Table 2. Atomic coordinates [$\times 10^4$], equivalent isotropic displacement parameters [$Å^2 \times 10^3$] and site occupancy factors. U_{eq} is defined as one third of the trace of the orthogonalized U^{ij} tensor.

Atom	*x*	*y*	*z*	U_{eq}	*S.o.f.*
C1	9208(4)	10323(6)	8473(3)	33(1)	1
C2	8716(3)	10836(5)	8032(3)	32(1)	1
C3	9155(4)	11769(5)	7726(3)	38(2)	1
C3A	9830(4)	11808(5)	7951(3)	40(2)	1
C4	10483(4)	12707(6)	7826(4)	51(2)	1
C5	11180(4)	12390(7)	8170(3)	51(2)	1
C6	11044(4)	11976(7)	8809(3)	47(2)	1
C7	10601(4)	10772(6)	8821(3)	40(2)	1
C7A	9913(4)	10916(5)	8424(3)	35(1)	1
C8	9021(4)	9267(6)	8895(3)	38(1)	1
C9	8732(3)	8192(5)	8511(3)	35(1)	1
C10	8473(4)	9717(7)	9397(3)	42(2)	1
C11'	8840(5)	10632(9)	9811(4)	65(2)	1
C11	8152(4)	8640(7)	9760(3)	43(2)	1
C12	7624(5)	9094(8)	10259(3)	57(2)	1
C12'	8301(6)	11056(9)	10293(4)	76(3)	1
C13	7998(6)	10006(10)	10667(4)	77(3)	1
C14	10168(4)	7153(6)	8280(3)	38(1)	1
C15	10911(4)	7525(7)	8246(3)	43(2)	1
C16	11462(4)	6860(8)	8524(4)	56(2)	1
C17	11283(5)	5783(8)	8844(4)	61(2)	1
C18	10561(6)	5395(7)	8882(4)	60(2)	1
C19	9992(5)	6060(6)	8603(3)	47(2)	1
C20	9007(3)	6655(5)	7483(3)	36(1)	1
C21	9466(4)	5853(6)	7171(4)	49(2)	1
C22	9162(5)	4886(6)	6865(4)	54(2)	1
C23	8436(5)	4675(6)	6839(4)	52(2)	1
C24	7958(4)	5428(6)	7145(3)	45(2)	1
C25	8237(4)	6429(6)	7473(3)	41(2)	1
C26	9263(3)	8396(6)	6141(3)	34(1)	1
C27	9957(4)	7802(7)	6179(3)	45(2)	1
C28	10115(5)	6795(8)	5835(4)	57(2)	1
C29	9576(5)	6327(8)	5443(4)	58(2)	1
C30	8901(5)	6887(7)	5404(3)	55(2)	1
C31	8724(4)	7933(7)	5745(3)	49(2)	1
C32	8101(3)	9967(5)	6609(3)	30(1)	1
C33	7636(4)	8989(7)	6747(4)	53(2)	1
C34	6872(4)	9170(8)	6826(4)	59(2)	1
C35	6569(4)	10332(8)	6772(4)	52(2)	1
C36	7018(4)	11334(7)	6643(4)	51(2)	1
C37	7793(3)	11145(6)	6555(3)	40(2)	1
C38	9414(4)	10972(6)	6056(3)	35(1)	1
C39	9096(4)	11026(7)	5484(3)	47(2)	1
C40	9325(4)	11905(7)	5073(3)	49(2)	1
C41	9884(4)	12728(6)	5224(3)	45(2)	1
C42	10213(4)	12649(6)	5780(3)	40(2)	1
C43	9989(4)	11771(6)	6194(3)	35(1)	1
Cl1	10898(1)	9765(2)	7159(1)	38(1)	1
P1	9416(1)	7967(1)	7893(1)	31(1)	1
P2	9126(1)	9787(2)	6604(1)	27(1)	1
Ru1	9621(1)	9927(1)	7565(1)	26(1)	1
C101	8585(7)	14028(11)	9608(7)	103(4)	1
C102	8572(7)	13672(11)	9038(5)	88(3)	1
C103	8126(7)	14177(9)	8632(6)	83(3)	1
C104	7534(6)	15370(8)	9351(6)	73(3)	1
C105	7639(5)	14989(9)	8798(5)	68(3)	1
C106	8054(12)	15000(11)	9819(6)	120(7)	1

APPENDIX III: X-RAY STRUCTURE OF RUTHENIUM COMPLEX 81

Table 3. Bond lengths [Å] and angles [°].

C1–C7A	1.424(9)	C18–H18	0.9500
C1–C2	1.432(9)	C19–H19	0.9500
C1–C8	1.525(9)	C20–C21	1.386(9)
C1–Ru1	2.188(7)	C20–C25	1.403(8)
C2–C3	1.456(9)	C20–P1	1.850(6)
C2–Ru1	2.166(6)	C21–C22	1.370(9)
C2–H2	0.9500	C21–H21	0.9500
C3–C3A	1.309(10)	C22–C23	1.322(12)
C3–Ru1	2.210(6)	C22–H22	0.9500
C3–H3	0.9500	C23–C24	1.368(12)
C3A–C7A	1.441(9)	C23–H23	0.9500
C3A–C4	1.554(9)	C24–C25	1.406(9)
C3A–Ru1	2.260(6)	C24–H24	0.9500
C4–C5	1.504(11)	C25–H25	0.9500
C4–H4A	0.9900	C26–C31	1.400(9)
C4–H4B	0.9900	C26–C27	1.406(9)
C5–C6	1.508(10)	C26–P2	1.853(6)
C5–H5A	0.9900	C27–C28	1.370(10)
C5–H5B	0.9900	C27–H27	0.9500
C6–C7	1.538(9)	C28–C29	1.396(11)
C6–H6A	0.9900	C28–H28	0.9500
C6–H6B	0.9900	C29–C30	1.359(12)
C7–C7A	1.522(9)	C29–H29	0.9500
C7–H7A	0.9900	C30–C31	1.408(11)
C7–H7B	0.9900	C30–H30	0.9500
C7A–Ru1	2.253(6)	C31–H31	0.9500
C8–C9	1.542(8)	C32–C33	1.389(9)
C8–C10	1.564(9)	C32–C37	1.408(8)
C8–H8	1.0000	C32–P2	1.846(6)
C9–P1	1.855(6)	C33–C34	1.394(10)
C9–H9A	0.9900	C33–H33	0.9500
C9–H9B	0.9900	C34–C35	1.388(11)
C10–C11'	1.508(11)	C34–H34	0.9500
C10–C11	1.538(10)	C35–C36	1.389(11)
C11'–C12'	1.514(12)	C35–H35	0.9500
C11'–H11A	0.9900	C36–C37	1.417(9)
C11'–H11B	0.9900	C36–H36	0.9500
C11–C12	1.539(10)	C37–H37	0.9500
C11–H11C	0.9900	C38–C43	1.384(9)
C11–H11D	0.9900	C38–C39	1.393(9)
C12–C13	1.504(12)	C38–P2	1.851(6)
C12–H12A	0.9900	C39–C40	1.387(10)
C12–H12B	0.9900	C39–H39	0.9500
C12'–C13	1.517(13)	C40–C41	1.387(10)
C12'–H12C	0.9900	C40–H40	0.9500
C12'–H12D	0.9900	C41–C42	1.370(10)
C13–H13A	0.9900	C41–H41	0.9500
C13–H13B	0.9900	C42–C43	1.389(9)
C14–C15	1.395(10)	C42–H42	0.9500
C14–C19	1.429(9)	C43–H43	0.9500
C14–P1	1.827(6)	Cl1–Ru1	2.4646(15)
C15–C16	1.373(10)	P1–Ru1	2.2937(17)
C15–H15	0.9500	P2–Ru1	2.3144(18)
C16–C17	1.412(13)	C101–C102	1.324(16)
C16–H16	0.9500	C101–C106	1.50(2)
C17–C18	1.363(13)	C101–H101	0.9500
C17–H17	0.9500	C102–C103	1.325(15)
C18–C19	1.397(10)	C102–H102	0.9500

C103–C105	1.299(14)	C7–C7A–Ru1	128.9(4)
C103–H103	0.9500	C1–C8–C9	108.2(6)
C104–C105	1.309(15)	C1–C8–C10	109.7(5)
C104–C106	1.45(2)	C9–C8–C10	115.0(6)
C104–H104	0.9500	C1–C8–H8	107.9
C105–H105	0.9500	C9–C8–H8	107.9
C106–H106	0.9500	C10–C8–H8	107.9
		C8–C9–P1	106.8(4)
C7A–C1–C2	108.4(6)	C8–C9–H9A	110.4
C7A–C1–C8	125.9(6)	P1–C9–H9A	110.4
C2–C1–C8	125.5(6)	C8–C9–H9B	110.4
C7A–C1–Ru1	73.8(4)	P1–C9–H9B	110.4
C2–C1–Ru1	69.9(4)	H9A–C9–H9B	108.6
C8–C1–Ru1	119.3(4)	C11'–C10–C11	110.7(6)
C1–C2–C3	105.1(5)	C11'–C10–C8	111.6(6)
C1–C2–Ru1	71.7(4)	C11–C10–C8	111.4(6)
C3–C2–Ru1	72.2(3)	C10–C11'–C12'	110.8(7)
C1–C2–H2	127.5	C10–C11'–H11A	109.5
C3–C2–H2	127.5	C12'–C11'–H11A	109.5
Ru1–C2–H2	120.6	C10–C11'–H11B	109.5
C3A–C3–C2	110.2(6)	C12'–C11'–H11B	109.5
C3A–C3–Ru1	75.1(4)	H11A–C11'–H11B	108.1
C2–C3–Ru1	68.9(3)	C10–C11–C12	111.0(6)
C3A–C3–H3	124.9	C10–C11–H11C	109.4
C2–C3–H3	124.9	C12–C11–H11C	109.4
Ru1–C3–H3	122.6	C10–C11–H11D	109.4
C3–C3A–C7A	110.6(6)	C12–C11–H11D	109.4
C3–C3A–C4	130.4(6)	H11C–C11–H11D	108.0
C7A–C3A–C4	118.7(6)	C13–C12–C11	112.0(7)
C3–C3A–Ru1	70.9(4)	C13–C12–H12A	109.2
C7A–C3A–Ru1	71.1(3)	C11–C12–H12A	109.2
C4–C3A–Ru1	129.3(4)	C13–C12–H12B	109.2
C5–C4–C3A	112.9(6)	C11–C12–H12B	109.2
C5–C4–H4A	109.0	H12A–C12–H12B	107.9
C3A–C4–H4A	109.0	C11'–C12'–C13	112.5(8)
C5–C4–H4B	109.0	C11'–C12'–H12C	109.1
C3A–C4–H4B	109.0	C13–C12'–H12C	109.1
H4A–C4–H4B	107.8	C11'–C12'–H12D	109.1
C4–C5–C6	114.3(6)	C13–C12'–H12D	109.1
C4–C5–H5A	108.7	H12C–C12'–H12D	107.8
C6–C5–H5A	108.7	C12–C13–C12'	109.4(7)
C4–C5–H5B	108.7	C12–C13–H13A	109.8
C6–C5–H5B	108.7	C12'–C13–H13A	109.8
H5A–C5–H5B	107.6	C12–C13–H13B	109.8
C5–C6–C7	110.9(6)	C12'–C13–H13B	109.8
C5–C6–H6A	109.5	H13A–C13–H13B	108.2
C7–C6–H6A	109.5	C15–C14–C19	118.8(6)
C5–C6–H6B	109.5	C15–C14–P1	122.4(5)
C7–C6–H6B	109.5	C19–C14–P1	118.7(5)
H6A–C6–H6B	108.0	C16–C15–C14	120.5(7)
C7A–C7–C6	108.6(6)	C16–C15–H15	119.7
C7A–C7–H7A	110.0	C14–C15–H15	119.7
C6–C7–H7A	110.0	C15–C16–C17	120.2(8)
C7A–C7–H7B	110.0	C15–C16–H16	119.9
C6–C7–H7B	110.0	C17–C16–H16	119.9
H7A–C7–H7B	108.4	C18–C17–C16	120.4(7)
C1–C7A–C3A	105.8(6)	C18–C17–H17	119.8
C1–C7A–C7	128.8(6)	C16–C17–H17	119.8
C3A–C7A–C7	125.1(6)	C17–C18–C19	120.2(8)
C1–C7A–Ru1	68.8(4)	C17–C18–H18	119.9
C3A–C7A–Ru1	71.6(4)	C19–C18–H18	119.9

C18–C19–C14	119.7(8)	C40–C39–H39	119.7
C18–C19–H19	120.1	C38–C39–H39	119.7
C14–C19–H19	120.1	C41–C40–C39	120.2(7)
C21–C20–C25	117.6(6)	C41–C40–H40	119.9
C21–C20–P1	120.1(5)	C39–C40–H40	119.9
C25–C20–P1	122.3(5)	C42–C41–C40	119.2(6)
C22–C21–C20	120.1(7)	C42–C41–H41	120.4
C22–C21–H21	120.0	C40–C41–H41	120.4
C20–C21–H21	120.0	C41–C42–C43	121.0(6)
C23–C22–C21	123.1(8)	C41–C42–H42	119.5
C23–C22–H22	118.4	C43–C42–H42	119.5
C21–C22–H22	118.4	C38–C43–C42	120.4(6)
C22–C23–C24	119.3(7)	C38–C43–H43	119.8
C22–C23–H23	120.4	C42–C43–H43	119.8
C24–C23–H23	120.4	C14–P1–C20	98.3(3)
C23–C24–C25	120.2(7)	C14–P1–C9	101.8(3)
C23–C24–H24	119.9	C20–P1–C9	101.8(3)
C25–C24–H24	119.9	C14–P1–Ru1	119.1(2)
C20–C25–C24	119.7(7)	C20–P1–Ru1	129.2(2)
C20–C25–H25	120.2	C9–P1–Ru1	102.4(2)
C24–C25–H25	120.2	C32–P2–C38	101.9(3)
C31–C26–C27	118.8(6)	C32–P2–C26	102.9(3)
C31–C26–P2	123.6(5)	C38–P2–C26	100.0(3)
C27–C26–P2	117.6(5)	C32–P2–Ru1	111.6(2)
C28–C27–C26	121.3(7)	C38–P2–Ru1	116.9(2)
C28–C27–H27	119.4	C26–P2–Ru1	121.0(2)
C26–C27–H27	119.4	C2–Ru1–C1	38.4(2)
C27–C28–C29	120.0(8)	C2–Ru1–C3	38.9(2)
C27–C28–H28	120.0	C1–Ru1–C3	62.8(2)
C29–C28–H28	120.0	C2–Ru1–C7A	63.2(2)
C30–C29–C28	119.3(7)	C1–Ru1–C7A	37.4(2)
C30–C29–H29	120.3	C3–Ru1–C7A	60.9(2)
C28–C29–H29	120.3	C2–Ru1–C3A	61.6(2)
C29–C30–C31	122.2(7)	C1–Ru1–C3A	61.8(2)
C29–C30–H30	118.9	C3–Ru1–C3A	34.0(2)
C31–C30–H30	118.9	C7A–Ru1–C3A	37.2(2)
C26–C31–C30	118.4(7)	C2–Ru1–P1	99.10(17)
C26–C31–H31	120.8	C1–Ru1–P1	80.76(17)
C30–C31–H31	120.8	C3–Ru1–P1	137.79(16)
C33–C32–C37	119.2(6)	C7A–Ru1–P1	102.59(17)
C33–C32–P2	121.0(5)	C3A–Ru1–P1	139.24(17)
C37–C32–P2	119.1(4)	C2–Ru1–P2	100.59(16)
C32–C33–C34	120.5(7)	C1–Ru1–P2	137.00(18)
C32–C33–H33	119.8	C3–Ru1–P2	93.68(18)
C34–C33–H33	119.8	C7A–Ru1–P2	154.15(17)
C35–C34–C33	120.2(7)	C3A–Ru1–P2	118.20(18)
C35–C34–H34	119.9	P1–Ru1–P2	99.75(6)
C33–C34–H34	119.9	C2–Ru1–Cl1	154.50(17)
C34–C35–C36	120.9(7)	C1–Ru1–Cl1	131.61(19)
C34–C35–H35	119.5	C3–Ru1–Cl1	118.37(18)
C36–C35–H35	119.5	C7A–Ru1–Cl1	97.35(17)
C35–C36–C37	118.8(6)	C3A–Ru1–Cl1	92.88(19)
C35–C36–H36	120.6	P1–Ru1–Cl1	101.36(6)
C37–C36–H36	120.6	P2–Ru1–Cl1	90.81(6)
C32–C37–C36	120.4(6)	C102–C101–C106	119.8(12)
C32–C37–H37	119.8	C102–C101–H101	120.1
C36–C37–H37	119.8	C106–C101–H101	120.1
C43–C38–C39	118.6(6)	C101–C102–C103	122.5(13)
C43–C38–P2	120.3(5)	C101–C102–H102	118.7
C39–C38–P2	121.0(5)	C103–C102–H102	118.7
C40–C39–C38	120.5(7)	C105–C103–C102	119.8(12)

C105–C103–H103	120.1	C103–C105–H105	117.2
C102–C103–H103	120.1	C104–C105–H105	117.2
C105–C104–C106	119.3(11)	C104–C106–C101	112.3(10)
C105–C104–H104	120.4	C104–C106–H106	123.8
C106–C104–H104	120.4	C101–C106–H106	123.8
C103–C105–C104	125.5(11)		

Symmetry transformations used to generate equivalent atoms:

APPENDIX III: X-RAY STRUCTURE OF RUTHENIUM COMPLEX **81**

Table 4. Anisotropic displacement parameters [$Å^2 \times 10^3$]. The anisotropic displacement factor exponent takes the form: $-2\pi^2[h^2a^{*2}U^{11} + \cdots + 2\,h\,k\,a^*\,b^*\,U^{12}]$.

Atom	U^{11}	U^{22}	U^{33}	U^{23}	U^{13}	U^{12}
C1	47(4)	20(3)	33(3)	−1(3)	−4(3)	−2(3)
C2	33(3)	38(3)	27(3)	−4(2)	−6(2)	0(2)
C3	64(4)	25(3)	25(3)	−3(2)	21(3)	4(3)
C3A	72(5)	26(3)	21(3)	−5(2)	12(3)	4(3)
C4	65(5)	40(4)	48(4)	−5(3)	1(4)	−21(3)
C5	52(4)	51(4)	51(4)	−9(3)	11(4)	−8(3)
C6	41(4)	49(4)	52(4)	−5(3)	−6(3)	−6(3)
C7	41(4)	44(4)	36(3)	−7(3)	−1(3)	−4(3)
C7A	43(3)	31(3)	31(3)	−8(2)	3(3)	−4(3)
C8	44(4)	34(3)	35(3)	−9(3)	−3(3)	1(3)
C9	35(3)	33(3)	39(3)	−4(3)	6(3)	−1(2)
C10	34(3)	68(5)	25(3)	0(3)	8(3)	10(3)
C11'	65(6)	82(6)	49(5)	−14(4)	14(4)	−28(5)
C11	44(4)	52(4)	34(4)	−4(3)	−2(3)	4(3)
C12	70(5)	69(5)	31(4)	9(4)	12(4)	−12(4)
C12'	80(6)	84(6)	64(6)	−41(5)	24(5)	−37(5)
C13	62(6)	139(10)	30(4)	−23(5)	16(4)	−37(6)
C14	47(4)	36(3)	32(3)	−1(3)	−6(3)	10(3)
C15	38(4)	46(4)	45(4)	−3(3)	−10(3)	1(3)
C16	37(4)	77(5)	54(5)	−7(4)	−8(3)	16(4)
C17	75(6)	65(5)	44(4)	−8(4)	−17(4)	35(5)
C18	95(7)	43(4)	41(4)	−7(3)	−22(4)	27(4)
C19	59(5)	39(4)	42(4)	4(3)	−7(3)	1(3)
C20	34(3)	39(3)	34(4)	3(3)	1(3)	−2(2)
C21	47(4)	44(4)	57(5)	−11(3)	−7(4)	3(3)
C22	60(5)	44(4)	56(5)	−15(3)	−24(4)	6(3)
C23	71(5)	37(4)	47(4)	−4(3)	−28(4)	−2(4)
C24	54(4)	44(4)	36(4)	6(3)	−18(3)	−8(3)
C25	39(3)	40(3)	45(4)	2(3)	1(3)	−5(3)
C26	36(3)	36(3)	29(3)	0(2)	1(3)	3(3)
C27	38(4)	52(4)	47(4)	−15(3)	0(3)	4(3)
C28	58(5)	59(5)	52(5)	−19(4)	5(4)	12(4)
C29	71(6)	60(5)	44(4)	−22(4)	3(4)	6(4)
C30	64(5)	61(5)	40(4)	−15(4)	−10(4)	−10(4)
C31	45(4)	58(4)	44(4)	−7(3)	−14(3)	−2(3)
C32	28(3)	32(3)	28(3)	2(2)	−1(2)	−1(2)
C33	28(3)	65(5)	68(5)	35(4)	−1(3)	2(3)
C34	32(4)	69(5)	76(6)	31(4)	0(4)	1(3)
C35	26(3)	72(5)	59(5)	4(4)	3(3)	8(3)
C36	39(4)	46(4)	70(5)	−11(4)	−7(4)	15(3)
C37	30(3)	37(3)	54(4)	−6(3)	−6(3)	−2(3)
C38	36(3)	46(4)	23(3)	5(3)	4(3)	−5(3)
C39	50(4)	58(4)	33(4)	7(3)	−10(3)	−16(4)
C40	56(5)	54(4)	37(4)	8(3)	−6(3)	−10(3)
C41	52(4)	35(3)	48(4)	8(3)	7(4)	0(3)
C42	43(4)	42(4)	35(4)	−5(3)	7(3)	−5(3)
C43	37(3)	41(3)	25(3)	2(3)	0(3)	−1(3)
Cl1	24(1)	52(1)	38(1)	−5(1)	6(1)	−5(1)
P1	33(1)	31(1)	30(1)	−2(1)	0(1)	4(1)
P2	27(1)	30(1)	23(1)	−1(1)	0(1)	−1(1)
Ru1	24(1)	31(1)	24(1)	−1(1)	1(1)	1(1)
C101	114(10)	81(8)	114(10)	−30(7)	−49(8)	8(7)
C102	98(8)	96(8)	70(7)	10(6)	9(6)	4(7)
C103	100(8)	58(5)	91(8)	13(5)	7(7)	−7(6)
C104	56(5)	53(5)	110(9)	−1(5)	26(6)	1(4)
C105	51(5)	78(6)	73(6)	13(5)	12(5)	−5(4)
C106	220(20)	89(8)	55(6)	−11(6)	28(9)	−69(10)

APPENDIX III: X-RAY STRUCTURE OF RUTHENIUM COMPLEX **81**

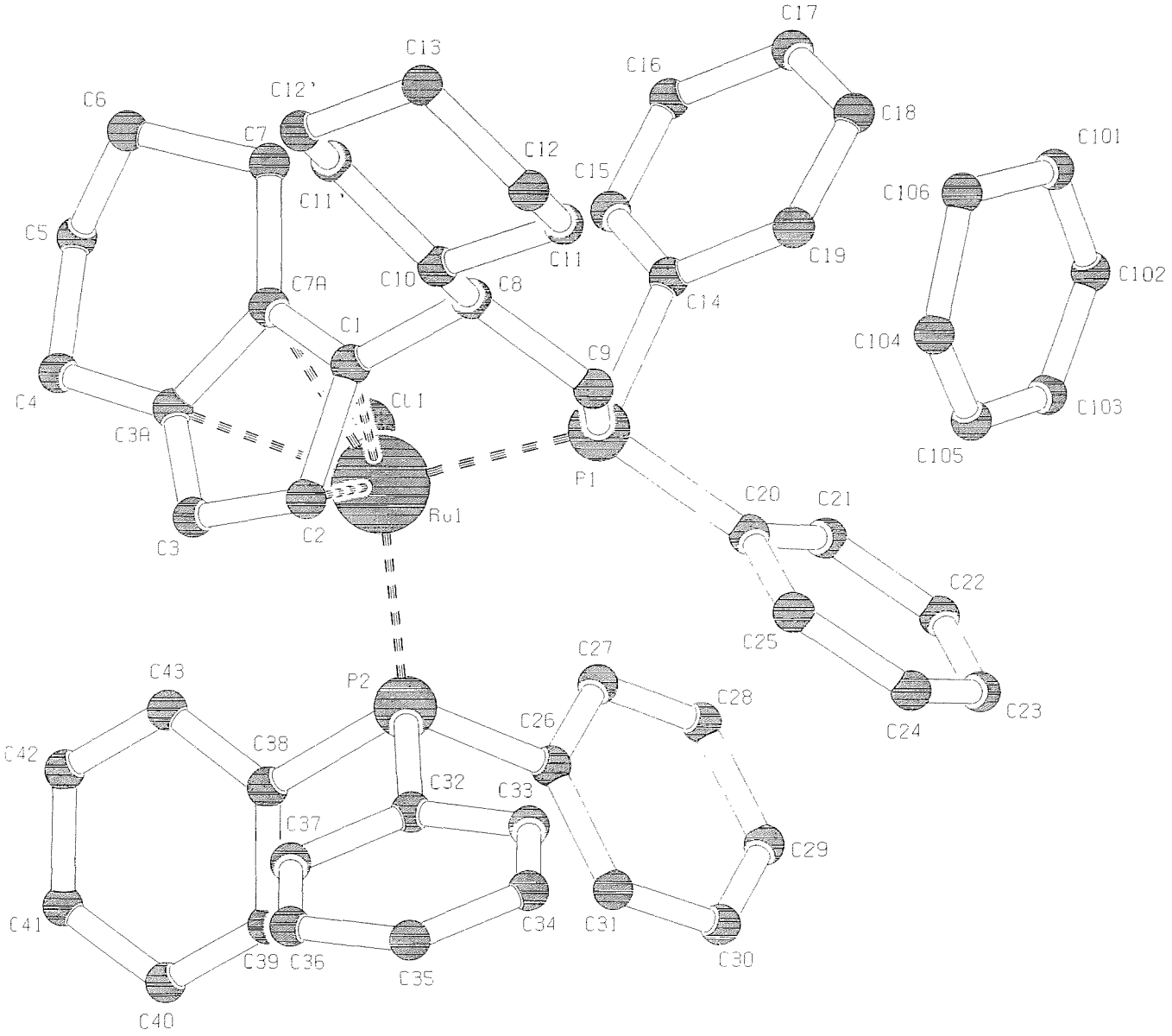

University of Southampton · Department of Chemistry

EPSRC National Crystallography Service

Table 1. Crystal data and structure refinement.

Identification code	**04sot0423 (DCP 115/1)**	
Empirical formula	$C_{49}H_{52}F_6NP_3Ru$	
Formula weight	962.90	
Temperature	120(2) K	
Wavelength	0.71073 Å	
Crystal system	Triclinic	
Space group	*P*–1	
Unit cell dimensions	a = 11.6409(5) Å	α = 105.529(5)°
	b = 12.5802(6) Å	β = 96.483(7)°
	c = 16.8044(11) Å	γ = 112.081(5)°
Volume	2133.4(2) Å^3	
Z	2	
Density (calculated)	1.499 Mg / m^3	
Absorption coefficient	0.543 mm^{-1}	
F(000)	992	
Crystal	Cut plate; light orange	
Crystal size	0.24 × 0.16 × 0.06 mm^3	
θ range for data collection	3.33 – 27.50°	
Index ranges	$-15 \le h \le 14$, $-15 \le k \le 16$, $-21 \le l \le 21$	
Reflections collected	35674	
Independent reflections	9730 [R_{int} = 0.0326]	
Completeness to θ = 27.50°	99.2 %	
Absorption correction	Semi-empirical from equivalents	
Max. and min. transmission	0.9681 and 0.8807	
Refinement method	Full-matrix least-squares on F^2	
Data / restraints / parameters	9730 / 0 / 750	
Goodness-of-fit on F^2	1.044	
Final *R* indices [$F^2 > 2\sigma(F^2)$]	*R1* = 0.0360, *wR2* = 0.0783	
R indices (all data)	*R1* = 0.0435, *wR2* = 0.0818	
Extinction coefficient	0.0027(4)	
Largest diff. peak and hole	0.739 and –0.786 e Å^{-3}	

Diffractometer: *Nonius KappaCCD* area detector (ϕ scans and ω scans to fill *asymmetric unit* sphere). **Cell determination:** DirAx (Duisenberg, A.J.M.(1992). J. Appl. Cryst. 25, 92-96.) **Data collection:** Collect (Collect: Data collection software, R. Hooft, Nonius B.V., 1998). **Data reduction and cell refinement**: *Denzo* (Z. Otwinowski & W. Minor, *Methods in Enzymology* (1997) Vol. **276**: *Macromolecular Crystallography*, part A, pp. 307–326; C. W. Carter, Jr. & R. M. Sweet, Eds., Academic Press). **Absorption correction**: *SORTAV* (R. H. Blessing, Acta Cryst. A**51** (1995) 33–37; R. H. Blessing, J. Appl. Cryst. **30** (1997) 421–426). **Structure solution**: *SHELXS97* (G. M. Sheldrick, Acta Cryst. (1990) A**46** 467–473). **Structure refinement**: *SHELXL97* (G. M. Sheldrick (1997), University of Göttingen, Germany). **Graphics:** Cameron - A Molecular Graphics Package. (D. M. Watkin, L. Pearce and C. K. Prout, Chemical Crystallography Laboratory, University of Oxford, 1993).

Special details:
The system was found to have higher symmetry than the data suggested. The Addsym module of Platon was used to change the symmetry.

APPENDIX IV: X-RAY STRUCTURE OF RUTHENIUM COMPLEX **82**

Table 2. Atomic coordinates [$\times 10^4$], equivalent isotropic displacement parameters [$Å^2 \times 10^3$] and site occupancy factors. U_{eq} is defined as one third of the trace of the orthogonalized U^{ij} tensor.

Atom	*x*	*y*	*z*	U_{eq}	*S.o.f.*
C1	7685(2)	1717(2)	2524(2)	21(1)	1
C2	6397(2)	1557(2)	2251(2)	22(1)	1
C3	6090(2)	1179(2)	1354(2)	23(1)	1
C3A	7174(2)	1114(2)	1048(1)	20(1)	1
C4	7296(3)	603(2)	170(2)	27(1)	1
C5	8679(3)	1036(3)	141(2)	33(1)	1
C6	9435(3)	808(3)	821(2)	36(1)	1
C7	9452(2)	1500(2)	1734(2)	26(1)	1
C7A	8155(2)	1462(2)	1790(1)	17(1)	1
C8	8451(2)	2174(2)	3434(2)	22(1)	1
C9	8358(2)	3334(2)	3909(2)	23(1)	1
C10	8069(2)	1228(2)	3901(2)	24(1)	1
C11	8395(3)	172(2)	3511(2)	30(1)	1
C11'	6676(3)	759(2)	3954(2)	29(1)	1
C12	8079(3)	−731(3)	3992(2)	39(1)	1
C12'	6362(3)	−152(3)	4435(2)	36(1)	1
C13	6696(3)	−1197(3)	4037(2)	42(1)	1
C14	10252(2)	5314(2)	3545(1)	19(1)	1
C15'	10732(2)	6397(2)	3370(2)	31(1)	1
C15	11126(2)	4964(2)	3903(1)	21(1)	1
C16'	12032(3)	7112(3)	3561(2)	36(1)	1
C16	12428(2)	5677(2)	4089(2)	26(1)	1
C17	12881(2)	6749(2)	3920(2)	30(1)	1
C18	7853(2)	5309(2)	3871(1)	22(1)	1
C19	8563(3)	6432(2)	4504(2)	30(1)	1
C19'	6529(3)	4789(3)	3741(2)	27(1)	1
C20	7952(3)	7009(3)	5006(2)	38(1)	1
C20'	5928(3)	5368(3)	4240(2)	35(1)	1
C21	6641(3)	6469(3)	4878(2)	39(1)	1
C22	5149(2)	4091(2)	1663(1)	18(1)	1
C23'	4955(2)	5140(2)	1762(2)	23(1)	1
C23	4247(2)	3120(2)	1821(2)	23(1)	1
C24	3170(2)	3190(2)	2062(2)	27(1)	1
C24'	3895(2)	5220(2)	2023(2)	29(1)	1
C25	2996(2)	4245(2)	2165(2)	28(1)	1
C26	7436(2)	5424(2)	1233(1)	17(1)	1
C27	8120(2)	6381(2)	1993(2)	20(1)	1
C27'	7547(2)	5649(2)	470(2)	21(1)	1
C28	8924(2)	7522(2)	1995(2)	23(1)	1
C28'	8363(2)	6793(2)	472(2)	25(1)	1
C29	9061(2)	7719(2)	1230(2)	26(1)	1
C30	5758(2)	3027(2)	153(1)	18(1)	1
C31	4503(2)	2725(2)	−234(2)	22(1)	1
C31'	6516(2)	2666(2)	−344(2)	20(1)	1
C32	4022(2)	2067(2)	−1096(2)	28(1)	1
C32'	6039(2)	2023(2)	−1204(2)	24(1)	1
C33	4785(3)	1720(2)	−1579(2)	27(1)	1
C34	9977(2)	4796(2)	1365(2)	22(1)	1
C35	11000(3)	5742(3)	1194(2)	34(1)	1
N1	9154(2)	4094(2)	1515(1)	20(1)	1
P1	8534(1)	4350(1)	3271(1)	18(1)	1
P2	6495(1)	3913(1)	1282(1)	15(1)	1
Ru1	7649(1)	3032(1)	1885(1)	15(1)	1
P3	2611(1)	198(1)	2795(1)	30(1)	1
F1	3287(2)	428(2)	2046(1)	45(1)	1
F2	3370(2)	1594(2)	3327(1)	66(1)	1
F3	1482(2)	440(2)	2367(1)	52(1)	1
F4	1857(2)	−1219(1)	2237(1)	44(1)	1
F5	3716(2)	−101(2)	3180(1)	59(1)	1
F6	1893(2)	−68(2)	3515(2)	75(1)	1

Table 3. Bond lengths [Å] and angles [°].

C1–C7A	1.414(3)	C16–C17	1.371(4)
C1–C2	1.437(3)	C16–H16A	0.92(3)
C1–C8	1.517(3)	C17–H17	0.92(3)
C1–Ru1	2.211(2)	C18–C19	1.390(3)
C2–C3	1.413(4)	C18–C19'	1.393(4)
C2–Ru1	2.175(2)	C18–P1	1.830(2)
C2–H2	0.98(3)	C19–C20	1.393(4)
C3–C3A	1.437(3)	C19–H19A	0.95(3)
C3–Ru1	2.206(2)	C19'–C20'	1.382(4)
C3–H3	0.88(3)	C19'–H19B	0.90(3)
C3A–C7A	1.435(3)	C20–C21	1.380(5)
C3A–C4	1.489(3)	C20–H20A	0.97(3)
C3A–Ru1	2.261(2)	C20'–C21	1.377(4)
C4–C5	1.504(4)	C20'–H20B	0.92(3)
C4–H4A	0.99(3)	C21–H21	0.93(3)
C4–H4B	0.96(3)	C22–C23'	1.391(3)
C5–C6	1.518(4)	C22–C23	1.393(3)
C5–H5A	1.07(3)	C22–P2	1.825(2)
C5–H5B	0.99(3)	C23'–C24'	1.384(3)
C6–C7	1.543(4)	C23'–H23B	0.91(3)
C6–H6A	1.08(3)	C23–C24	1.387(3)
C6–H6B	0.98(3)	C23–H23A	0.94(3)
C7–C7A	1.508(3)	C24–C25	1.385(4)
C7–H7A	0.97(3)	C24–H24A	0.93(3)
C7–H7B	0.99(3)	C24'–C25	1.380(4)
C7A–Ru1	2.236(2)	C24'–H24B	0.91(3)
C8–C9	1.515(3)	C25–H25	0.94(3)
C8–C10	1.552(3)	C26–C27	1.393(3)
C8–H8	1.05(3)	C26–C27'	1.394(3)
C9–P1	1.848(2)	C26–P2	1.833(2)
C9–H9A	0.99(3)	C27–C28	1.387(3)
C9–H9B	0.95(3)	C27–H27A	0.95(3)
C10–C11	1.519(3)	C27'–C28'	1.393(3)
C10–C11'	1.526(4)	C27'–H27B	0.93(3)
C10–H10	1.07(3)	C28–C29	1.388(4)
C11–C12	1.525(4)	C28–H28A	0.91(3)
C11–H11A	1.02(3)	C28'–C29	1.377(4)
C11–H11B	0.98(3)	C28'–H28B	0.95(3)
C11'–C12'	1.532(4)	C29–H29	0.93(3)
C11'–H11C	1.02(3)	C30–C31	1.392(3)
C11'–H11D	0.95(3)	C30–C31'	1.396(3)
C12–C13	1.511(5)	C30–P2	1.833(2)
C12–H12A	0.94(3)	C31–C32	1.388(3)
C12–H12B	1.02(4)	C31–H31A	0.91(3)
C12'–C13	1.517(4)	C31'–C32'	1.380(3)
C12'–H12C	0.99(3)	C31'–H31B	0.94(3)
C12'–H12D	0.95(2)	C32–C33	1.380(4)
C13–H13A	1.12(3)	C32–H32A	0.93(3)
C13–H13B	1.00(4)	C32'–C33	1.386(4)
C14–C15	1.390(3)	C32'–H32B	0.93(3)
C14–C15'	1.390(3)	C33–H33	1.00(3)
C14–P1	1.831(2)	C34–N1	1.140(3)
C15'–C16'	1.384(4)	C34–C35	1.453(3)
C15'–H15B	0.94(3)	C35–H35A	0.93(4)
C15–C16	1.385(3)	C35–H35B	0.90(5)
C15–H15A	0.96(3)	C35–H35C	0.91(4)
C16'–C17	1.379(4)	N1–Ru1	2.0423(19)
C16'–H16B	0.90(3)	P1–Ru1	2.3112(6)

APPENDIX IV: X-RAY STRUCTURE OF RUTHENIUM COMPLEX **82**

P2–Ru1	2.3380(6)	C7–C7A–Ru1	124.43(15)
P3–F2	1.5744(19)	C9–C8–C1	108.10(19)
P3–F6	1.585(2)	C9–C8–C10	111.73(19)
P3–F5	1.5872(18)	C1–C8–C10	114.56(19)
P3–F1	1.5919(18)	C9–C8–H8	107.6(14)
P3–F3	1.5950(18)	C1–C8–H8	107.2(14)
P3–F4	1.6031(17)	C10–C8–H8	107.4(14)
		C8–C9–P1	111.85(16)
C7A–C1–C2	107.6(2)	C8–C9–H9A	107.9(15)
C7A–C1–C8	125.4(2)	P1–C9–H9A	102.7(15)
C2–C1–C8	126.8(2)	C8–C9–H9B	113.3(16)
C7A–C1–Ru1	72.45(12)	P1–C9–H9B	109.9(16)
C2–C1–Ru1	69.53(13)	H9A–C9–H9B	111(2)
C8–C1–Ru1	119.94(15)	C11–C10–C11'	110.5(2)
C3–C2–C1	107.6(2)	C11–C10–C8	111.1(2)
C3–C2–Ru1	72.36(13)	C11'–C10–C8	114.2(2)
C1–C2–Ru1	72.22(13)	C11–C10–H10	108.7(15)
C3–C2–H2	126.3(18)	C11'–C10–H10	106.0(15)
C1–C2–H2	125.8(18)	C8–C10–H10	106.0(15)
Ru1–C2–H2	126.1(18)	C10–C11–C12	111.4(2)
C2–C3–C3A	109.4(2)	C10–C11–H11A	108.0(16)
C2–C3–Ru1	70.02(13)	C12–C11–H11A	109.4(16)
C3A–C3–Ru1	73.36(12)	C10–C11–H11B	106.7(17)
C2–C3–H3	128.0(18)	C12–C11–H11B	110.7(17)
C3A–C3–H3	122.6(18)	H11A–C11–H11B	111(2)
Ru1–C3–H3	121.5(17)	C10–C11'–C12'	111.8(2)
C7A–C3A–C3	105.9(2)	C10–C11'–H11C	106.5(16)
C7A–C3A–C4	122.5(2)	C12'–C11'–H11C	111.3(16)
C3–C3A–C4	130.8(2)	C10–C11'–H11D	106.8(17)
C7A–C3A–Ru1	70.45(12)	C12'–C11'–H11D	104.1(17)
C3–C3A–Ru1	69.14(12)	H11C–C11'–H11D	116(2)
C4–C3A–Ru1	132.57(16)	C13–C12–C11	111.7(2)
C3A–C4–C5	110.6(2)	C13–C12–H12A	111(2)
C3A–C4–H4A	108.1(15)	C11–C12–H12A	112(2)
C5–C4–H4A	109.1(15)	C13–C12–H12B	103(2)
C3A–C4–H4B	113.5(17)	C11–C12–H12B	107(2)
C5–C4–H4B	109.2(17)	H12A–C12–H12B	111(3)
H4A–C4–H4B	106(2)	C13–C12'–C11'	110.9(2)
C4–C5–C6	111.2(2)	C13–C12'–H12C	109.2(17)
C4–C5–H5A	110.7(16)	C11'–C12'–H12C	110.1(17)
C6–C5–H5A	107.8(16)	C13–C12'–H12D	109.4(13)
C4–C5–H5B	109.7(18)	C11'–C12'–H12D	107.2(13)
C6–C5–H5B	107.2(19)	H12C–C12'–H12D	110(2)
H5A–C5–H5B	110(2)	C12–C13–C12'	110.9(2)
C5–C6–C7	113.5(2)	C12–C13–H13A	107.8(17)
C5–C6–H6A	105.5(17)	C12'–C13–H13A	109.3(17)
C7–C6–H6A	108.1(16)	C12–C13–H13B	113(2)
C5–C6–H6B	110.6(18)	C12'–C13–H13B	109(2)
C7–C6–H6B	108.5(18)	H13A–C13–H13B	107(3)
H6A–C6–H6B	111(2)	C15–C14–C15'	117.6(2)
C7A–C7–C6	110.8(2)	C15–C14–P1	121.16(17)
C7A–C7–H7A	108.6(18)	C15'–C14–P1	121.17(18)
C6–C7–H7A	112.3(18)	C16'–C15'–C14	121.2(2)
C7A–C7–H7B	109.6(18)	C16'–C15'–H15B	118.5(19)
C6–C7–H7B	106.9(18)	C14–C15'–H15B	120.3(19)
H7A–C7–H7B	109(2)	C16–C15–C14	121.1(2)
C1–C7A–C3A	109.4(2)	C16–C15–H15A	119.3(16)
C1–C7A–C7	128.4(2)	C14–C15–H15A	119.6(16)
C3A–C7A–C7	122.2(2)	C17–C16'–C15'	120.1(2)
C1–C7A–Ru1	70.47(12)	C17–C16'–H16B	118(2)
C3A–C7A–Ru1	72.35(12)	C15'–C16'–H16B	122(2)

C17–C16–C15	120.4(2)	C31–C30–P2	123.65(17)
C17–C16–H16A	121.6(18)	C31'–C30–P2	117.60(17)
C15–C16–H16A	118.0(18)	C32–C31–C30	120.1(2)
C16–C17–C16'	119.6(2)	C32–C31–H31A	119.2(16)
C16–C17–H17	123.1(18)	C30–C31–H31A	120.6(16)
C16'–C17–H17	117.3(18)	C32'–C31'–C30	121.0(2)
C19–C18–C19'	118.9(2)	C32'–C31'–H31B	119.6(15)
C19–C18–P1	124.6(2)	C30–C31'–H31B	119.4(15)
C19'–C18–P1	116.06(18)	C33–C32–C31	120.4(2)
C18–C19–C20	120.0(3)	C33–C32–H32A	119.4(18)
C18–C19–H19A	118.2(17)	C31–C32–H32A	120.2(18)
C20–C19–H19A	121.8(17)	C31'–C32'–C33	119.6(2)
C20'–C19'–C18	120.8(3)	C31'–C32'–H32B	120.1(16)
C20'–C19'–H19B	120.6(18)	C33–C32'–H32B	120.2(16)
C18–C19'–H19B	118.6(18)	C32–C33–C32'	120.1(2)
C21–C20–C19	120.3(3)	C32–C33–H33	119.1(16)
C21–C20–H20A	121.8(19)	C32'–C33–H33	120.8(16)
C19–C20–H20A	117.9(19)	N1–C34–C35	176.7(3)
C21–C20'–C19'	120.0(3)	C34–C35–H35A	109(2)
C21–C20'–H20B	120(2)	C34–C35–H35B	111(3)
C19'–C20'–H20B	120(2)	H35A–C35–H35B	111(4)
C20'–C21–C20	120.1(3)	C34–C35–H35C	112(3)
C20'–C21–H21	119(2)	H35A–C35–H35C	112(3)
C20–C21–H21	121(2)	H35B–C35–H35C	103(4)
C23'–C22–C23	118.6(2)	C34–N1–Ru1	172.25(18)
C23'–C22–P2	122.46(17)	C18–P1–C14	104.99(11)
C23–C22–P2	118.85(17)	C18–P1–C9	97.92(11)
C24'–C23'–C22	120.6(2)	C14–P1–C9	104.23(11)
C24'–C23'–H23B	118.9(17)	C18–P1–Ru1	125.40(8)
C22–C23'–H23B	120.5(17)	C14–P1–Ru1	116.53(7)
C24–C23–C22	120.7(2)	C9–P1–Ru1	104.10(8)
C24–C23–H23A	119.8(17)	C22–P2–C26	102.58(10)
C22–C23–H23A	119.5(17)	C22–P2–C30	101.58(10)
C25–C24–C23	120.0(2)	C26–P2–C30	101.38(10)
C25–C24–H24A	120.1(17)	C22–P2–Ru1	121.99(7)
C23–C24–H24A	119.9(17)	C26–P2–Ru1	115.95(7)
C25–C24'–C23'	120.4(2)	C30–P2–Ru1	110.60(7)
C25–C24'–H24B	119.1(19)	N1–Ru1–C2	161.61(8)
C23'–C24'–H24B	120.5(19)	N1–Ru1–C3	137.32(9)
C24'–C25–C24	119.7(2)	C2–Ru1–C3	37.62(9)
C24'–C25–H25	120.1(17)	N1–Ru1–C1	125.26(8)
C24–C25–H25	120.1(17)	C2–Ru1–C1	38.25(9)
C27–C26–C27'	118.4(2)	C3–Ru1–C1	62.77(9)
C27–C26–P2	118.43(17)	N1–Ru1–C7A	98.84(7)
C27'–C26–P2	123.09(17)	C2–Ru1–C7A	62.87(8)
C28–C27–C26	121.0(2)	C3–Ru1–C7A	62.14(8)
C28–C27–H27A	118.4(16)	C1–Ru1–C7A	37.07(8)
C26–C27–H27A	120.5(16)	N1–Ru1–C3A	103.90(8)
C28'–C27'–C26	120.5(2)	C2–Ru1–C3A	63.21(9)
C28'–C27'–H27B	119.2(16)	C3–Ru1–C3A	37.50(9)
C26–C27'–H27B	120.3(16)	C1–Ru1–C3A	62.64(8)
C27–C28–C29	119.9(2)	C7A–Ru1–C3A	37.20(8)
C27–C28–H28A	121.3(18)	N1–Ru1–P1	89.78(6)
C29–C28–H28A	118.8(18)	C2–Ru1–P1	93.67(7)
C29–C28'–C27'	120.3(2)	C3–Ru1–P1	131.07(7)
C29–C28'–H28B	120.7(17)	C1–Ru1–P1	80.57(6)
C27'–C28'–H28B	118.9(17)	C7A–Ru1–P1	106.60(6)
C28'–C29–C28	119.8(2)	C3A–Ru1–P1	142.20(6)
C28'–C29–H29	120.1(17)	N1–Ru1–P2	85.75(5)
C28–C29–H29	120.0(17)	C2–Ru1–P2	110.88(7)
C31–C30–C31'	118.7(2)	C3–Ru1–P2	94.18(6)

C1–Ru1–P2	148.95(6)	F2–P3–F3	90.72(11)
C7A–Ru1–P2	149.49(6)	F6–P3–F3	89.86(12)
C3A–Ru1–P2	112.35(6)	F5–P3–F3	177.18(12)
P1–Ru1–P2	103.56(2)	F1–P3–F3	88.93(11)
F2–P3–F6	92.40(13)	F2–P3–F4	178.71(12)
F2–P3–F5	91.80(12)	F6–P3–F4	88.88(12)
F6–P3–F5	91.29(13)	F5–P3–F4	88.03(10)
F2–P3–F1	89.31(11)	F1–P3–F4	89.41(10)
F6–P3–F1	177.91(13)	F3–P3–F4	89.41(10)
F5–P3–F1	89.84(11)		

Symmetry transformations used to generate equivalent atoms:

APPENDIX IV: X-RAY STRUCTURE OF RUTHENIUM COMPLEX 82

Table 4. Anisotropic displacement parameters [$Å^2 \times 10^3$]. The anisotropic displacement factor exponent takes the form: $-2\pi^2[h^2a^{*2}U^{11} + \cdots + 2\,h\,k\,a^*\,b^*\,U^{12}]$.

Atom	U^{11}	U^{22}	U^{33}	U^{23}	U^{13}	U^{12}
C1	27(1)	16(1)	24(1)	10(1)	11(1)	10(1)
C2	22(1)	15(1)	27(1)	8(1)	7(1)	6(1)
C3	13(1)	13(1)	39(1)	10(1)	−3(1)	2(1)
C3A	23(1)	10(1)	23(1)	4(1)	2(1)	6(1)
C4	39(1)	21(1)	22(1)	5(1)	3(1)	16(1)
C5	42(2)	34(2)	26(1)	7(1)	12(1)	20(1)
C6	37(2)	45(2)	39(2)	16(1)	19(1)	28(1)
C7	22(1)	26(1)	31(1)	8(1)	3(1)	15(1)
C7A	18(1)	11(1)	22(1)	5(1)	3(1)	7(1)
C8	22(1)	21(1)	22(1)	9(1)	5(1)	9(1)
C9	23(1)	22(1)	22(1)	10(1)	4(1)	7(1)
C10	30(1)	23(1)	20(1)	8(1)	3(1)	11(1)
C11	35(2)	26(1)	33(2)	14(1)	8(1)	14(1)
C11'	32(1)	23(1)	33(1)	11(1)	10(1)	11(1)
C12	53(2)	32(2)	46(2)	23(1)	15(2)	24(1)
C12'	41(2)	34(2)	37(2)	20(1)	15(1)	14(1)
C13	54(2)	31(2)	49(2)	25(1)	15(2)	18(1)
C14	19(1)	18(1)	16(1)	4(1)	1(1)	5(1)
C15'	25(1)	26(1)	38(2)	16(1)	−4(1)	5(1)
C15	22(1)	21(1)	19(1)	5(1)	5(1)	9(1)
C16'	28(1)	25(1)	44(2)	17(1)	0(1)	1(1)
C16	24(1)	32(1)	25(1)	8(1)	6(1)	15(1)
C17	19(1)	30(1)	30(1)	6(1)	3(1)	2(1)
C18	29(1)	23(1)	18(1)	9(1)	4(1)	16(1)
C19	38(2)	26(1)	26(1)	8(1)	1(1)	16(1)
C19'	30(1)	35(1)	21(1)	11(1)	8(1)	18(1)
C20	64(2)	30(1)	28(1)	9(1)	7(1)	30(2)
C20'	40(2)	51(2)	33(2)	24(1)	19(1)	30(1)
C21	62(2)	48(2)	34(2)	22(1)	23(1)	42(2)
C22	16(1)	19(1)	17(1)	5(1)	3(1)	7(1)
C23'	21(1)	20(1)	30(1)	10(1)	8(1)	9(1)
C23	20(1)	21(1)	30(1)	10(1)	8(1)	9(1)
C24	20(1)	30(1)	33(1)	14(1)	10(1)	9(1)
C24'	26(1)	26(1)	40(2)	10(1)	11(1)	16(1)
C25	21(1)	35(1)	33(1)	10(1)	11(1)	14(1)
C26	13(1)	16(1)	23(1)	9(1)	5(1)	8(1)
C27	17(1)	20(1)	24(1)	9(1)	4(1)	9(1)
C27'	21(1)	21(1)	24(1)	9(1)	7(1)	10(1)
C28	18(1)	17(1)	30(1)	6(1)	1(1)	7(1)
C28'	25(1)	27(1)	31(1)	16(1)	13(1)	13(1)
C29	20(1)	19(1)	41(2)	16(1)	10(1)	7(1)
C30	18(1)	14(1)	20(1)	7(1)	3(1)	5(1)
C31	21(1)	22(1)	25(1)	7(1)	4(1)	10(1)
C31'	21(1)	18(1)	22(1)	6(1)	6(1)	8(1)
C32	23(1)	25(1)	27(1)	6(1)	−4(1)	7(1)
C32'	32(1)	19(1)	22(1)	7(1)	11(1)	12(1)
C33	35(1)	18(1)	22(1)	4(1)	1(1)	9(1)
C34	18(1)	19(1)	29(1)	8(1)	7(1)	9(1)
C35	25(1)	29(1)	52(2)	21(1)	19(1)	8(1)
N1	17(1)	16(1)	25(1)	6(1)	4(1)	8(1)
P1	17(1)	16(1)	19(1)	7(1)	2(1)	6(1)
P2	14(1)	13(1)	17(1)	5(1)	4(1)	6(1)
Ru1	12(1)	12(1)	19(1)	5(1)	4(1)	5(1)
P3	26(1)	28(1)	37(1)	14(1)	8(1)	13(1)
F1	48(1)	35(1)	54(1)	20(1)	25(1)	13(1)
F2	87(2)	36(1)	49(1)	−5(1)	−9(1)	19(1)
F3	39(1)	47(1)	84(1)	31(1)	11(1)	28(1)
F4	27(1)	26(1)	75(1)	18(1)	9(1)	7(1)
F5	34(1)	56(1)	86(2)	34(1)	−9(1)	16(1)
F6	105(2)	93(2)	69(1)	51(1)	58(1)	60(2)

APPENDIX IV: X-RAY STRUCTURE OF RUTHENIUM COMPLEX **82**

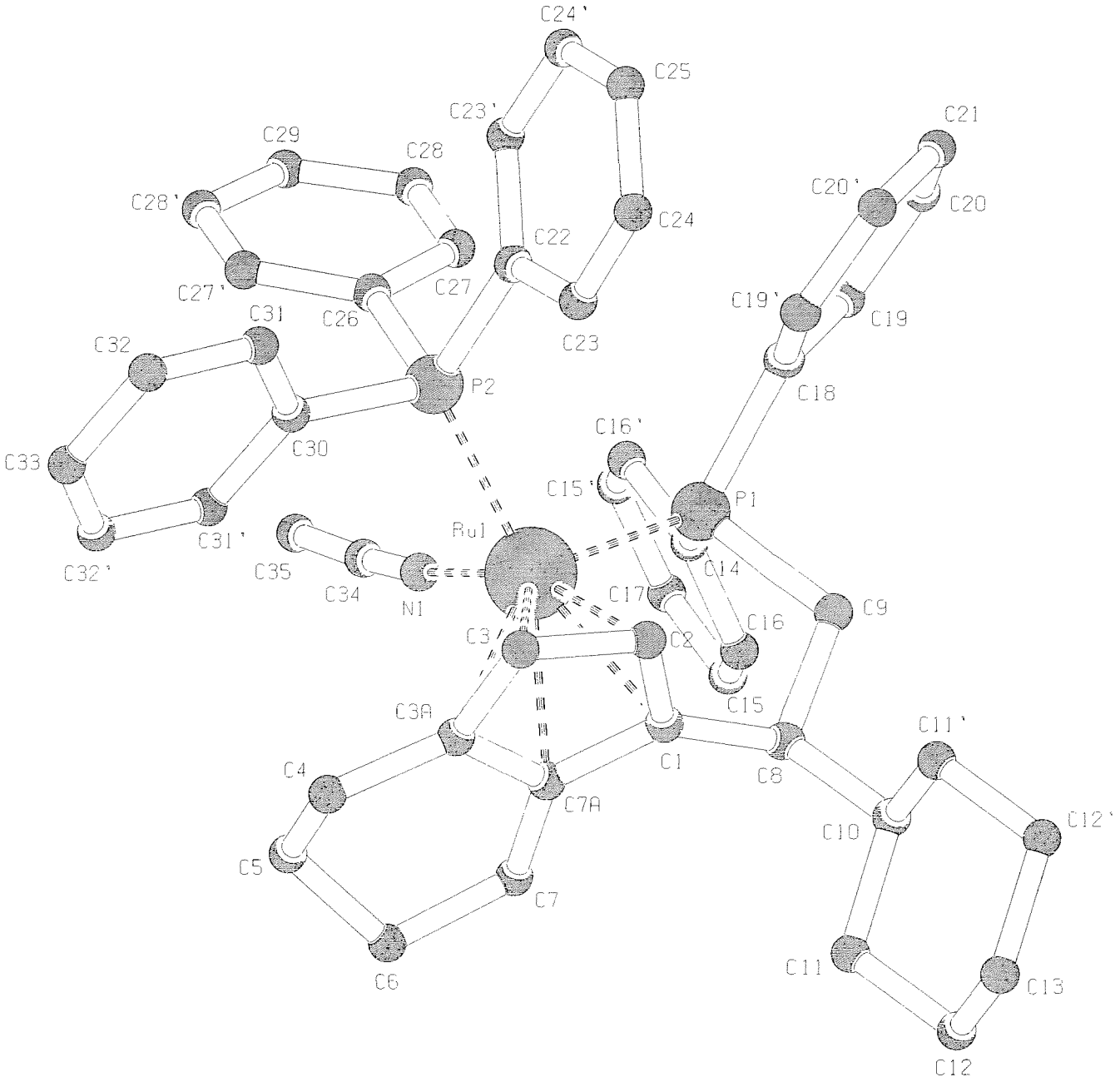

University of Southampton · Department of Chemistry
EPSRC National Crystallography Service

Table 1. Crystal data and structure refinement.

Identification code	**04sot0700 (DCP156/1)**	
Empirical formula	$C_{42}H_{43}ClP_2Ru$	
Formula weight	746.22	
Temperature	120(2) K	
Wavelength	0.71073 Å	
Crystal system	Monoclinic	
Space group	*Pc*	
Unit cell dimensions	$a = 11.0846(8)$ Å	$\alpha = 90°$
	$b = 23.7847(12)$ Å	$\beta = 123.825(5)°$
	$c = 16.5912(12)$ Å	$\gamma = 90°$
Volume	3633.8(4) Å^3	
Z	4 (2 molecules in ASU)	
Density (calculated)	1.364 Mg / m^3	
Absorption coefficient	0.622 mm^{-1}	
F(000)	1544	
Crystal	Slab; dark red	
Crystal size	0.20 × 0.15 × 0.08 mm^3	
θ range for data collection	3.17 – 27.50°	
Index ranges	$-14 \le h \le 12$, $-30 \le k \le 26$, $-21 \le l \le 21$	
Reflections collected	45086	
Independent reflections	14611 [$R_{int} = 0.0527$]	
Completeness to $\theta = 27.50°$	99.6 %	
Absorption correction	Semi–empirical from equivalents	
Max. and min. transmission	0.9519 and 0.8857	
Refinement method	Full-matrix least-squares on F^2	
Data / restraints / parameters	14611 / 2 / 830	
Goodness-of-fit on F^2	1.067	
Final *R* indices [$F^2 > 2\sigma(F^2)$]	*R1* = 0.0422, *wR2* = 0.0807	
R indices (all data)	*R1* = 0.0695, *wR2* = 0.0887	
Absolute structure parameter	0.002(18)	
Extinction coefficient	0.00034(16)	
Largest diff. peak and hole	0.863 and −0.531 e Å^{-3}	

Diffractometer: *Nonius KappaCCD* area detector (ϕ scans and ω scans to fill *asymmetric unit* sphere). **Cell determination:** DirAx (Duisenberg, A.J.M.(1992). J. Appl. Cryst. 25, 92-96.) **Data collection:** Collect (Collect: Data collection software, R. Hooft, Nonius B.V., 1998). **Data reduction and cell refinement**: *Denzo* (Z. Otwinowski & W. Minor, *Methods in Enzymology* (1997) Vol. **276**: *Macromolecular Crystallography*, part A, pp. 307–326; C. W. Carter, Jr. & R. M. Sweet, Eds., Academic Press). **Absorption correction**: *SORTAV* (R. H. Blessing, Acta Cryst. A**51** (1995) 33–37; R. H. Blessing, J. Appl. Cryst. **30** (1997) 421–426). **Structure solution**: *SHELXS97* (G. M. Sheldrick, Acta Cryst. (1990) A**46** 467–473). **Structure refinement**: *SHELXL97* (G. M. Sheldrick (1997), University of Göttingen, Germany). **Graphics:** Cameron - A Molecular Graphics Package. (D. M. Watkin, L. Pearce and C. K. Prout, Chemical Crystallography Laboratory, University of Oxford, 1993).

Special details:

APPENDIX V: X-RAY STRUCTURE OF RUTHENIUM COMPLEX **112**

Table 2. Atomic coordinates [$\times 10^4$], equivalent isotropic displacement parameters [$Å^2 \times 10^3$] and site occupancy factors. U_{eq} is defined as one third of the trace of the orthogonalized U^{ij} tensor.

Atom	*x*	*y*	*z*	U_{eq}	*S.o.f.*
C1	9495(5)	1766(2)	−665(3)	27(1)	1
C2	10281(5)	2009(2)	273(3)	26(1)	1
C3	9413(5)	1952(2)	662(3)	26(1)	1
C4	9651(6)	2125(2)	1556(3)	31(1)	1
C5	8590(6)	2016(2)	1723(4)	36(1)	1
C6	7315(6)	1734(2)	1046(4)	35(1)	1
C7	7043(5)	1560(2)	167(4)	32(1)	1
C8	8104(5)	1662(2)	−37(3)	26(1)	1
C9	8180(5)	1535(2)	−865(3)	28(1)	1
C10	7013(6)	1231(2)	−1765(3)	32(1)	1
C11	6356(6)	1605(2)	−2659(3)	41(1)	1
C12	5765(6)	2147(2)	−2535(4)	57(2)	1
C13	5157(8)	2531(2)	−3407(4)	85(2)	1
C14	4011(10)	2228(2)	−4342(5)	118(4)	1
C16	5182(7)	1313(2)	−3590(4)	61(2)	1
C17	7630(5)	666(2)	−1841(3)	30(1)	1
C18	7134(6)	129(2)	−506(3)	26(1)	1
C19	7253(5)	204(2)	364(3)	27(1)	1
C20	6133(6)	21(2)	456(4)	33(1)	1
C21	4898(5)	−217(2)	−318(4)	31(1)	1
C22	4774(5)	−287(2)	−1179(3)	33(1)	1
C23	5865(5)	−123(2)	−1278(3)	29(1)	1
C24	9277(5)	−323(2)	−716(3)	23(1)	1
C25	9481(5)	−460(2)	−1443(3)	28(1)	1
C26	10086(5)	−971(2)	−1436(3)	32(1)	1
C27	10457(6)	−1349(2)	−711(4)	37(1)	1
C28	10272(5)	−1223(2)	20(3)	36(1)	1
C29	9675(5)	−717(2)	24(3)	29(1)	1
C30	12459(5)	1062(2)	−324(3)	22(1)	1
C31	12010(5)	704(2)	−1100(3)	31(1)	1
C32	12152(6)	849(2)	−1853(4)	43(1)	1
C33	12764(6)	1359(2)	−1824(4)	39(1)	1
C34	13190(5)	1720(2)	−1071(3)	32(1)	1
C35	13036(5)	1578(2)	−322(3)	29(1)	1
C36	13703(5)	1218(2)	1698(3)	27(1)	1
C37	15122(5)	1164(2)	1944(4)	32(1)	1
C38	16280(6)	1418(2)	2767(4)	41(1)	1
C39	16024(6)	1727(2)	3355(4)	42(1)	1
C40	14633(6)	1785(2)	3139(4)	36(1)	1
C41	13471(6)	1541(2)	2309(3)	31(1)	1
C42	12797(6)	132(2)	892(4)	30(1)	1
Cl1	10859(1)	595(1)	1844(1)	26(1)	1
P1	8603(1)	355(1)	−622(1)	22(1)	1
P2	12184(1)	863(1)	627(1)	23(1)	1
Ru1	9971(1)	1082(1)	323(1)	20(1)	1
C15	4525(8)	1694(2)	−4481(4)	76(2)	1
C101	5025(5)	3285(2)	−877(3)	28(1)	1
C102	5817(5)	3019(2)	52(3)	23(1)	1
C103	4963(5)	3051(2)	449(3)	26(1)	1
C104	5167(6)	2855(2)	1314(3)	34(1)	1
C105	4084(6)	2928(2)	1464(4)	37(1)	1
C106	2787(7)	3198(2)	789(4)	44(2)	1
C107	2534(6)	3410(2)	−60(4)	37(1)	1
C108	3628(5)	3341(2)	−251(3)	27(1)	1
C109	3706(5)	3501(2)	−1052(3)	29(1)	1
C110	2561(6)	3823(2)	−1935(3)	37(1)	1
C111	1872(7)	3456(2)	−2846(4)	59(2)	1
C112	1192(8)	2922(2)	−2735(4)	77(2)	1
C113	586(9)	2529(3)	−3587(5)	115(3)	1

C114	−490(11)	2818(3)	−4504(6)	124(4)	1
C115	82(10)	3335(3)	−4653(5)	113(3)	1
C116	752(8)	3741(2)	−3757(4)	78(2)	1
C117	3174(5)	4381(2)	−1994(3)	33(1)	1
C118	2652(5)	4891(2)	−649(3)	24(1)	1
C119	1400(6)	5135(2)	−1424(3)	32(1)	1
C120	262(6)	5273(2)	−1338(4)	37(1)	1
C121	404(6)	5192(2)	−472(4)	33(1)	1
C122	1657(6)	4948(2)	303(4)	33(1)	1
C123	2771(5)	4796(2)	210(3)	29(1)	1
C124	4801(5)	5368(2)	−846(3)	24(1)	1
C125	5134(5)	5768(2)	−135(3)	29(1)	1
C126	5683(5)	6289(2)	−142(3)	32(1)	1
C127	5915(5)	6415(2)	−862(3)	35(1)	1
C128	5611(5)	6027(2)	−1567(3)	32(1)	1
C129	5034(5)	5509(2)	−1572(3)	28(1)	1
C130	7935(5)	3964(2)	−518(3)	22(1)	1
C131	7437(5)	4334(2)	−1292(3)	28(1)	1
C132	7492(6)	4185(2)	−2085(3)	33(1)	1
C133	8061(6)	3670(2)	−2084(3)	34(1)	1
C134	8542(5)	3303(2)	−1329(3)	31(1)	1
C135	8484(5)	3446(2)	−540(3)	28(1)	1
C136	9261(5)	3801(2)	1522(3)	23(1)	1
C137	10648(5)	3836(2)	1715(3)	30(1)	1
C138	11831(6)	3596(2)	2551(3)	37(1)	1
C139	11611(6)	3328(2)	3202(3)	38(1)	1
C140	10244(6)	3282(2)	3008(3)	31(1)	1
C141	9051(6)	3515(2)	2172(3)	28(1)	1
C142	8354(6)	4889(2)	750(3)	24(1)	1
Cl2	6364(1)	4396(1)	1698(1)	25(1)	1
P3	4149(1)	4684(1)	−764(1)	23(1)	1
P4	7713(1)	4160(1)	463(1)	21(1)	1
Ru2	5501(1)	3940(1)	153(1)	19(1)	1

APPENDIX V: X-RAY STRUCTURE OF RUTHENIUM COMPLEX **112**

Table 3. Bond lengths [Å] and angles [°].

C1–C9	1.415(6)	C25–C26	1.385(6)
C1–C2	1.416(6)	C25–H25	0.9500
C1–Ru1	2.155(4)	C26–C27	1.368(6)
C1–H1	0.9500	C26–H26	0.9500
C2–C3	1.433(6)	C27–C28	1.372(6)
C2–Ru1	2.240(4)	C27–H27	0.9500
C2–H2	0.9500	C28–C29	1.375(6)
C3–C4	1.416(6)	C28–H28	0.9500
C3–C8	1.432(6)	C29–H29	0.9500
C3–Ru1	2.318(4)	C30–C35	1.383(5)
C4–C5	1.376(6)	C30–C31	1.384(6)
C4–H4	0.9500	C30–P2	1.830(4)
C5–C6	1.393(7)	C31–C32	1.386(6)
C5–H5	0.9500	C31–H31	0.9500
C6–C7	1.378(6)	C32–C33	1.377(6)
C6–H6	0.9500	C32–H32	0.9500
C7–C8	1.415(6)	C33–C34	1.367(6)
C7–H7	0.9500	C33–H33	0.9500
C8–C9	1.454(6)	C34–C35	1.388(6)
C8–Ru1	2.273(4)	C34–H34	0.9500
C9–C10	1.508(6)	C35–H35	0.9500
C9–Ru1	2.152(4)	C36–C37	1.394(6)
C10–C11	1.524(6)	C36–C41	1.405(6)
C10–C17	1.543(6)	C36–P2	1.838(5)
C10–H10	1.0000	C37–C38	1.388(6)
C11–C12	1.512(7)	C37–H37	0.9500
C11–C16	1.524(7)	C38–C39	1.372(7)
C11–H11	1.0000	C38–H38	0.9500
C12–C13	1.516(7)	C39–C40	1.383(7)
C12–H12A	0.9900	C39–H39	0.9500
C12–H12B	0.9900	C40–C41	1.385(6)
C13–C14	1.532(8)	C40–H40	0.9500
C13–H13A	0.9900	C41–H41	0.9500
C13–H13B	0.9900	C42–P2	1.828(4)
C14–C15	1.462(9)	C42–H42A	0.9800
C14–H14A	0.9900	C42–H42B	0.9800
C14–H14B	0.9900	C42–H42C	0.9800
C16–C15	1.530(7)	Cl1–Ru1	2.4316(10)
C16–H16A	0.9900	P1–Ru1	2.2589(12)
C16–H16B	0.9900	P2–Ru1	2.2717(12)
C17–P1	1.836(4)	C15–H15A	0.9900
C17–H17A	0.9900	C15–H15B	0.9900
C17–H17B	0.9900	C101–C109	1.419(6)
C18–C19	1.386(6)	C101–C102	1.427(6)
C18–C23	1.404(6)	C101–Ru2	2.151(4)
C18–P1	1.824(5)	C101–H101	0.9500
C19–C20	1.402(6)	C102–C103	1.426(6)
C19–H19	0.9500	C102–Ru2	2.240(4)
C20–C21	1.374(7)	C102–H102	0.9500
C20–H20	0.9500	C103–C104	1.404(6)
C21–C22	1.368(6)	C103–C108	1.450(6)
C21–H21	0.9500	C103–Ru2	2.322(4)
C22–C23	1.365(6)	C104–C105	1.365(6)
C22–H22	0.9500	C104–H104	0.9500
C23–H23	0.9500	C105–C106	1.393(8)
C24–C25	1.384(5)	C105–H105	0.9500
C24–C29	1.405(5)	C106–C107	1.371(7)
C24–P1	1.820(4)	C106–H106	0.9500

C107–C108	1.423(6)	C133–H133	0.9500
C107–H107	0.9500	C134–C135	1.388(6)
C108–C109	1.430(6)	C134–H134	0.9500
C108–Ru2	2.289(4)	C135–H135	0.9500
C109–C110	1.508(6)	C136–C137	1.387(6)
C109–Ru2	2.149(4)	C136–C141	1.400(6)
C110–C117	1.518(6)	C136–P4	1.845(4)
C110–C111	1.531(6)	C137–C138	1.394(6)
C110–H110	1.0000	C137–H137	0.9500
C111–C116	1.481(8)	C138–C139	1.387(6)
C111–C112	1.541(8)	C138–H138	0.9500
C111–H111	1.0000	C139–C140	1.368(7)
C112–C113	1.506(8)	C139–H139	0.9500
C112–H11C	0.9900	C140–C141	1.392(6)
C112–H11D	0.9900	C140–H140	0.9500
C113–C114	1.480(9)	C141–H141	0.9500
C113–H11K	0.9900	C142–P4	1.834(4)
C113–H11L	0.9900	C142–H14C	0.9800
C114–C115	1.467(11)	C142–H14D	0.9800
C114–H11I	0.9900	C142–H14E	0.9800
C114–H11J	0.9900	Cl2–Ru2	2.4351(10)
C115–C116	1.571(8)	P3–Ru2	2.2695(11)
C115–H11G	0.9900	P4–Ru2	2.2684(12)
C115–H11H	0.9900		
C116–H11E	0.9900	C9–C1–C2	109.9(4)
C116–H11F	0.9900	C9–C1–Ru1	70.7(2)
C117–P3	1.843(4)	C2–C1–Ru1	74.5(2)
C117–H11A	0.9900	C9–C1–H1	125.1
C117–H11B	0.9900	C2–C1–H1	125.1
C118–C123	1.375(6)	Ru1–C1–H1	121.4
C118–C119	1.390(6)	C1–C2–C3	107.5(4)
C118–P3	1.840(5)	C1–C2–Ru1	68.0(2)
C119–C120	1.386(7)	C3–C2–Ru1	74.7(2)
C119–H119	0.9500	C1–C2–H2	126.3
C120–C121	1.369(6)	C3–C2–H2	126.3
C120–H120	0.9500	Ru1–C2–H2	122.7
C121–C122	1.390(6)	C4–C3–C8	120.2(4)
C121–H121	0.9500	C4–C3–C2	131.6(4)
C122–C123	1.375(6)	C8–C3–C2	108.2(4)
C122–H122	0.9500	C4–C3–Ru1	126.5(3)
C123–H123	0.9500	C8–C3–Ru1	70.1(2)
C124–C125	1.396(5)	C2–C3–Ru1	68.8(2)
C124–C129	1.404(5)	C5–C4–C3	118.3(5)
C124–P3	1.816(4)	C5–C4–H4	120.8
C125–C126	1.383(6)	C3–C4–H4	120.8
C125–H125	0.9500	C4–C5–C6	121.8(5)
C126–C127	1.388(6)	C4–C5–H5	119.1
C126–H126	0.9500	C6–C5–H5	119.1
C127–C128	1.376(6)	C7–C6–C5	121.5(5)
C127–H127	0.9500	C7–C6–H6	119.2
C128–C129	1.388(6)	C5–C6–H6	119.2
C128–H128	0.9500	C6–C7–C8	118.8(4)
C129–H129	0.9500	C6–C7–H7	120.6
C130–C135	1.385(6)	C8–C7–H7	120.6
C130–C131	1.393(5)	C7–C8–C3	119.4(4)
C130–P4	1.835(4)	C7–C8–C9	133.1(4)
C131–C132	1.396(6)	C3–C8–C9	107.5(4)
C131–H131	0.9500	C7–C8–Ru1	126.2(3)
C132–C133	1.377(6)	C3–C8–Ru1	73.5(3)
C132–H132	0.9500	C9–C8–Ru1	66.4(2)
C133–C134	1.368(6)	C1–C9–C8	106.9(4)

APPENDIX V: X-RAY STRUCTURE OF RUTHENIUM COMPLEX **112**

C1–C9–C10	128.5(4)	C21–C22–H22	119.6
C8–C9–C10	124.6(4)	C22–C23–C18	121.1(4)
C1–C9–Ru1	71.0(2)	C22–C23–H23	119.5
C8–C9–Ru1	75.4(2)	C18–C23–H23	119.5
C10–C9–Ru1	120.9(3)	C25–C24–C29	118.8(4)
C9–C10–C11	111.5(4)	C25–C24–P1	123.8(3)
C9–C10–C17	108.9(4)	C29–C24–P1	117.4(3)
C11–C10–C17	115.0(4)	C24–C25–C26	120.7(4)
C9–C10–H10	107.0	C24–C25–H25	119.6
C11–C10–H10	107.0	C26–C25–H25	119.6
C17–C10–H10	107.0	C27–C26–C25	119.5(4)
C12–C11–C10	112.0(4)	C27–C26–H26	120.2
C12–C11–C16	109.7(4)	C25–C26–H26	120.2
C10–C11–C16	113.3(4)	C26–C27–C28	120.8(4)
C12–C11–H11	107.2	C26–C27–H27	119.6
C10–C11–H11	107.2	C28–C27–H27	119.6
C16–C11–H11	107.2	C27–C28–C29	120.4(4)
C11–C12–C13	112.3(5)	C27–C28–H28	119.8
C11–C12–H12A	109.1	C29–C28–H28	119.8
C13–C12–H12A	109.1	C28–C29–C24	119.7(4)
C11–C12–H12B	109.1	C28–C29–H29	120.1
C13–C12–H12B	109.1	C24–C29–H29	120.1
H12A–C12–H12B	107.9	C35–C30–C31	118.4(4)
C12–C13–C14	111.1(5)	C35–C30–P2	121.7(3)
C12–C13–H13A	109.4	C31–C30–P2	119.8(3)
C14–C13–H13A	109.4	C30–C31–C32	121.5(4)
C12–C13–H13B	109.4	C30–C31–H31	119.3
C14–C13–H13B	109.4	C32–C31–H31	119.3
H13A–C13–H13B	108.0	C33–C32–C31	119.3(5)
C15–C14–C13	113.1(6)	C33–C32–H32	120.3
C15–C14–H14A	109.0	C31–C32–H32	120.3
C13–C14–H14A	109.0	C34–C33–C32	119.9(4)
C15–C14–H14B	109.0	C34–C33–H33	120.1
C13–C14–H14B	109.0	C32–C33–H33	120.1
H14A–C14–H14B	107.8	C33–C34–C35	120.9(4)
C11–C16–C15	112.8(4)	C33–C34–H34	119.6
C11–C16–H16A	109.0	C35–C34–H34	119.6
C15–C16–H16A	109.0	C30–C35–C34	120.1(4)
C11–C16–H16B	109.0	C30–C35–H35	120.0
C15–C16–H16B	109.0	C34–C35–H35	120.0
H16A–C16–H16B	107.8	C37–C36–C41	118.0(4)
C10–C17–P1	106.1(3)	C37–C36–P2	121.2(3)
C10–C17–H17A	110.5	C41–C36–P2	120.8(4)
P1–C17–H17A	110.5	C38–C37–C36	121.5(5)
C10–C17–H17B	110.5	C38–C37–H37	119.3
P1–C17–H17B	110.5	C36–C37–H37	119.3
H17A–C17–H17B	108.7	C39–C38–C37	119.2(5)
C19–C18–C23	118.2(4)	C39–C38–H38	120.4
C19–C18–P1	119.9(4)	C37–C38–H38	120.4
C23–C18–P1	121.9(3)	C38–C39–C40	120.9(5)
C18–C19–C20	119.8(4)	C38–C39–H39	119.6
C18–C19–H19	120.1	C40–C39–H39	119.6
C20–C19–H19	120.1	C39–C40–C41	120.0(5)
C21–C20–C19	120.5(4)	C39–C40–H40	120.0
C21–C20–H20	119.7	C41–C40–H40	120.0
C19–C20–H20	119.7	C40–C41–C36	120.3(5)
C22–C21–C20	119.7(4)	C40–C41–H41	119.9
C22–C21–H21	120.2	C36–C41–H41	119.9
C20–C21–H21	120.2	P2–C42–H42A	109.5
C23–C22–C21	120.7(5)	P2–C42–H42B	109.5
C23–C22–H22	119.6	H42A–C42–H42B	109.5

P2–C42–H42C	109.5	C104–C103–C102	133.3(5)
H42A–C42–H42C	109.5	C104–C103–C108	119.3(4)
H42B–C42–H42C	109.5	C102–C103–C108	107.4(4)
C24–P1–C18	100.41(19)	C104–C103–Ru2	127.3(3)
C24–P1–C17	106.30(19)	C102–C103–Ru2	68.7(2)
C18–P1–C17	102.9(2)	C108–C103–Ru2	70.4(2)
C24–P1–Ru1	126.07(15)	C105–C104–C103	119.1(5)
C18–P1–Ru1	116.53(15)	C105–C104–H104	120.4
C17–P1–Ru1	102.18(14)	C103–C104–H104	120.4
C42–P2–C30	103.6(2)	C104–C105–C106	122.1(5)
C42–P2–C36	100.8(2)	C104–C105–H105	118.9
C30–P2–C36	102.2(2)	C106–C105–H105	118.9
C42–P2–Ru1	118.88(17)	C107–C106–C105	121.6(5)
C30–P2–Ru1	115.26(14)	C107–C106–H106	119.2
C36–P2–Ru1	113.85(15)	C105–C106–H106	119.2
C9–Ru1–C1	38.35(17)	C106–C107–C108	118.3(5)
C9–Ru1–C2	63.65(17)	C106–C107–H107	120.8
C1–Ru1–C2	37.53(15)	C108–C107–H107	120.8
C9–Ru1–P1	80.01(12)	C107–C108–C109	132.5(5)
C1–Ru1–P1	105.35(12)	C107–C108–C103	119.5(4)
C2–Ru1–P1	141.78(12)	C109–C108–C103	108.0(4)
C9–Ru1–P2	130.58(13)	C107–C108–Ru2	127.5(3)
C1–Ru1–P2	96.87(13)	C109–C108–Ru2	66.0(2)
C2–Ru1–P2	93.78(13)	C103–C108–Ru2	72.9(3)
P1–Ru1–P2	101.73(4)	C101–C109–C108	107.5(4)
C9–Ru1–C8	38.24(15)	C101–C109–C110	126.6(4)
C1–Ru1–C8	62.65(17)	C108–C109–C110	125.8(5)
C2–Ru1–C8	61.88(17)	C101–C109–Ru2	70.8(3)
P1–Ru1–C8	96.95(11)	C108–C109–Ru2	76.6(3)
P2–Ru1–C8	155.51(11)	C110–C109–Ru2	120.0(3)
C9–Ru1–C3	62.64(16)	C109–C110–C117	110.0(4)
C1–Ru1–C3	61.66(16)	C109–C110–C111	111.0(4)
C2–Ru1–C3	36.59(15)	C117–C110–C111	115.4(4)
P1–Ru1–C3	133.26(12)	C109–C110–H110	106.6
P2–Ru1–C3	123.52(12)	C117–C110–H110	106.6
C8–Ru1–C3	36.35(15)	C111–C110–H110	106.6
C9–Ru1–Cl1	145.36(13)	C116–C111–C110	114.9(5)
C1–Ru1–Cl1	159.17(12)	C116–C111–C112	108.2(5)
C2–Ru1–Cl1	121.68(12)	C110–C111–C112	111.1(5)
P1–Ru1–Cl1	94.76(4)	C116–C111–H111	107.5
P2–Ru1–Cl1	84.06(4)	C110–C111–H111	107.5
C8–Ru1–Cl1	110.17(11)	C112–C111–H111	107.5
C3–Ru1–Cl1	100.47(12)	C113–C112–C111	113.1(6)
C14–C15–C16	112.4(5)	C113–C112–H11C	109.0
C14–C15–H15A	109.1	C111–C112–H11C	109.0
C16–C15–H15A	109.1	C113–C112–H11D	109.0
C14–C15–H15B	109.1	C111–C112–H11D	109.0
C16–C15–H15B	109.1	H11C–C112–H11D	107.8
H15A–C15–H15B	107.9	C114–C113–C112	111.1(6)
C109–C101–C102	109.1(4)	C114–C113–H11K	109.4
C109–C101–Ru2	70.7(2)	C112–C113–H11K	109.4
C102–C101–Ru2	74.4(2)	C114–C113–H11L	109.4
C109–C101–H101	125.5	C112–C113–H11L	109.4
C102–C101–H101	125.5	H11K–C113–H11L	108.0
Ru2–C101–H101	121.1	C115–C114–C113	112.8(8)
C103–C102–C101	107.9(4)	C115–C114–H11I	109.0
C103–C102–Ru2	75.0(2)	C113–C114–H11I	109.0
C101–C102–Ru2	67.7(2)	C115–C114–H11J	109.0
C103–C102–H102	126.0	C113–C114–H11J	109.0
C101–C102–H102	126.0	H11I–C114–H11J	107.8
Ru2–C102–H102	122.9	C114–C115–C116	112.1(7)

C114–C115–H11G	109.2	C131–C132–H132	120.5
C116–C115–H11G	109.2	C134–C133–C132	120.9(4)
C114–C115–H11H	109.2	C134–C133–H133	119.6
C116–C115–H11H	109.2	C132–C133–H133	119.6
H11G–C115–H11H	107.9	C133–C134–C135	120.5(4)
C111–C116–C115	111.7(5)	C133–C134–H134	119.7
C111–C116–H11E	109.3	C135–C134–H134	119.7
C115–C116–H11E	109.3	C130–C135–C134	119.7(4)
C111–C116–H11F	109.3	C130–C135–H135	120.2
C115–C116–H11F	109.3	C134–C135–H135	120.2
H11E–C116–H11F	107.9	C137–C136–C141	119.3(4)
C110–C117–P3	106.1(3)	C137–C136–P4	121.1(3)
C110–C117–H11A	110.5	C141–C136–P4	119.5(4)
P3–C117–H11A	110.5	C136–C137–C138	120.9(4)
C110–C117–H11B	110.5	C136–C137–H137	119.6
P3–C117–H11B	110.5	C138–C137–H137	119.6
H11A–C117–H11B	108.7	C139–C138–C137	119.1(5)
C123–C118–C119	119.9(5)	C139–C138–H138	120.4
C123–C118–P3	119.5(4)	C137–C138–H138	120.4
C119–C118–P3	120.6(3)	C140–C139–C138	120.4(5)
C120–C119–C118	120.1(4)	C140–C139–H139	119.8
C120–C119–H119	120.0	C138–C139–H139	119.8
C118–C119–H119	120.0	C139–C140–C141	121.0(4)
C121–C120–C119	119.7(5)	C139–C140–H140	119.5
C121–C120–H120	120.1	C141–C140–H140	119.5
C119–C120–H120	120.1	C140–C141–C136	119.2(5)
C120–C121–C122	120.1(4)	C140–C141–H141	120.4
C120–C121–H121	119.9	C136–C141–H141	120.4
C122–C121–H121	119.9	P4–C142–H14C	109.5
C123–C122–C121	120.2(4)	P4–C142–H14D	109.5
C123–C122–H122	119.9	H14C–C142–H14D	109.5
C121–C122–H122	119.9	P4–C142–H14E	109.5
C118–C123–C122	120.0(5)	H14C–C142–H14E	109.5
C118–C123–H123	120.0	H14D–C142–H14E	109.5
C122–C123–H123	120.0	C124–P3–C118	100.79(19)
C125–C124–C129	118.3(4)	C124–P3–C117	106.25(19)
C125–C124–P3	118.4(3)	C118–P3–C117	102.3(2)
C129–C124–P3	123.2(3)	C124–P3–Ru2	127.36(15)
C126–C125–C124	120.9(4)	C118–P3–Ru2	115.83(15)
C126–C125–H125	119.6	C117–P3–Ru2	101.50(15)
C124–C125–H125	119.6	C142–P4–C130	104.25(19)
C125–C126–C127	119.6(4)	C142–P4–C136	99.7(2)
C125–C126–H126	120.2	C130–P4–C136	102.4(2)
C127–C126–H126	120.2	C142–P4–Ru2	119.33(16)
C128–C127–C126	120.8(4)	C130–P4–Ru2	113.76(15)
C128–C127–H127	119.6	C136–P4–Ru2	115.10(14)
C126–C127–H127	119.6	C109–Ru2–C101	38.55(17)
C127–C128–C129	119.7(4)	C109–Ru2–C102	63.74(17)
C127–C128–H128	120.2	C101–Ru2–C102	37.87(15)
C129–C128–H128	120.2	C109–Ru2–P4	130.28(13)
C128–C129–C124	120.7(4)	C101–Ru2–P4	95.90(13)
C128–C129–H129	119.6	C102–Ru2–P4	92.71(13)
C124–C129–H129	119.6	C109–Ru2–P3	80.26(12)
C135–C130–C131	119.5(4)	C101–Ru2–P3	104.68(12)
C135–C130–P4	121.8(3)	C102–Ru2–P3	141.65(12)
C131–C130–P4	118.6(3)	P4–Ru2–P3	101.49(4)
C130–C131–C132	120.4(4)	C109–Ru2–C108	37.42(16)
C130–C131–H131	119.8	C101–Ru2–C108	62.25(17)
C132–C131–H131	119.8	C102–Ru2–C108	61.54(16)
C133–C132–C131	119.1(4)	P4–Ru2–C108	154.05(11)
C133–C132–H132	120.5	P3–Ru2–C108	97.82(12)

C109–Ru2–C103	62.65(16)	C101–Ru2–Cl2	159.72(12)
C101–Ru2–C103	61.94(15)	C102–Ru2–Cl2	121.91(12)
C102–Ru2–C103	36.36(15)	P4–Ru2–Cl2	85.28(4)
P4–Ru2–C103	122.27(13)	P3–Ru2–Cl2	94.87(4)
P3–Ru2–C103	134.43(13)	C108–Ru2–Cl2	110.28(12)
C108–Ru2–C103	36.64(16)	C103–Ru2–Cl2	100.35(11)
C109–Ru2–Cl2	144.43(13)		

Symmetry transformations used to generate equivalent atoms:

APPENDIX V: X-RAY STRUCTURE OF RUTHENIUM COMPLEX 112

Table 4. Anisotropic displacement parameters [$Å^2 \times 10^3$]. The anisotropic displacement factor exponent takes the form: $-2\pi^2[h^2a^{*2}U^{11} + \cdots + 2\,h\,k\,a^*\,b^*\,U^{12}]$.

Atom	U^{11}	U^{22}	U^{33}	U^{23}	U^{13}	U^{12}
C1	31(3)	15(2)	32(3)	11(2)	15(3)	3(2)
C2	23(3)	16(2)	31(3)	0(2)	11(3)	−1(2)
C3	21(3)	14(2)	34(3)	2(2)	9(3)	1(2)
C4	31(3)	21(2)	29(3)	2(2)	9(3)	7(2)
C5	42(4)	21(2)	44(3)	4(2)	23(3)	9(2)
C6	31(3)	27(3)	51(4)	−2(2)	24(3)	6(2)
C7	19(3)	15(2)	51(3)	0(2)	12(3)	2(2)
C8	20(3)	16(2)	31(3)	6(2)	8(2)	9(2)
C9	23(3)	16(2)	31(3)	12(2)	7(2)	5(2)
C10	31(3)	23(2)	26(3)	4(2)	7(2)	5(2)
C11	40(4)	25(3)	28(3)	8(2)	1(3)	−1(2)
C12	44(4)	29(3)	50(4)	9(2)	−3(3)	7(3)
C13	84(6)	41(3)	46(4)	16(3)	−16(4)	15(3)
C14	131(8)	51(4)	43(4)	12(3)	−31(4)	5(4)
C16	62(5)	29(3)	39(3)	10(2)	−5(3)	5(3)
C17	28(3)	26(2)	27(3)	1(2)	10(2)	−2(2)
C18	26(3)	17(2)	31(3)	0(2)	14(3)	1(2)
C19	19(3)	25(2)	31(3)	0(2)	10(2)	1(2)
C20	34(3)	32(3)	36(3)	4(2)	21(3)	−1(2)
C21	24(3)	30(3)	41(3)	2(2)	19(3)	−2(2)
C22	20(3)	26(2)	33(3)	−4(2)	3(2)	−7(2)
C23	23(3)	29(2)	29(3)	−7(2)	10(2)	−6(2)
C24	23(3)	15(2)	23(2)	−1(2)	9(2)	−2(2)
C25	25(3)	28(2)	29(3)	−5(2)	14(2)	−9(2)
C26	33(3)	27(2)	43(3)	0(2)	25(3)	1(2)
C27	33(3)	28(3)	52(3)	−2(2)	25(3)	7(2)
C28	40(4)	27(2)	33(3)	8(2)	17(3)	3(2)
C29	29(3)	27(3)	28(3)	4(2)	15(2)	8(2)
C30	13(2)	23(2)	26(2)	6(2)	9(2)	5(2)
C31	32(3)	21(2)	42(3)	−3(2)	22(3)	−3(2)
C32	58(4)	35(3)	46(3)	0(2)	34(3)	0(3)
C33	38(4)	44(3)	44(3)	0(2)	29(3)	−6(3)
C34	27(3)	26(2)	45(3)	3(2)	20(3)	−5(2)
C35	27(3)	28(3)	26(3)	−3(2)	11(2)	−3(2)
C36	21(3)	25(2)	28(3)	6(2)	10(2)	1(2)
C37	25(3)	23(2)	43(3)	5(2)	16(3)	−1(2)
C38	17(3)	36(3)	48(3)	6(2)	5(3)	−3(2)
C39	29(3)	40(3)	37(3)	−6(2)	6(3)	−5(2)
C40	26(3)	29(3)	35(3)	−5(2)	5(3)	−6(2)
C41	28(3)	25(2)	28(3)	3(2)	9(3)	2(2)
C42	25(3)	23(2)	39(3)	6(2)	17(3)	6(2)
Cl1	23(1)	27(1)	25(1)	5(1)	11(1)	2(1)
P1	21(1)	20(1)	20(1)	2(1)	9(1)	0(1)
P2	18(1)	20(1)	28(1)	2(1)	11(1)	1(1)
Ru1	17(1)	17(1)	23(1)	2(1)	8(1)	1(1)
C15	86(6)	46(4)	40(4)	11(3)	0(4)	−2(4)
C101	31(3)	19(2)	31(3)	−9(2)	16(3)	−7(2)
C102	21(3)	17(2)	30(3)	−1(2)	13(2)	0(2)
C103	28(3)	17(2)	29(3)	−8(2)	14(3)	−4(2)
C104	42(4)	22(2)	44(3)	−4(2)	27(3)	−5(2)
C105	55(4)	18(2)	56(4)	−4(2)	42(3)	−8(2)
C106	57(5)	30(3)	72(4)	−17(3)	53(4)	−21(3)
C107	29(3)	22(2)	53(3)	−16(2)	19(3)	−9(2)
C108	21(3)	14(2)	43(3)	−12(2)	16(3)	−7(2)
C109	24(3)	22(2)	26(3)	−9(2)	5(2)	−7(2)
C110	27(3)	31(3)	32(3)	−9(2)	4(3)	2(2)
C111	53(4)	59(4)	33(3)	−20(3)	3(3)	3(3)
C112	76(6)	34(3)	59(4)	−15(3)	−2(4)	−7(3)

C113	101(7)	68(5)	73(6)	−23(4)	−15(5)	7(5)
C114	156(9)	33(4)	82(6)	−11(4)	3(6)	−15(5)
C115	105(7)	91(6)	40(4)	−23(4)	−24(4)	9(5)
C116	85(6)	54(4)	43(4)	−7(3)	3(4)	−1(4)
C117	31(3)	34(3)	22(2)	−2(2)	8(2)	8(2)
C118	20(3)	21(2)	27(3)	−4(2)	11(2)	−5(2)
C119	28(3)	32(3)	32(3)	16(2)	15(3)	4(2)
C120	22(3)	35(3)	40(3)	16(2)	9(3)	1(2)
C121	28(3)	25(2)	49(3)	4(2)	24(3)	3(2)
C122	29(3)	40(3)	35(3)	3(2)	20(3)	2(2)
C123	29(3)	27(2)	28(3)	4(2)	14(3)	8(2)
C124	22(3)	21(2)	22(2)	5(2)	8(2)	6(2)
C125	32(3)	28(3)	22(2)	−1(2)	12(2)	−2(2)
C126	30(3)	31(2)	32(3)	−5(2)	15(3)	−3(2)
C127	32(3)	26(3)	44(3)	12(2)	20(3)	2(2)
C128	29(3)	38(3)	32(3)	9(2)	19(3)	4(2)
C129	28(3)	33(3)	23(2)	6(2)	14(2)	6(2)
C130	20(3)	25(2)	18(2)	0(2)	9(2)	−2(2)
C131	26(3)	28(2)	25(2)	2(2)	12(2)	1(2)
C132	36(3)	36(3)	25(3)	6(2)	16(3)	1(2)
C133	38(4)	37(3)	31(3)	−5(2)	21(3)	2(2)
C134	40(3)	20(2)	34(3)	−3(2)	23(3)	0(2)
C135	26(3)	26(3)	29(3)	1(2)	13(3)	1(2)
C136	19(3)	21(2)	18(2)	−2(2)	4(2)	−4(2)
C137	27(3)	27(2)	31(3)	1(2)	12(2)	2(2)
C138	24(3)	32(3)	37(3)	−4(2)	7(3)	4(2)
C139	30(3)	32(3)	27(3)	1(2)	0(3)	3(2)
C140	38(4)	27(2)	22(3)	4(2)	12(3)	4(2)
C141	33(3)	24(2)	25(3)	−4(2)	16(3)	−6(2)
C142	24(3)	22(2)	32(3)	−5(2)	19(3)	−3(2)
Cl2	24(1)	29(1)	20(1)	−3(1)	11(1)	−1(1)
P3	22(1)	23(1)	19(1)	0(1)	10(1)	2(1)
P4	21(1)	19(1)	22(1)	0(1)	12(1)	0(1)
Ru2	18(1)	19(1)	19(1)	−1(1)	8(1)	−1(1)

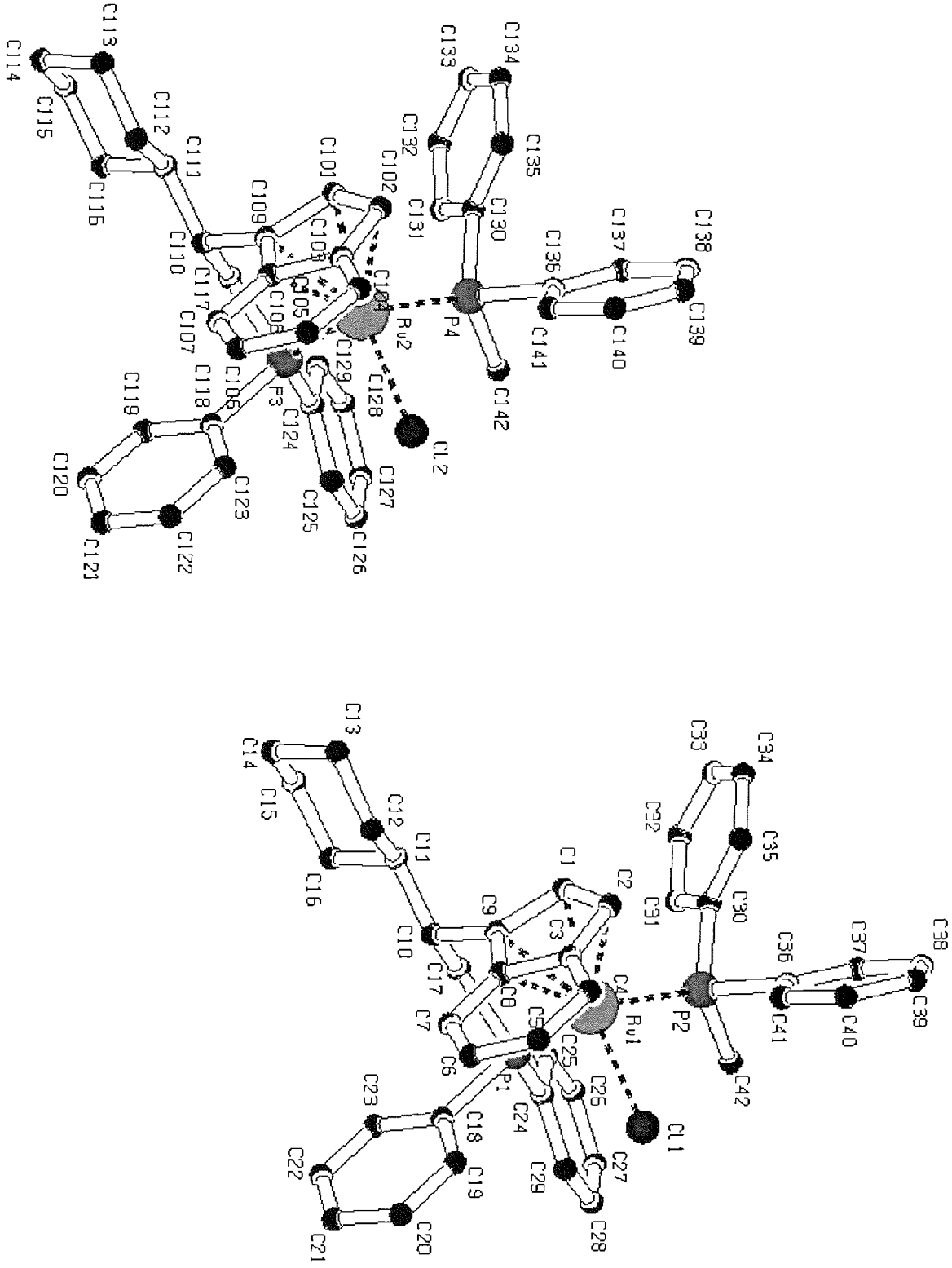
C113
C114
C115
C112
C111
C116
C110
C109
C101
C102
C132
C133
C134
C135
C131
C130
C136
C137
C138
C139
C140
C141
C142
C103
C104
C105
C108
C107
C106
C129
C128
C118
C119
C124
P3
Ru2
P4
Cl2
C120
C123
C125
C127
C121
C122
C126
C13
C14
C15
C12
C11
C16
C10
C9
C1
C2
C3
C17
C8
C4
C7
C5
C6
C25
P1
Ru1
P2
C33
C34
C92
C35
C31
C30
C36
C37
C38
C39
C40
C41
C42
C23
C18
C24
C26
Cl1
C22
C19
C29
C27
C28
C21
C20

University of Southampton · Department of Chemistry
EPSRC National Crystallography Service

Table 1. Crystal data and structure refinement.

Identification code	**04sot0782 (DCP165/2)**	
Empirical formula	$C_{37}H_{41}ClP_2Ru$	
Formula weight	684.16	
Temperature	120(2) K	
Wavelength	0.71073 Å	
Crystal system	Orthorhombic	
Space group	*Pbca*	
Unit cell dimensions	a = 18.93(2) Å	α = 90°
	b = 16.508(13) Å	β = 90°
	c = 20.610(5) Å	γ = 90°
Volume	6441(9) Å^3	
Z	8	
Density (calculated)	1.411 Mg / m^3	
Absorption coefficient	0.694 mm^{-1}	
F(000)	2832	
Crystal	Cut block; dark red	
Crystal size	0.16 × 0.10 × 0.08 mm^3	
θ range for data collection	2.92 – 27.50°	
Index ranges	$-24 \le h \le 24$, $-19 \le k \le 19$, $-26 \le l \le 16$	
Reflections collected	38570	
Independent reflections	7146 [R_{int} = 0.2476]	
Completeness to θ = 27.50°	96.6 %	
Absorption correction	Semi-empirical from equivalents	
Max. and min. transmission	0.9466 and 0.8970	
Refinement method	Full-matrix least-squares on F^2	
Data / restraints / parameters	7146 / 0 / 371	
Goodness-of-fit on F^2	0.972	
Final R indices [$F^2 > 2\sigma(F^2)$]	$R1$ = 0.0792, $wR2$ = 0.1273	
R indices (all data)	$R1$ = 0.1949, $wR2$ = 0.1611	
Extinction coefficient	0.0011(2)	
Largest diff. peak and hole	1.514 and −3.492 e Å^{-3}	

Diffractometer: *Nonius KappaCCD* area detector (ϕ scans and ω scans to fill *asymmetric unit* sphere). **Cell determination:** DirAx (Duisenberg, A.J.M.(1992). J. Appl. Cryst. 25, 92-96.) **Data collection:** Collect (Collect: Data collection software, R. Hooft, Nonius B.V., 1998). **Data reduction and cell refinement**: *Denzo* (Z. Otwinowski & W. Minor, *Methods in Enzymology* (1997) Vol. **276**: *Macromolecular Crystallography*, part A, pp. 307–326; C. W. Carter, Jr. & R. M. Sweet, Eds., Academic Press). **Absorption correction**: *SORTAV* (R. H. Blessing, Acta Cryst. A**51** (1995) 33–37; R. H. Blessing, J. Appl. Cryst. **30** (1997) 421–426). **Structure solution**: *SHELXS97* (G. M. Sheldrick, Acta Cryst. (1990) A**46** 467–473). **Structure refinement**: *SHELXL97* (G. M. Sheldrick (1997), University of Göttingen, Germany). **Graphics:** Cameron - A Molecular Graphics Package. (D. M. Watkin, L. Pearce and C. K. Prout, Chemical Crystallography Laboratory, University of Oxford, 1993).

Special details:

APPENDIX VI: X-RAY STRUCTURE OF RUTHENIUM COMPLEX **113**

Table 2. Atomic coordinates [$\times 10^4$], equivalent isotropic displacement parameters [$Å^2 \times 10^3$] and site occupancy factors. U_{eq} is defined as one third of the trace of the orthogonalized U^{ij} tensor.

Atom	*x*	*y*	*z*	U_{eq}	*S.o.f.*
Ru1	758(1)	1573(1)	1644(1)	15(1)	1
Cl1	24(1)	362(1)	1716(1)	21(1)	1
P1	1087(1)	1420(1)	2697(1)	17(1)	1
P2	−98(1)	2501(1)	1832(1)	15(1)	1
C1	1735(2)	2163(4)	1442(2)	20(1)	1
C2	1833(3)	1345(4)	1220(2)	22(1)	1
C3	1375(3)	1223(4)	677(2)	23(1)	1
C4	1279(3)	528(4)	272(2)	30(2)	1
C5	825(3)	600(5)	−242(2)	36(2)	1
C6	454(3)	1315(5)	−365(2)	35(2)	1
C7	508(3)	1992(4)	30(2)	26(2)	1
C8	980(3)	1945(4)	572(2)	15(1)	1
C9	1181(3)	2528(4)	1071(2)	18(1)	1
C10	880(3)	3379(4)	1120(2)	17(1)	1
C11	1483(3)	4016(4)	1135(2)	21(1)	1
C12	1962(3)	3957(5)	535(2)	28(2)	1
C13	1598(3)	4266(5)	−75(2)	37(2)	1
C14	1326(4)	5121(5)	10(3)	43(2)	1
C15	833(3)	5195(5)	609(3)	36(2)	1
C16	1220(3)	4878(4)	1208(3)	27(2)	1
C17	378(3)	3459(4)	1707(2)	19(1)	1
C18	−577(3)	2644(4)	2593(2)	15(1)	1
C19	−585(3)	3361(4)	2947(2)	17(1)	1
C20	−1008(3)	3415(4)	3501(2)	19(1)	1
C21	−1424(3)	2779(4)	3695(2)	23(1)	1
C22	−1414(3)	2055(4)	3353(2)	23(1)	1
C23	−1000(3)	1992(4)	2799(2)	22(1)	1
C24	−872(3)	2564(4)	1281(2)	19(1)	1
C25	−1346(3)	3203(4)	1319(2)	21(1)	1
C26	−1954(3)	3222(4)	940(2)	25(2)	1
C27	−2085(3)	2581(4)	515(2)	27(2)	1
C28	−1620(3)	1942(4)	478(2)	24(1)	1
C29	−1008(3)	1925(4)	859(2)	19(1)	1
C30	1866(3)	769(4)	2789(2)	19(1)	1
C31	1813(3)	−17(4)	2534(2)	23(1)	1
C32	2364(3)	−556(4)	2605(2)	28(2)	1
C33	2988(3)	−325(4)	2912(2)	27(2)	1
C34	3051(3)	452(4)	3151(2)	26(2)	1
C35	2495(3)	993(4)	3096(2)	21(1)	1
C36	480(3)	926(4)	3264(2)	29(2)	1
C37	1319(3)	2331(4)	3146(2)	28(2)	1

APPENDIX VI: X-RAY STRUCTURE OF RUTHENIUM COMPLEX 113

Table 3. Bond lengths [Å] and angles [°].

Ru1–C9	2.127(6)	C20–H20	0.9500
Ru1–C1	2.131(5)	C21–C22	1.388(9)
Ru1–C2	2.246(5)	C21–H21	0.9500
Ru1–P2	2.264(2)	C22–C23	1.389(6)
Ru1–P1	2.2713(13)	C22–H22	0.9500
Ru1–C8	2.331(4)	C23–H23	0.9500
Ru1–C3	2.380(5)	C24–C29	1.391(8)
Ru1–Cl1	2.439(2)	C24–C25	1.387(8)
P1–C37	1.819(6)	C25–C26	1.392(7)
P1–C30	1.834(6)	C25–H25	0.9500
P1–C36	1.832(6)	C26–C27	1.397(8)
P2–C18	1.828(5)	C26–H26	0.9500
P2–C17	1.838(6)	C27–C28	1.375(9)
P2–C24	1.857(5)	C27–H27	0.9500
C1–C9	1.431(7)	C28–C29	1.400(7)
C1–C2	1.437(9)	C28–H28	0.9500
C1–H1	0.9500	C29–H29	0.9500
C2–C3	1.430(7)	C30–C35	1.398(7)
C2–H2	0.9500	C30–C31	1.403(9)
C3–C8	1.424(8)	C31–C32	1.379(8)
C3–C4	1.430(8)	C31–H31	0.9500
C4–C5	1.371(7)	C32–C33	1.393(8)
C4–H4	0.9500	C32–H32	0.9500
C5–C6	1.396(10)	C33–C34	1.378(9)
C5–H5	0.9500	C33–H33	0.9500
C6–C7	1.386(9)	C34–C35	1.386(8)
C6–H6	0.9500	C34–H34	0.9500
C7–C8	1.432(6)	C35–H35	0.9500
C7–H7	0.9500	C36–H36A	0.9800
C8–C9	1.459(7)	C36–H36B	0.9800
C9–C10	1.519(8)	C36–H36C	0.9800
C10–C17	1.544(6)	C37–H37A	0.9800
C10–C11	1.553(8)	C37–H37B	0.9800
C10–H10	1.0000	C37–H37C	0.9800
C11–C16	1.515(9)		
C11–C12	1.537(7)	C9–Ru1–C1	39.27(19)
C11–H11	1.0000	C9–Ru1–C2	64.3(2)
C12–C13	1.521(7)	C1–Ru1–C2	38.2(2)
C12–H12A	0.9900	C9–Ru1–P2	82.07(16)
C12–H12B	0.9900	C1–Ru1–P2	110.15(19)
C13–C14	1.512(10)	C2–Ru1–P2	145.90(18)
C13–H13A	0.9900	C9–Ru1–P1	120.61(14)
C13–H13B	0.9900	C1–Ru1–P1	89.96(13)
C14–C15	1.553(8)	C2–Ru1–P1	96.01(13)
C14–H14A	0.9900	P2–Ru1–P1	96.20(5)
C14–H14B	0.9900	C9–Ru1–C8	37.9(2)
C15–C16	1.527(8)	C1–Ru1–C8	62.50(17)
C15–H15A	0.9900	C2–Ru1–C8	60.83(18)
C15–H15B	0.9900	P2–Ru1–C8	96.42(15)
C16–H16A	0.9900	P1–Ru1–C8	152.27(13)
C16–H16B	0.9900	C9–Ru1–C3	62.0(2)
C17–H17A	0.9900	C1–Ru1–C3	61.4(2)
C17–H17B	0.9900	C2–Ru1–C3	35.86(17)
C18–C19	1.391(8)	P2–Ru1–C3	131.16(15)
C18–C23	1.407(8)	P1–Ru1–C3	129.67(14)
C19–C20	1.398(7)	C8–Ru1–C3	35.2(2)
C19–H19	0.9500	C9–Ru1–Cl1	148.86(13)
C20–C21	1.372(8)	C1–Ru1–Cl1	151.81(17)

C2–Ru1–Cl1	113.80(18)	C17–C10–C11	112.2(4)
P2–Ru1–Cl1	97.83(9)	C9–C10–H10	107.5
P1–Ru1–Cl1	90.44(5)	C17–C10–H10	107.5
C8–Ru1–Cl1	112.11(14)	C11–C10–H10	107.5
C3–Ru1–Cl1	97.59(16)	C16–C11–C12	109.5(5)
C37–P1–C30	103.8(3)	C16–C11–C10	113.4(5)
C37–P1–C36	101.2(3)	C12–C11–C10	112.0(5)
C30–P1–C36	100.2(3)	C16–C11–H11	107.2
C37–P1–Ru1	117.4(2)	C12–C11–H11	107.2
C30–P1–Ru1	112.62(15)	C10–C11–H11	107.2
C36–P1–Ru1	119.13(18)	C13–C12–C11	112.0(4)
C18–P2–C17	104.6(2)	C13–C12–H12A	109.2
C18–P2–C24	97.2(2)	C11–C12–H12A	109.2
C17–P2–C24	104.6(3)	C13–C12–H12B	109.2
C18–P2–Ru1	126.13(18)	C11–C12–H12B	109.2
C17–P2–Ru1	102.05(19)	H12A–C12–H12B	107.9
C24–P2–Ru1	119.92(19)	C14–C13–C12	111.9(5)
C9–C1–C2	108.7(5)	C14–C13–H13A	109.2
C9–C1–Ru1	70.2(3)	C12–C13–H13A	109.2
C2–C1–Ru1	75.2(3)	C14–C13–H13B	109.2
C9–C1–H1	125.7	C12–C13–H13B	109.2
C2–C1–H1	125.7	H13A–C13–H13B	107.9
Ru1–C1–H1	120.6	C13–C14–C15	111.7(5)
C3–C2–C1	107.6(5)	C13–C14–H14A	109.3
C3–C2–Ru1	77.2(3)	C15–C14–H14A	109.3
C1–C2–Ru1	66.6(3)	C13–C14–H14B	109.3
C3–C2–H2	126.2	C15–C14–H14B	109.3
C1–C2–H2	126.2	H14A–C14–H14B	107.9
Ru1–C2–H2	121.6	C16–C15–C14	109.1(5)
C8–C3–C4	121.1(5)	C16–C15–H15A	109.9
C8–C3–C2	108.7(5)	C14–C15–H15A	109.9
C4–C3–C2	130.3(6)	C16–C15–H15B	109.9
C8–C3–Ru1	70.5(3)	C14–C15–H15B	109.9
C4–C3–Ru1	128.3(4)	H15A–C15–H15B	108.3
C2–C3–Ru1	66.9(3)	C11–C16–C15	113.5(5)
C5–C4–C3	117.5(6)	C11–C16–H16A	108.9
C5–C4–H4	121.2	C15–C16–H16A	108.9
C3–C4–H4	121.2	C11–C16–H16B	108.9
C4–C5–C6	121.9(6)	C15–C16–H16B	108.9
C4–C5–H5	119.1	H16A–C16–H16B	107.7
C6–C5–H5	119.1	C10–C17–P2	109.7(4)
C7–C6–C5	122.6(5)	C10–C17–H17A	109.7
C7–C6–H6	118.7	P2–C17–H17A	109.7
C5–C6–H6	118.7	C10–C17–H17B	109.7
C6–C7–C8	117.4(6)	P2–C17–H17B	109.7
C6–C7–H7	121.3	H17A–C17–H17B	108.2
C8–C7–H7	121.3	C19–C18–C23	119.1(5)
C3–C8–C7	119.4(5)	C19–C18–P2	124.5(4)
C3–C8–C9	107.9(4)	C23–C18–P2	116.3(4)
C7–C8–C9	132.6(6)	C18–C19–C20	119.3(5)
C3–C8–Ru1	74.3(3)	C18–C19–H19	120.4
C7–C8–Ru1	129.9(3)	C20–C19–H19	120.4
C9–C8–Ru1	63.5(3)	C21–C20–C19	121.2(6)
C1–C9–C8	106.9(5)	C21–C20–H20	119.4
C1–C9–C10	129.0(5)	C19–C20–H20	119.4
C8–C9–C10	123.9(4)	C20–C21–C22	120.3(5)
C1–C9–Ru1	70.5(3)	C20–C21–H21	119.9
C8–C9–Ru1	78.7(3)	C22–C21–H21	119.9
C10–C9–Ru1	120.5(3)	C23–C22–C21	119.3(6)
C9–C10–C17	111.3(4)	C23–C22–H22	120.4
C9–C10–C11	110.6(4)	C21–C22–H22	120.4

C22–C23–C18	120.8(6)	C30–C31–H31	119.9
C22–C23–H23	119.6	C31–C32–C33	120.8(6)
C18–C23–H23	119.6	C31–C32–H32	119.6
C29–C24–C25	119.4(5)	C33–C32–H32	119.6
C29–C24–P2	119.1(4)	C34–C33–C32	119.4(6)
C25–C24–P2	121.3(4)	C34–C33–H33	120.3
C24–C25–C26	121.4(5)	C32–C33–H33	120.3
C24–C25–H25	119.3	C33–C34–C35	120.2(5)
C26–C25–H25	119.3	C33–C34–H34	119.9
C27–C26–C25	118.8(6)	C35–C34–H34	119.9
C27–C26–H26	120.6	C34–C35–C30	121.0(6)
C25–C26–H26	120.6	C34–C35–H35	119.5
C28–C27–C26	120.2(5)	C30–C35–H35	119.5
C28–C27–H27	119.9	P1–C36–H36A	109.5
C26–C27–H27	119.9	P1–C36–H36B	109.5
C27–C28–C29	120.9(6)	H36A–C36–H36B	109.5
C27–C28–H28	119.5	P1–C36–H36C	109.5
C29–C28–H28	119.5	H36A–C36–H36C	109.5
C24–C29–C28	119.3(6)	H36B–C36–H36C	109.5
C24–C29–H29	120.3	P1–C37–H37A	109.5
C28–C29–H29	120.3	P1–C37–H37B	109.5
C35–C30–C31	118.3(5)	H37A–C37–H37B	109.5
C35–C30–P1	125.2(5)	P1–C37–H37C	109.5
C31–C30–P1	116.5(4)	H37A–C37–H37C	109.5
C32–C31–C30	120.2(5)	H37B–C37–H37C	109.5
C32–C31–H31	119.9		

Symmetry transformations used to generate equivalent atoms:

APPENDIX VI: X-RAY STRUCTURE OF RUTHENIUM COMPLEX **113**

Table 4. Anisotropic displacement parameters [$Å^2 \times 10^3$]. The anisotropic displacement factor exponent takes the form: $-2\pi^2[h^2a^{*2}U^{11} + \cdots + 2\,h\,k\,a^*\,b^*\,U^{12}]$.

Atom	U^{11}	U^{22}	U^{33}	U^{23}	U^{13}	U^{12}
Ru1	16(1)	17(1)	11(1)	−2(1)	0(1)	0(1)
Cl1	23(1)	18(1)	24(1)	−1(1)	−4(1)	−1(1)
P1	19(1)	21(1)	12(1)	−1(1)	−1(1)	1(1)
P2	16(1)	17(1)	12(1)	−1(1)	2(1)	1(1)
C1	14(2)	34(5)	13(2)	−5(2)	0(2)	−3(3)
C2	15(2)	28(5)	23(2)	3(3)	1(2)	3(3)
C3	26(3)	26(4)	15(2)	−4(2)	5(2)	0(3)
C4	29(3)	36(5)	25(2)	−10(3)	2(2)	0(3)
C5	40(3)	46(6)	21(2)	−12(3)	−1(3)	2(4)
C6	32(3)	52(6)	20(2)	−6(3)	−6(2)	−6(3)
C7	23(3)	38(5)	16(2)	2(3)	−2(2)	2(3)
C8	21(2)	15(4)	9(2)	3(2)	3(2)	−2(2)
C9	21(2)	21(4)	11(2)	1(2)	3(2)	2(3)
C10	20(2)	11(4)	19(2)	1(2)	3(2)	−5(2)
C11	24(3)	19(4)	21(2)	3(2)	2(2)	−4(3)
C12	22(3)	34(5)	29(3)	7(3)	9(2)	0(3)
C13	48(4)	42(5)	21(2)	7(3)	10(3)	3(4)
C14	53(4)	40(6)	37(3)	15(3)	4(3)	1(4)
C15	34(3)	37(5)	37(3)	8(3)	6(3)	4(3)
C16	31(3)	19(4)	31(3)	−1(3)	2(2)	−10(3)
C17	25(3)	16(4)	16(2)	0(2)	4(2)	0(3)
C18	20(2)	8(4)	16(2)	0(2)	−1(2)	0(2)
C19	21(2)	16(4)	15(2)	2(2)	0(2)	−2(3)
C20	28(3)	14(4)	16(2)	−2(2)	−4(2)	1(3)
C21	26(3)	23(4)	21(2)	2(3)	4(2)	8(3)
C22	23(2)	21(4)	26(2)	5(3)	7(2)	2(3)
C23	19(2)	21(4)	25(2)	−5(3)	4(2)	−1(3)
C24	19(2)	26(4)	11(2)	4(2)	2(2)	5(3)
C25	30(3)	20(4)	15(2)	1(2)	−2(2)	−1(3)
C26	27(3)	23(5)	25(2)	5(3)	−1(2)	6(3)
C27	31(3)	30(5)	20(2)	0(3)	−9(2)	2(3)
C28	33(3)	21(4)	19(2)	−8(2)	−2(2)	−1(3)
C29	21(2)	14(4)	20(2)	0(2)	0(2)	−1(3)
C30	21(3)	24(4)	11(2)	1(2)	1(2)	1(3)
C31	26(3)	27(4)	17(2)	−2(3)	−1(2)	1(3)
C32	30(3)	27(5)	27(3)	0(3)	2(2)	3(3)
C33	27(3)	24(5)	28(3)	7(3)	5(2)	10(3)
C34	24(3)	26(5)	26(2)	2(3)	0(2)	2(3)
C35	21(2)	26(4)	16(2)	−1(3)	−1(2)	−2(3)
C36	30(3)	36(5)	21(2)	7(3)	2(2)	−3(3)
C37	28(3)	38(5)	17(2)	−6(3)	−6(2)	6(3)

APPENDIX VI: X-RAY STRUCTURE OF RUTHENIUM COMPLEX **113**